New multiproxy record of the Jenkyns Event (a.k.a. Toarcian Oceanic Anoxic Event) from the Mecsek Mountains (Hungary): Differences, duration and drivers

Tamás Müller[1,2], Gregory D. Price[3], Dávid Bajnai[1,4], Anita Nyerges[1,5], Dóra Kesjár[6], Béla Raucsik[7], Andrea Varga[7], Katalin Judik[6], József Fekete[6], Zoltán May[8], József Pálfy[1,5]

[1] Department of Physical and Applied Geology, Eötvös Loránd University, Pázmány Péter sétány 1/C, H-1117, Budapest, Hungary

[2] Earth Science Institute, Slovak Academy of Sciences, Dúbravská cesta 9, 840 05, Bratislava, Slovak Republic

[3] School of Geography, Earth & Environmental Sciences, Plymouth University, Drake Circus, PL4 8AA, Plymouth, United Kingdom

[4] Institut für Geowissenschaften, J. W. Goethe-Universität, Altenhöferallee 1, 60438, Frankfurt, Germany

[5] MTA-MTM-ELTE Research Group for Paleontology, POB 137, H-1431, Budapest, Hungary

[6] Institute for Geological and Geochemical Research, Hungarian Academy of Sciences, Budaörsi út 45, H-1112, Budapest, Hungary

[7] Department of Mineralogy, Geochemistry and Petrology, University of Szeged, Egyetem utca 2, H-6722, Szeged, Hungary

[8] Research Centre for Natural Sciences, Hungarian Academy of Sciences, Institute of Materials and Environmental Chemistry, Magyar tudósok körútja 2, H-1117, Budapest, Hungary

ABSTRACT

The oceanic anoxic event in the Early Toarcian, often referred to as T-OAE, led to widespread deposition of organic-rich black shales and geochemical anomalies in elemental distribution and multiple isotope systems in the Early Jurassic ocean. Best characterized by its hallmark carbon isotope anomaly, the event is widely regarded as a prime example of rapid greenhouse warming-related changes in the Mesozoic Earth system. However, despite numerous studies, details of its forcing mechanisms, exact duration, and the role of regional effects remain debated. Here we present new data (high resolution organic carbon isotope, calcareous nannofossil and elemental geochemical analyses) from the black shale-bearing Lower Toarcian section in the Réka Valley, Hungary, with the aim of assessing any regional differences in the sedimentary and geochemical record and their bearing on the underlying oceanographic and climatic processes. Following a short segment with a positive trend at the base of the section, values of our carbon isotope data are turning to a negative trend with a steep, stepwise drop in two negative shifts, reaching their minimum before a positive trend with oscillations characterizing the top part of the section examined. The shape of the curve and nannoplankton biostratigraphy (recognition of zones NJ5b, NJ6 and NJ7) allow reliable correlation of our data with the global carbon isotope perturbation recorded elsewhere in the Early Toarcian. We propose here that it would be fitting to rename the T-OAE as the Jenkyns Event, to honour the seminal contributions of Hugh Jenkyns. Our cyclostratigraphic analysis suggests that the duration of the negative isotope excursion at Réka Valley is 200 kyr, 350 kyr, or 1 Myr, depending on which astronomical forcing parameter controls the most prominent cyclicity. Spectroscopic analyses suggest that the source of the organic matter, marine algae according to previous studies, did not change considerably during the main negative carbon isotope excursion. The variability observed in major element concentrations and enrichments relative to the average shale in the Réka Valley black shales can be regarded as mixtures of terrigenous aluminosilicates and calcium carbonate as two endmembers. Consequently, the terrigenous compositional endmember of the studied black shales consists of a mixture of an illitic/smectitic and a kaolinitic clay, supports previous suggestions of increased weathering under extremely humid climate in the hinterland during the Jenkyns Event.

Keywords oceanic anoxic event, Early Jurassic, Toarcian, carbon isotopes, elemental geochemistry, cyclostratigraphy, nannoplankton biostratigraphy, Fourier transform infrared spectroscopy

INTRODUCTION

The Earth system experienced a major global perturbation in the Early Toarcian (Early Jurassic, 182 Ma; Jenkyns, 2010). This event is widely recognized by occurrences of organic-rich black shale in the marine sedimentary record. Regionally, it has been exceptionally well studied in stratigraphic successions of the Yorkshire coast in England, where the widespread Jet Rock also represents a level of notable extinction among benthic organisms (Hallam, 1967). Global developments of similar organic-rich sediments in the Cretaceous were termed Oceanic Anoxic Events by Schlanger & Jenkyns (1976), and it was Hugh Jenkyns who first recognized the analogy and significance of Toarcian deposits and first used a remarkable positive stable carbon isotope excursion (CIE) to characterize its development (Jenkyns, 1985, 1988). Shortly thereafter, signs of a negative CIE interrupting the positive trend were noted by Jenkyns & Clayton (1986, 1997), following an earlier description by Küspert (1982), and described in detail from Yorkshire by Hesselbo et al. (2000). Students and co-workers of Hugh Jenkyns developed high-resolution chemostratigraphies in many Lower Toarcian sections worldwide, including the Paris Basin (Hermoso et al., 2012), the Lusitanian Basin (Hesselbo et al., 2007), western Tethyan margin (Woodfine et al., 2008; Sabatino et al., 2009; Kafousia et al., 2011), and outside Europe in Argentina's Neuquén Basin (Al-Suwaidi et al., 2010; 2016). Together with other studies from the Panthalassa in western Canada (Caruthers et al, 2011) and Japan (Gröcke et al., 2011; Izumi et al., 2012; Kemp & Izumi, 2014), the global nature of the Toarcian CIE has been well-established.

The significance of Tethyan manganese deposits of Early Toarcian age was also recognized by Jenkyns et al. (1991). The Jenkyns school pioneered the use of other isotope systems, including nitrogen (Jenkyns et al., 2001), strontium (Jones et al., 1994), and sulphur (Gill et al., 2011) to further characterize the processes and drivers of the Early Toarcian perturbation.

Much has been learned from the sedimentary and geochemical record of the Toarcian and other, similar, anoxic events and commonly related biotic turnover in the Mesozoic and beyond, summarized in a comprehensive review by Jenkyns (2010), widely utilized for chemostratigraphy and paleoceanographic reconstructions (Jenkyns et al., 2002) and presented as prime examples of rapid greenhouse warming events (Jenkyns, 2003).

The name Toarcian Oceanic Anoxic Event (or T-OAE) has been commonly used recently; alternatively it is also referred to as *Posidonienschiefer* event for its typical development in southern Germany (Jenkyns, 2010). However, there are many similar events in Earth history which are named after pioneers of their study, notably including the Early Cretaceous (Valanginian) Weissert Event (Erba et al., 2004). We propose here that it would be fitting to rename the T-OAE as Jenkyns Event, to honour Hugh Jenkyns' seminal contribution to its understanding, and this name will be used throughout this paper.

Hugh Jenkyns worked on several Toarcian sections in Hungary in the Transdanubian Range (Jenkyns et al., 1991). Another occurrence of organic-rich shale in southern Hungary is shown by Jenkyns (1988), from the Mecsek Mts. The present paper describes new results from the Réka Valley section in the Mecsek Mts., the best outcrop of a 12 m thick black shale unit, first connected with the Jenkyns Event by Dulai et al. (1992). More recent studies at this locality reported on and characterized its high organic carbon content, the black shales containing ~4 to ~8% total organic carbon with kerogen type suggestive of marine algal source (Varga et al., 2007). The carbon isotope composition of the organic matter and both the carbon and oxygen isotope composition of the carbonate fraction were also measured, albeit on a small suite of 10 samples only. Although the carbonate fraction was affected by diagenetic overprint, the organic matter yielded negative $\delta^{13}C_{org}$ values between -28.6‰ and –30.9‰ (Varga et al., 2007), raising the possibility of correlation with the minima of other European sections. A clay mineralogical study confirmed elevated weathering under hot and humid conditions (Raucsik & Varga, 2008), whereas changes in palynomorph assemblages were used to infer the sequence of environmental and biotic change (Baranyi, 2012). Despite these advances, detailed comparison of this section with other coeval sedimentary records of the Jenkyns Event has been hindered by insufficient biostratigraphy (only preliminary ammonoid (Galácz, 1991) and calcareous nannoplankton studies (Baldanza et al., 1995) exist) and the low resolution of previous carbon isotope data (Varga et al., 2007).

Geographically distinct records of the Jenkyns Event suggest regional differences in its expression (e.g. Schmid-Röhl et al., 2002; Hermoso et al., 2009; Kafousia et al., 2011), therefore new data from underexplored sections could help refine our understanding of the regional effects. Another outstanding issue is the timing and duration of this event. The synchrony of environmental changes has been approached by ammonoid and nannoplankton biostratigraphic correlation (Jenkyns & Clayton, 1997; Mattioli et al., 2008), but some discrepancies remain in the details of biostratigraphic boundaries, onset of black shale sedimentation and phases of the CIE. Orbitally forced cyclicity in the CIE and sedimentary proxies were first recognized by Kemp et al. (2005) and subsequently documented from several sections, but identification of the dominant control remains controversial. This uncertainty affects estimates of the duration of the black shale interval and the negative CIE, where opinions range between ~170–620 kyr (Suan et al., 2008b; Kemp et al., 2011; Huang & Hesselbo, 2014; Boulila et al., 2014). Resolving these issues may be of significance with respect to identifying the drivers of this event, widely regarded to be triggered by volcanism of the Karoo-Ferrar LIP (Pálfy & Smith, 2000) and related greenhouse warming, amplified by methane injection through either gas-hydrate dissociation in marine sediments (Hesselbo et al., 2000) or thermogenic methane from sill emplacement (McElwain et al., 2005; Svensen et al., 2007).

To address these issues, we present here new data from the Lower Toarcian black shale in the Réka Valley, Hungary. From a new, high-resolution suite of samples, a calcareous nannoplankton biostratigraphic framework is developed, and a $\delta^{13}C_{org}$ curve is presented on the basis of 182 measurements. Because both a well-developed negative CIE and prominent cyclicity are observed in the signal, infrared reflectance spectra and elemental abundance data were obtained on the same samples by FTIR and XRF instruments, respectively. Cyclostratigraphic analysis is used to provide a range of astrochronologic estimates for the duration of the black shale interval, the negative CIE, and the largely correlative NJ6 nannoplankton zone. The shape of the $\delta^{13}C$ curve, the magnitude of the CIE and the amplitude of its cycles are compared with other sections for new insights. Elemental geochemical data are utilized to characterize the weathering regime and climate in the continental hinterland. The results are then used to assess the regional differences in the sedimentary and geochemical record of the Jenkyns Event, and their bearing on the underlying oceanographic and climatic processes.

GEOLOGICAL SETTING AND STRATIGRAPHY

The Mecsek Mountains are located in the southwestern part of the Pannonian Basin in Hungary (Fig. 1). This east-west trending mountain range is the only area within Hungary with surface exposures of the Mecsek structural unit, which comprises a thick package of Permian and Mesozoic strata, and itself forms part of the Tisza Mega-unit (Csontos & Vörös, 2004; Haas & Péró, 2004). The Tisza Mega-unit was part of the European margin after the Variscan orogenic cycle in the Late Palaeozoic and Early Mesozoic. Its separation from the European continental margin started with the Middle Jurassic rifting and later Mesozoic tectonic movements in the Tethys. The Mecsek Unit reached its present day position through complex tectonic processes related to the Alpine orogeny in the Paleogene and Neogene (Csontos et al., 2002). The Late Triassic and Early Jurassic evolution of the Mecsek Basin was controlled by a half-graben system related to continental rifting between the Tisza block and the European margin. Gradual deepening during the Late Sinemurian and Pliensbachian led to the deposition of the intensively bioturbated Hosszúhetény Calcareous Marl Formation in an open marine basin (Raucsik & Merényi, 2000). This lithofacies is named informally as spotted marl and it represents the equivalent of the widely known "Fleckenmergel" or "Allgäu" facies of the European margin of the Neotethys (Horváth & Galácz, 2006; Főzy, 2012). The Upper Pliensbachian and lowermost Toarcian part of the formation is monotonous spotted marl with intercalated turbiditic sandstone beds, crinoidal limestone and organic-rich limestone, reflecting an environment where sea level, climate change, and tectonically controlled subsidence influenced the depositional regime (Raucsik & Varga, 2008). In the Lower Toarcian, organic-rich silty claystone, marlstone and a distinctive, ~12 m thick black shale succession occurs, recently distinguished as a separate lithostratigraphic unit, the Rékavölgy Formation (Főzy, 2012). The organic-rich, in some parts laminated, shale suggests anoxic conditions in the Mecsek Basin in the Early Toarcian and is recognized as the local stratigraphic expression of the Jenkyns Event (Dulai et al., 1992; Varga et al., 2007). In the overlying strata the spotted marl facies returns and continues up to the Bajocian, lithostratigraphically assigned to the Komló Calcareous Marl Formation.

The studied section at Réka Valley provides the best outcrop of the recessive, and elsewhere only very poorly exposed, Lower Toarcian black shale unit. The section is located in a narrow tributary valley of the northern side of the NE-SW trending Réka Valley, south of the village of Óbánya, in the eastern part of the Mecsek Mountains. The basal part of the section comprises bioturbated and clay-rich spotted marl facies with intercalated sandstone beds, overlain by a ~12 m thick succession of organic rich black shale, including intervals of brown to grey bituminous laminated shale, with intercalated beds and lenses of calcareous and sandy turbidite. Fish remains, pyrite framboids, fragments of plant remains and bivalves are common in the black shale (Dulai et al., 1992; Raucsik & Varga, 2008). In the overlying strata at the top of the measured section the spotted marl facies returns.

The age and ammonite biostratigraphy of the section has not been precisely defined due to the scarcity of index species. Ammonites of the genus *Hildaites* from the black shale and *Harpoceras* cf. *exaratum* from the highest part of the black shale interval suggest the presence of the Lower Toarcian Falciferum ammonite standard zone (Galácz, 1991; Dulai et al., 1992). The assignment was supported by limited calcareous nannofossil data reported in Baldanza et al. (1995) and Varga et al. (2009).

MATERIAL AND METHODS

In our field work in August 2014, the intermittent natural outcrops at the steep side of the tributary ravine of Réka Valley were cleaned to access the unweathered rock for sampling. Four parallel trenches with adequate overlap were excavated to connect and expand the natural outcrops, allowing measurement and description of a detailed sedimentary section. The total thickness of the sampled interval of the section is 19.5 m on which high resolution sampling has been carried out applying 0.05 m spacing, wherever outcrop conditions permitted. In total, 460 bulk sediment samples, 100–200 g each, were obtained from the partially overlapping measured stratigraphic sections RVA, RVB, RVC and RVD. Easily recognizable lithologic marker horizons allow the accurate correlation of these sections with earlier studies made at Réka Valley. Splits of the collected samples were investigated for calcareous nannofossil content, organic carbon stable isotope measurements, elemental geochemistry and infrared spectroscopic analyses.

Calcareous nannofossils

The calcareous nannoplankton assemblage was studied in 68 smear slides from the section, at a regular sampling resolution of 0.3 m, except for five levels where sandstone interbeds were avoided. Slide preparation followed the standard technique described by Bown (1998) which is known to retain the original composition of the nannoplankton assemblages of the sediments. The slides were studied in oil immersion at 1000$^\times$ magnification under cross-polarized light using an Olympus BX51 microscope. Forty fields of view per slide were scanned and all of the observed specimens were counted to assess the abundance distribution of nannoflora.

Organic carbon isotope analysis

Bulk organic matter carbon isotope analysis was performed on 182 samples from the studied stratigraphic interval. Parts of the section were analysed either with a 0.1 m or with an increased 0.05 m sample spacing, as outcrop conditions did not allow completely uniform sampling steps throughout (see Supplementary Data). First, ~1 g of the sample material was powdered by using an agate mortar and pestle. The powdered materials were then placed in centrifuge tubes and then treated two times with 10% HCl (agitated and left for 1 hour after each treatment) to remove all the carbonate phases. The remaining solution was pipetted off and replaced with deionized H_2O. After leaving the sediment to settle for two hours, this neutralisation process was repeated ten times. Carbon isotope analysis of the remaining organic matter was conducted at Plymouth

University, using an Isoprime isotope ratio mass spectrometer connected to an Isoprime Microcube elemental analyser. Carbon isotope ratios are expressed using the internationally accepted δ notation in per mil (‰) relative to the Vienna Pee Dee belemnite (VPDB) standard. Instrument calibration was achieved using three international standards, USGS 40 (l-glutamic acid, $\delta^{13}C$ = -26.389‰), USGS 24 (graphite, $\delta^{13}C$ = -16.049‰) and IAEA CH-7 (polyethylene, $\delta^{13}C$ = -32.151‰). The standard deviation on replicates in run analyses of the USGS 40 standard was ±0.12‰.

Elemental geochemical analyses

The use of a handheld XRF device was chosen to efficiently gather elemental abundance data for cyclostratigraphic and elemental geochemical analyses. The measurements were made on 2–3 g of powdered bulk rock material from a suite of 184 samples that represents a 10 cm stratigraphic resolution. Powdered samples were poured onto a piece of paper and were piled up to achieve an appropriate height (1-2 cm) of the sample column. The sensor was pressed directly against the powder during measurements. The instrument's nozzle was thoroughly cleaned after each measurement. The instrument used for this study was a Thermo Scientific Niton XL3t 900 GOLDD+ (Geometrically Optimized Large Area Drift Detector) portable XRF analyser with 50 kV X-ray tube with silver target (Ag anode). Helium purging was also applied for appropriate measuring of light elements (Mg, Al, Si, S, Cl, P). The apparatus has several company-preset calibrations for given matrices, of which the Mining and TestAllGeo calibrations were used for our samples. The average uncertainty of the XRF measurements is 15-20%, depending on the particular element (see Supplementary Data). For the measurements three different certified standards were used (DC72301, GBW07111 and a Hungarian one (from SZIKTTI)). A total of 22 elements (Ti, Mo, Zr, Sr, Rb, Th, Pb, As, Zn, Cu, Fe, Mn, Cr, Ca, K, S, Ba, Nb, Al, P, Si, Mg) were measured. Duration of each measurement was 120 seconds or more, using four energy filters ('Main, Low, High, Light') for 30 seconds each, except for the 'Light' filter which was applied for slightly longer to obtain more accurate values of light elements (Mg, Al, Si, P, S, Cl). The standardless fundamental parameters method with Compton-normalization was used by the XRF apparatus for quantitative analysis and results were also checked by viewing the corresponding spectra with the NDT (Niton Data Transfer, version 8.0.0) software. Mathematical and statistical data processing was done using Excel and Statistica 12 software packages. The different elemental signals derived from XRF measurements are independent of each other, therefore show the variations in the content of the various elements in the bulk rock sample. Analytical quality data including detection limits and precision are tabulated in the Supplementary Data.

Fourier transform infrared spectroscopy (FTIR)

Infrared spectroscopy uses IR radiation to measure what fraction of the incident radiation is absorbed at a particular wavelength, which can be used to establish semi-quantitative measures of mineral and organic matter composition (Farmer, 1974; Griffiths, 1983; Thompson et al., 2009). FTIR uses Fourier transform to convert the raw wavelength data collected by a detector into spectra (Griffith, 1983). Attenuated total reflectance (ATR) is a rapid technique which is a useful initial step to characterize minerals and organic matter with minimal sample preparation (Stuart, 2004). ATR is based on the phenomenon of total internal reflection (Bruno, 1999) and measures the changes which occur in an internally reflected infrared beam which come in contact with the sample through a diamond crystal. When the sample is placed in contact with the ATR crystal the resulting evanescent wave is attenuated in the regions of the IR spectrum where the sample absorbs energy (Stuart, 2004). Measurements were carried out on splits from the same suite of 184 samples at 0.1 m spacing as used for the stable isotope and XRF analyses. The samples were first ground into powder using an agate mortar and pestle. For each sample 16 scans were recorded in the 4000–400 cm^{-1} spectral range with a resolution of 4 cm^{-1}. The measurements were carried out using a Bruker Vertex 70 spectrometer controlled by OPUS 7.2 software, at the Institute for Geological and Geochemical Research of the Hungarian Academy of Sciences.

Time series analysis for cyclostratigraphy and astrochronology

Cyclostratigraphic analyses were made on bulk rock $\delta^{13}C_{org}$, $CaCO_3$, and $CH2_{FTIR}$ signals. The turbidite beds were excluded from the stratigraphy as these strata are instantaneous event deposits that do not record the cyclic variations in the studied proxies. Thus the analyses were performed using a corrected section thickness of 18.5 m.

Data processing was performed using Matlab (2015b) along with R (3.2.4) and the Astrochron R package (Meyers, 2014). Prior to the spectral analysis, the raw data series were linearly interpolated every 0.1 m, long-term trends were removed, and the data series was padded with zeros to 256 data points to accelerate calculations (Cooley & Tukey, 1965). The $\delta^{13}C$ dataset was detrended using a second order polynomial regression, as this method provided the best result for removing the long-term trend of the negative excursion without affecting the low-frequency cyclicities. The $CaCO_3$ and the $CH2_{FTIR}$ signals were detrended using linear regressions. For spectral analyses the multitaper method was used by applying three 2π-tapers (2π-MTM; Thomson, 1982). Confidence levels were calculated using robust red-noise modelling, modified according to Tukey's end-point rule (Tukey, 1977; Mann & Lees 1996; Meyers, 2014). To isolate certain frequencies from the rest of the series, Taner band-pass filters were applied (Taner, 2003). The length of the Milankovitch periodicities in the Toarcian were calculated from the La2004 astronomical solution (short eccentricity: 100 kyr, obliquity: 35 kyr, precession: 25 kyr; Laskar et al., 2004).

RESULTS

Nannofossil assemblages and biostratigraphy

The preservation of coccoliths in the studied material is good and has not been affected by significant diagenetic overprint, as no calcite resorption or overgrowth was observed. The diversity is intermediate, a total of 12 taxa have been identified. A reduced size of coccoliths is noted along the section, especially noticeable in the dominant genus *Lotharingius* (Fig. S1 A-B), with specimens commonly as small as 4-5 μm.

Most of the biostratigraphically important Late Pliensbachian–Early Toarcian calcareous nannoplankton species are well represented in the section, allowing the recognition of calcareous nannoplankton bioevents which are used here as the primary means of age assignment, in the absence of a good ammonite record.

Three nannoplankton zones, NJ5b, NJ6 and NJ7 have been recognized using the biostratigraphic scheme of Bown (1998). The zonal assignments are based on the following primary and secondary nannofossil marker events.

Lotharingius hauffi (Fig. S1A-B), *Lotharingius sigillatus* (Fig. S1E), *Biscutum finchii* (Fig. S1C), and *Crepidolithus impontus* (Fig. S1D) were found in the lowermost sample. Based on their co-occurrence, the base of the studied section is assigned to the NJ5b *Crepidolithus impontus* Subzone. The Pliensbachian-Toarcian boundary is thought to fall within this subzone but it is not recognized in the studied material. The first occurence (FO) of *Carinolithus superbus* (Fig. S1F) is recorded at 7.1 m and used to define the base of NJ6 *Carinolithus superbus* Zone. Its upper boundary and the base of the overlying NJ7 *Discorhabdus striatus* Zone is recognized by the FO of *Discorhabdus striatus* (Fig. S1G) and the last occurrence (LO) of *Biscutum finchii* at 14.85 m.

Beside the zonal marker species, *Bussonius prinsii* (Fig. S1H), *Watznaueria sp*. (Fig. S1J), *Orthogonoides hamiltoniae* (Fig. S1L), *Zeugrhabdotus erectus* (Fig. S1I), and *Schizosphaerella* sp. (Fig. S1K) occur in the Lower Toarcian calcareous nannoplankton assemblage. *Lotharingius* and *Crepidolithus* are numerically dominant over other taxa in the assemblage. *Mitrolithus jansae* has not been recorded, its absence is notable as it is a characteristic species of Tethyan nannoplankton assemblages at several other localities.

The abundance of the nannofossil assemblage is insufficient for a fully quantitative palaeoecological analysis, as viewing 40 fields of view per slide yielded less than 100 specimens in a large number of samples. However, counting all the observed specimens allowed generation of an abundance distribution curve, suitable for a first-order approximation for nannoplankton productivity changes (Fig. 2). In the calcareous marl in the lower part of the section, the nannofossil abundance is variable. Higher up, in the carbonate-poor and organic-rich shale the abundance is generally low except for two significant peaks (at 10.8 and 13.3 m) which correlate with maxima in the $CaCO_3$ content. In the upper marl interval, from 15.6 m, the nannofossil abundance starts to increase and reaches a third major peak at 17.9 m, again coincident with a $CaCO_3$ maximum. The abundance increase is coincident with the positive trend in the $\delta^{13}C_{org}$ data.

The zonal nannoplankton biostratigraphy presented here is the best tool for chronostratigraphic subdivision in the section, through correlation with standard ammonoid zones established in other European sections. The NJ5 *Lotharingius hauffi* Zone is correlative to the ammonoid standard Margaritatus, Spinatum and Tenuicostatum zones, i.e. it ranges from the Upper Pliensbachian to the lowermost Toarcian. The NJ5b subzone, recognized in the studied section, is restricted to the Spinatum and Tenuicostatum zones and straddles the stage boundary. Zone NJ6 is correlated with the Falciferum Zone in the Lower Toarcian and includes the most organic-rich sediments both in this section and at other localities. The NJ7 *Discorhabdus striatus* Zone is correlated with an interval encompassing the topmost Falciferum to Levesquei zones, from the Lower to Upper Toarcian, of which here only the lowermost part is present.

Carbon isotope record

In general, the $\delta^{13}C_{org}$ data obtained from bulk organic matter show negative values (on average -30.84‰) and characteristic patterns throughout the sampled section (Fig. 2). The $\delta^{13}C_{org}$ values range from -32.9‰ to -27.6‰, with an average of -30.9‰. Changing trends in the $\delta^{13}C_{org}$ curve allow us to distinguish three intervals, with potential for chemostratigraphy and interpretation of changes in the carbon cycle. The boundaries of these intervals, together with some other local minima, maxima, and inflection points in the curve are noted as useful features for correlation with other sections. Interval 1 is restricted to the lowermost 2.1 m and is characterized by an overall positive trend up to -27.6‰ at 1.8 m, followed by a sharp drop of –4.2‰ over the next 0.3 m, reaching -31.8‰. The inflection point at 1.8 m marks the onset of the CIE. Interval 2 lies between 2.1–14.8 m, and it starts with a transient rebound followed by a second step of a somewhat less steep drop of –3.2‰, to a value of 32.4‰ at 3.7 m. This interval includes the lithologic change at the termination of spotted marl facies and the onset of black shale sedimentation at 2.65 m. Carbon isotope values remain very negative, reach their minimum at 7.0 m, and show cyclic oscillations of an amplitude of ~2‰ throughout Interval 2. An overall positive trend with continuing oscillations characterizes Interval 3 in the top part of the section. It starts at an inflection point at 14.8 m, marking the recovery phase after the CIE, with a rebound to less negative values of up to –27.8‰. This interval includes the uppermost 1.5 m of the black shale and the overlying spotted marl. The studied part of the section terminates without any flattening of the $\delta^{13}C_{org}$ curve.

Elemental geochemistry and carbonate content

Statistical evaluation of the concentration data (see the Supplementary Data) revealed distinguishable groups of the elements analysed by the XRF method. The first group includes Si, Al, Ti, K, Zr, Rb and, at lower positive coefficients, Th, Mg, and Pb. These elements are commonly carried by detrital aluminosilicate phases in siliciclastic sedimentary rocks. Ca and Sr form the second group, associated with $CaCO_3$ phases. Fe, Mn and Cr comprise the third group at a lower level of significance. Cu, Zn and Mo show moderate positive correlation coefficients and are separated from all other measured elements. The remainder of the elements (S, P, Ba) do not show significant correlation.

In order to evaluate the elemental geochemistry of the studied samples in the framework of dilution of detrital components by $CaCO_3$, organic matter and authigenic minerals, the elemental concentrations are normalized by Al and enrichment factors relative to average shale (Wedepohl, 1991) are calculated. The enrichment factor for any element, hereafter EF(e), is calculated as follows:

$$EF(e) = (C(e)sample/C(Al)sample)/(C(e)shale/C(Al)shale)$$

where C is the concentration.

The Al-normalised EFs of the major elements considerably fluctuate in the samples. Si, Ti, Mg and K are depleted relative to the average shale, whereas Ca shows a moderate overall enrichment with mean EF of 2.78. Fe, Mn and P have positive mean EF values of <2, thus they do not display significant authigenic enrichment (see Supplementary Data).

Large ion radius lithophile elements such as Rb, Sr, Ba and Pb show different distributions regarding their mean EFs. A general depletion in Rb characterizes the entire studied section. Although EF values for Sr, Ba and Pb are generally <2, there are six, two and one samples of these elements, respectively, which yield moderate authigenic enrichments with EF>2. Concentrations and the EFs of the transitional elements (As, Cr, Cu, Mo, Zn) vary widely, remaining under detection limit in numerous samples. However, Mo shows significant enrichment, Cu and Zn show a mean depletion within this group of redox sensitive elements. Mean EF values of As and Cr remain <2 (see Supplementary Data).

The carbonate content was determined by using the molecular weight of calcium carbonate (Ca wt% x 2.5). The distribution of $CaCO_3$ along the section is not showing any remarkable trend either. Although a significant drop to a minimum value of 1.6 wt% can be observed around ~2.2 m and an abrupt peak where the values are increasing to 20 wt% at ~11 m. Nevertheless, a gentle general increase in the carbonate content is apparent upward in the section.

Fourier transform infrared spectroscopy (FTIR)

The characteristic wave numbers of the identified bands of the organic matter appear at 2850 cm^{-1} and 2925 cm^{-1} which represents C-H and C-H2 bonds (Stuart, 2004; Movasaghi et al., 2008). The carbonate molecules have two characteristic peaks in stretching vibration mode (where interaction with infrared radiation induces a change in the bond length among the atoms, and such changes in the dipole of the molecule cause the observed absorption). These are considered the most prominent absorption features, at 1420 cm^{-1} and 876 cm^{-1} (Chester & Elderfield, 1967; Muller et al., 2014). The baseline was automatically corrected in the Opus 7.2 software by rubber band correction with 64 baseline points and two iterations of joining the points of lowest absorbance on a peak (Stuart, 2004). An integration method was set up using peak intensity to a local baseline to measure the organic matter and carbonate variation during the whole section. The organic matter was not observable in the lower part of the section. The stratigraphically lowest sample with calculated peak intensity value occurs at 2.8 m and the highest one is at 17.4 m. The results are presented in the Supplementary Data and in Fig. S2. Apparently, cyclic changes in the spectra occur throughout the section in both the CH and CH2 peaks. The highest intensity values range between 0.0038 and 0.0049 with peaks at 3.7, 5.9, 7.0, 9.2, 11.2 and 15.1 m. The magnitude of oscillation between the highest and lowest values reaches 0.004 over stratigraphic intervals of 0.4–0.8 m. The three carbonate bands appear throughout the entire record but we processed only the 1420 cm^{-1} band which represents the CO_2^{-3} stretching, whereas the other two bands overlapped through the whole section with the Si-O and Al-Al-OH and Al-Mg-OH bands, which are characteristic for common silicate minerals (Madejová & Komadel, 2001).

Cyclostratigraphy and astrochronology

The 2π–MTM power spectrum of the $\delta^{13}C_{org}$ signal shows a peak over 99% confidence level (CL) at 1.60 m, and peaks reaching 95% CL at 0.37 and 0.25 m (Fig. 3). The 2π–MTM power spectrum of the $CaCO_3$ signal shows peaks over 99% CL at 2.13, 0.29 and 0.24 m, a peak reaching 95% CL at 0.39 m, and a peak reaching 90% CL at 1.11 m. The 1.60-m peak in the $\delta^{13}C_{org}$ signal and the 2.13-m peak in the $CaCO_3$ signal have higher spectral power compared to the other cyclicities. The multitaper analyses of the $CH2_{FTIR}$ signal shows peaks over 95% CL at 2.33, 1.60, 0.98, 0.78, 0.44, 0.29, 0.27 and 0.23 m. The more equalized power of the peaks on this latter power spectrum is due to the incomplete data series.

To isolate the prominent cyclicity from the rest of the series band pass-filters were applied. The frequency domains of the filter were set to include the most prominent 1.1 m – 2.3 m cyclicity, present in all three proxy signals, but to exclude the low-power and high-frequency cyclicities. The peaks adjacent to the prominent cyclicity in the low-frequency domain are thought to represent the modulation of the prominent cyclicity caused by the variations in the sedimentation rate and are therefore included in the filters. Of particular interest is Interval 2 that corresponds to the CIE and in which ten key cycles occur in the $\delta^{13}C_{org}$ and the $CaCO_3$ signals in the same phase. Two additional cycles are detected in the preceding Interval 1 and three to four cycles can be counted in Interval 3. In the $CH2_{FTIR}$ signal 7–10 cycles can be distinguished between 3 m and the end of Interval 2 (Fig. 3).

DISCUSSION

Nannoplankton biostratigraphy of the Jenkyns Event

Due to the scarcity of macrofossils and a lack of a detailed ammonoid biostratigraphic study, nannofossils offer good independent support for correlation of the CIE at Réka Valley and other sections. Previously, Baldanza et al. (1995) studied five samples, including two from the lower half of the black shale and three from the underlying beds from this locality. Without providing clear evidence, a correlation of the black shale with the ammonite standard Falciferum Zone was suggested. Two other samples from the black shale were previously studied by E. Mattioli, whose identifications were reported in Varga et al. (2009). Although none of the zonal indices were found, *Carinolithus poulnabronei* from the lower and *Wautzneria fossacincta* and *W. colacicchii* from the upper sample led her to establish the presence of the *C. superbus* and *D. striatus* zones (Mattioli in Varga et al. 2009).

In this study, the base of both the NJ6 and NJ7 zones are more tightly constrained, on the basis of the FO of *C. superbus* and *D. striatus*, respectively. There are only a handful of other sections where the sequence of calcareous nannoplankton bioevents and the onset and termination of both the black shale sedimentation and the CIE can be assessed. At Réka Valley, the base of Zone NJ6 falls within the black shale, thus it follows the onset of the CIE and deposition of organic-rich sediments. This is in contrast with other sections, as the FO of *C. superbus* precedes the start of the Jenkyns Event in Dotternhausen, Yorkshire, Pozzale (Mattioli et al., 2004), Peniche (Mattioli et al., 2008) and the Paris Basin (Mattioli et al., 2008; Boulila et al., 2014). Because the nannoplankton abundance in this part of the Réka Valley section is rather low, and there are few other indices of this zone apart from its primary marker species, the unexpectedly high local FO of *C. superbus* may be due to collection failure. On the other hand, the boundary between zones NJ6 and NJ7 is firmly established by the closely spaced LO of *B. finchii* and the FO of *D. striatus*. This level occurs immediately below the top of the black shale, in the last part of the CIE characterized by rising $\delta^{13}C$ values. This stratigraphic position is equivalent to that observed in Dotternhausen (Mattioli et al., 2008). In Peniche (Mattioli et al., 2008) this zonal boundary was not recorded at the level predicted by the chemostratigraphic correlation, whereas in the Paris Basin (Mattioli et al., 2008; Boulila et al., 2014) it occurs significantly higher than the termination of the CIE. Apparently the rarity of marker bioevents around the Jenkyns Event, exacerbated by a drop in abundance of coccoliths broadly coincident with the onset of CIE as also noted in other sections (Hermoso et al., 2012), may compromise the precision of nannofossil biostratigraphy in this interval.

Several authors discussed the palaeoecological significance of Toarcian calcareous nannoplankton taxa (Baldanza et al., 1995; Mattioli et al., 2004, 2008; Ferreira et al., 2015). The assemblage of the studied section is dominated by *Lotharingius*, thriving under mesotrophic to eutrophic conditions and stratified water masses. Another common genus, *Watznaueria*, is thought to tolerate elevated surface water temperatures. The small size of *Lotharingius* may be a response to the calcification crisis related to the Jenkyns Event (Tremolada et al., 2005), also reflected in the overall low abundance of nannoplankton. The transient peaks of abundance during the CIE could represent of periods of blooms under temporarily ameliorating environmental conditions.

Chemostratigraphical correlation of the Réka Valley section

The $\delta^{13}C$ record of the Jenkyns Event is eminently suitable for stratigraphic correlation for its characteristic pattern replicated through numerous high-resolution studies worldwide (Jenkyns, 2003; Al-Suwaidi et al. 2010; Caruthers et al. 2011; Kemp & Izumi, 2014; Al-Suwaidi et al. 2016). The majority of the data originates from European sections, of which correlation is presented here with Peniche in the Lusitanian Basin (Hesselbo et al., 2007), Yorkshire (Hesselbo et al, 2000; Kemp et al., 2005, 2011), the Sancerre core (Hermoso et al., 2009, 2012) and Lorraine (Ruebsam et al., 2014) in the Paris Basin, the Denkingen core (Suan et al., 2015) near the longer known Dotternhausen section (Röhl et al., 2001) in SW Germany, and the Tethyan sections of Valdorbia in the Appenines (Sabatino et al., 2009) and Sega d'Ala in the Trento Platform of the Southern Alps (Woodfine et al., 2008). The suggested chemostratigraphical correlations are illustrated in Fig. 4. The simple subdivision of Hesselbo et al. (2007) is followed here, because it was developed in the GSSP section for the Toarcian stage at Peniche, it is based on consistently high quality and high resolution data, and it gained wide acceptance (Suan et al., 2008b; Kemp et al., 2011; Huang & Hesselbo, 2014). The three intervals identified in the Réka Valley $\delta^{13}C$ curve are therefore correlative to those separated by distinctive levels labelled 1 to 4 in Hesselbo et al. (2007).

Level 1, the Pliensbachian-Toarcian CIE is not captured in the Réka Valley section which starts higher up. The onset of the CIE associated with the Jenkyns Event is marked by a sharp and large drop in $\delta^{13}C$ values in all sections. The 4.2‰ shift in Réka Valley is among the largest recorded for the initial step in $\delta^{13}C_{org}$ data. Level 2 marks the local minimum reached in this step, and the beginning of Interval 2, i. e. the main negative CIE. At the base of Interval 2, a transient rebound and a second step of a major negative shift is also well correlatable among all sections. In the Réka Valley section, this second step is also well expressed and its magnitude (–3.2‰) is one of the largest recorded anywhere. The same holds true for the next several cycles, as Interval 2 is characterized in nearly all sections by cyclic fluctuations which are decreasing in magnitude upsection. Despite the similarities in this pattern, subtle differences exist in the overall shape of the curve in Interval 2. Réka Valley displays a bowl-shaped curve, with sustained negative values over a considerable stratigraphic distance, resembling those from Peniche, Yorkshire, SW Germany, and Valdorbia. Sancerre and Lorraine from the Paris Basin are characterized by V-shaped curves with a more pronounced, narrow minimum. Records from the shallow marine sections of the Trento Platform differ in their "Aladdin lantern" shape, where a minimum is reached in the lowermost part of Interval 2, followed by a gentle rise in values.

Level 3 is also present in every section. This level is defined by the inflection point heralding the recovery from the CIE, from where a gradually increasing trend in $\delta^{13}C$ values is observed in Interval 3. However, the definition of this level remains ambiguous in certain sections.

Level 4 is marked by termination of the gradual shift to more positive values and a flattening of the $\delta^{13}C$ curve at Peniche and all the other expanded sections. This level is not captured in the data from Réka Valley, where it is predicted to occur higher upsection, in a part not sampled in the present study.

The carbon isotope record of the Jenkyns Event

The remarkable carbon isotope anomaly during the Jenkyns Event is commonly characterized by a broad positive excursion with a sudden interruption by an abrupt, globally observed negative excursion (CIE). The proposed sources of the isotopically light carbon include volcanic degassing of CO_2 during the magmatism of the Karoo-Ferrar large igneous province, thermogenic methane generated through related sill emplacement (McElwain et al., 2005; Svensen et al., 2007), or the dissociation of methane-hydrate from deep-sea sediments driven by concomitant greenhouse warming (Hesselbo et al., 2000; Kemp et al., 2005). The carbon isotope anomaly is preserved in different records, including bulk carbonate, belemnite skeletal carbonate, bulk organic matter and fossil wood (e.g. Hesselbo et al., 2000, 2007; Schouten et al., 2000; Suan et al., 2008a, 2010; Sabatino et al., 2009; Ullmann et al., 2014), suggesting that both the ocean and atmosphere system were affected. However, the magnitude of the CIE differs among the records, with typically larger shifts in bulk $\delta^{13}C_{org}$ (e.g. -7‰ in Sancerre; Hermoso et al., 2012) than in bulk $\delta^{13}C_{carb}$ (e.g. from 3‰ in Peniche; Hesselbo- et al., 2007, to -6‰ in Sancerre, Hermoso et al., 2012). Changes in the contribution of various sources of organic matter, isotopically lighter marine algal OM versus heavier terrestrial plant OM, was suggested to explain the difference (van de Schootbrugge, 2013) and supported by measured changes in the Hydrogen Index (Suan et al., 2015).

In this context, it is instructive to analyse the Réka Valley $\delta^{13}C_{org}$ curve which shows similar features, trends and values to other sections from the European epicontinental seaway. The magnitude of the observed CIE (5.3‰, defined as the difference between the value at the start of the CIE and the most negative value) is not exceptional as it falls within the range of observations from other locations. On the other hand, the magnitude of the first and second step in the negative shift at the beginning of the CIE exceeds that of Yorkshire, which otherwise features one of the largest overall $\delta^{13}C_{carb}$ anomalies of -8‰ (Kemp et al., 2011). The magnitude of the first two negative steps in the CIE observed at Réka Valley is challenging to explain. The Mecsek Basin was located close to the European margin of the Neotethys in the Early Jurassic (Horváth & Galácz, 2006). This palaeogeographic setting may have facilitated local development of upwelling and related CO_2-recycling, which could further affect the isotopic composition of C_{org} (Schouten et al., 2000), beside the global addition of isotopically light carbon from methane-hydrate dissociation and volcanic sources. Regional differences in the δ^{13}Corg records of the Jenkyns Event are more commonly ascribed to changes in the organic matter source and variation in the ratio between terrestrial and marine organic matter (French et al., 2014; Suan et al., 2015). The lack of further, more detailed organic geochemical studies preclude a definitive explanation but existing data favour the speculation of paleoceanographic drivers. Cyclic fluctuations in $\delta^{13}C_{org}$ during the CIE are also well developed in Réka Valley. Our FTIR measurements are useful to quantify and characterize the organic content and its variation throughout the section. One region commonly used for the assessment of organic matter in sedimentary rocks is the methylene group at 2800 cm^{-1} – 3000 cm^{-1} and the vibrational stretching of CH2 at 2850 cm^{-1} and CH stretching at 2923 cm^{-1} (Movasaghi et al., 2008; Pistorius et al., 2009). These two bands occur throughout the section, but their detection was compromised in the lowermost 3 m and at the top of the section in the spotted marl facies, due to the overlap with the OH stretching bands of the clay minerals and other silicates. The two methylene bands show a good correlation (r=0.77) and similar variation throughout the section, arguing against significant changes in organic matter sourcing. The organic matter probably originates from marine algae, as suggested by Rock Eval pyrolysis in a previous study (Varga et al., 2007), but proper identification by FTIR is not possible due to the lack of these bands in the FTIR spectra. However, similar and largely synchronous cyclicity in the CH and CH2 signals (see below) argues against strong variations in the source of organic matter.

Major environmental change affected the plankton communities before and after the Jenkyns Event, but a largely invariable marine algal source for the OM during the CIE is further supported by recent results of Baranyi (2012). Her study of palynomorphs in the Réka Valley section documents a significant change in the dinoflagellate assemblage to an impoverished *Nannoceratopsis*-dominated community, broadly coeval with the initial two steps of the CIE preceding the onset of black shale deposition. This stage was followed by the temporary disappearance of all dinoflagellates, and high abundance of sphaeromorphs, regarded to belong to the opportunistic group of prasinophyte algae, together with a lack of terrestrially derived phytoclasts. This stage is equivalent to the interval of black shale deposition, and is followed by the gradual return of more diverse palynomorph assemblages.

Cyclic fluctuations in the $\delta^{13}C_{org}$ curve in Réka Valley is not restricted to Interval 2, it occurs in Interval 1 and 3 as well. Analogous, similarly persistent orbitally forced fluctuations in $\delta^{13}C_{org}$ are reported from the Hettangian and Lower Sinemurian mudrocks in SW England (Ruhl et al., 2010).

Differences in the shape of the CIE, described in the context of chemostratigraphic correlation above, may have a bearing on the regional differences in development of the Jenkyns Event. The bowl-shaped curve of Réka Valley is similar to other sections in the European epicontinental seaway, explained by their palaeogeographic position (Fig. 1). However, the protracted CIE without a start of rebound is more clearly expressed here than in other sections. This feature is useful for model-data comparisons, as modelling studies attempt to simulate the cause and effect of the carbon cycle perturbation (Beerling & Brentnall, 2007).

Duration of the Jenkyns Event

The duration of the Jenkyns Event is still debated despite the plethora of published studies on Toarcian localities. Short eccentricity, obliquity as well as precession were all proposed by various authors as the dominant factor driving the cyclic changes. The new data from Réka Valley are used here to provide astrochronological estimates for the duration of the CIE, understood in the narrow sense to be represented by Interval 2 in Fig. 4, and our new results are discussed in the context of previously published studies.

One of the first cyclostratigraphic studies on the Jenkyns Event was based on $CaCO_3$ and $\delta^{13}C_{org}$ signals measured in the Yorkshire section (Kemp et al., 2005). The authors identified precession as the dominant astronomical forcing parameter, considering radiometrically dated correlative sections and the likely dominant astronomical forcing parameter at the palaeolatitude of deposition. Suan et al. (2008b) proposed a ~550 kyr duration for the main negative excursion, corresponding to Interval 2 in Réka Valley, based on $CaCO_3$ measurements from Peniche and grayscale signal from Dotternhausen, and assigned the dominant forcing to short eccentricity. Sabatino et al. (2009) analysed $CaCO_3$ and $\delta^{13}C_{org}$ signals from Valdorbia and the Monte Mangart section in the Julian Alps (Italy/Slovenia) and assigned a ~500 kyr duration for the negative CIE suggesting short eccentricity forcing. Kemp et al. (2011) revised the cyclostratigraphy of the Yorkshire section by making new, high-resolution $\delta^{13}C_{org}$, $CaCO_3$, and sulphur concentration measurements, and proposed two possible durations for the negative excursion assuming precession or obliquity as the key driver of the cyclic changes: the minimum duration of the excursion based on 21 kyr precession cycles is calculated as 168–189 kyr, whereas the maximum duration for the same interval, based on 36 kyr obliquity forcing, is 288–324 kyr. Boulila et al. (2014) studied the ~165 m long section of the Sancerre core from the Paris Basin. They made high-resolution magnetic susceptibility measurements, in which signal they identified long and short eccentricity, obliquity, precession and sub-Milankovitch cyclicities. For the CIE they estimated a duration of ~300 kyr, while suggesting obliquity as the dominant forcing factor. Huang & Hesselbo (2014) provided new cyclostratigraphic constraints for the Peniche, Yorkshire, Dotternhausen, and the Valdorbia sections. Based on the bulk rock $\delta^{13}C_{carb}$ signal from Peniche, which is considered to be the most complete section, they suggest a 620 kyr duration for the negative excursion. They argue that the prominent cyclicity revealed by the previous studies is, in fact, the short eccentricity signal. They also suggest that the main forcing parameter behind the climate change shifted from precession-eccentricity before the CIE to obliquity during the CIE, and then back to precession-eccentricity. Ruebsam et al. (2014) presented magnetic susceptibility measurements from Lorraine in the Paris Basin, from which a ~600 kyr duration for the CIE was proposed. Apart from the cyclostratigraphic estimates, independent age constraints based on belemnite $^{87}Sr/^{86}Sr$ stratigraphy in Yorkshire provide an approximate duration of ~560 kyr for the CIE of the Jenkyns Event (i.e. equivalent of Interval 2) (McArthur et al., 2000).

In the Réka Valley section a key ~2 m cyclicity is present in the $\delta^{13}C_{org}$ and the $CaCO_3$ signals, while the $CH2_{FTIR}$ signal records a cyclicity of comparable frequency. Unambiguous identification of the specific orbital components is not possible based on the available data, therefore we propose three possible durations for the CIE based on short eccentricity, obliquity, or precession forcing. Ten prominent cycles are counted in the part of the analysed signals that match the correlative interval of the CIE related to the Jenkyns Event. The best estimate for the duration of the negative excursion at Réka Valley, based on precession, obliquity and short eccentricity, is therefore 200 kyr, 350 kyr, and 1 Myr, respectively.

The cyclicity observed in the carbon isotope records of several European sections are interpreted to reflect orbitally controlled short pulses of methane-hydrate dissociation events (Sabatino et al. 2009; Kemp et al. 2011; Huang & Hesselbo, 2014). Similarities between the Réka Valley and other European section's carbon isotope record suggest that the same phenomenon exerted a major control on the carbon isotope record in the Réka Valley. In addition, both the $\delta^{13}C_{org}$ and the $CaCO_3$ signals are also thought to reflect fluctuations in the productivity of marine organisms, as their main cyclicity is in the same phase.

Palaeoenvironmental interpretation from elemental geochemistry

The conspicuous grouping of elements by their abundance in the samples, the variability in major element concentrations, and enrichment factors relative to the average shale suggest that the black shale is best regarded as a mixture of two endmembers, terrigenous aluminosilicates and marine carbonates (Fig. 5A-B). Despite the rather monotonous lithology, a wide range of compositional fluctuations are depicted in the Al-Si-Ca and Al-K-Ca ternary systems. This observation suggests that the significant changes in chemical composition are controlled primarily by a dilution effect. In addition, the scatter and position of the data points show that the terrigenous component of the studied samples can be characterised as Al-enriched shale.

Consequently, the terrigenous compositional endmember of the studied black shales consists of a mixture of an illitic/smectitic and a kaolinitic clay with an enhanced role of the kaolinite, a clay mineral which contains stochiometrically only Si^{4+} and Al^{3+} in its layer silicate structure, contrary to illite and smectite which contain other cations as well (Weaver, 1989; Moore & Reynolds, 1997). Previous clay mineral studies documented that the Réka Valley black shale has high kaolinite content suggesting elevated weathering rates in the hinterland during deposition (Raucsik & Merényi, 2000; Raucsik & Varga, 2008). The Early Toarcian global warming and a resultant acceleration of the hydrological cycle delivered nutrients and freshwater to shelf seas worldwide by enhanced weathering and runoff (Bailey et al., 2003; Jenkyns, 2003; Cohen at al., 2004). A high proportion of kaolinite occurs in Lower Toarcian strata in the Peritethyan areas of the European epicontinental seaway (Dera et al., 2009), in the Lombardian Basin of the Southern Alps (Deconinck & Bernoulli, 1991), in the hemipelagic Lusitanian Basin (Duarte, 1998) and the Polish Basin (Brański, 2010), suggesting increased humidity and intense weathering in the continental hinterland during the Jenkyns Event. The observed shift in the trend of data points can be caused by a kaolinite-rich terrigenous load relative to the average shale, therefore our present geochemical data support the scenario of increased continental hydrolysis during the Jenkyns Event in the hinterland of the Mecsek Basin.

According to Plank & Langmuir (1998), geochemical variations in elemental composition, including the abundance of some alkaline metals (K, Rb, Cs), are linked to changes in the lithological composition, as their ratios in sediments are controlled by continental input and can be characterized using the K_2O/Rb ratio. In marine sediments, the alkaline elements are mainly hosted in terrigenous minerals and their distributions are predominantly controlled by dilution of biogenic material. Low K_2O/Rb ratios are characteristic features of highly weathered and recycled sources because Rb (together with Cs) tends to be less mobile during the hydrolysis than K (Nesbitt et al. 1980; Tanaka & Watanabe, 2015). High K_2O/Rb ratios are typical of sediments rich in rock fragments derived from acidic volcanics or volcaniclastics and of sediments that have suffered K metasomatism (Plank & Langmuir, 1998). The studied samples are sharply divided into two populations, one of which shows high Rb content relative to the overall trend with K_2O/Rb ratio typical of siliciclastics derived from the upper continental crustal rocks (Fig. 6). Samples falling in this field likely represent intervals of extremely enhanced continental weathering. The stratigraphic distribution of these samples shows that more than half of them cluster in the lower part of the section between 2.4 m and 5.5 m, in the lower part (i. e. first two cycles) in Interval 2, suggesting that weathering was most intense at the beginning of the CIE. A similar timing of peak weathering is suggested by a Ca isotope anomaly in the Peniche section (Brazier et al., 2015).

CONCLUSIONS

Deposition of a 12 m thick black shale unit in the Lower Toarcian section of Réka Valley has been previously associated with anoxic conditions during the Jenkyns Event, but results from a high-resolution sampling are reported here for the first time. The new data from the Mecsek basin, located east of other well-studied sites in the Early Jurassic European epicontinental seaway, adds to our understanding of overall similarities and subtle regional differences of the sedimentary and geochemical record of the Jenkyns Event. Nannoplankton biostratigraphy allow recognition of Lower Jurassic zones NJ5b, NJ6 and NJ7 and permit correlation with several classical sections. The obtained $\delta^{13}C_{org}$ curve is subdivided into three intervals, which are readily correlatable with those established at Peniche (Hesselbo et al., 2007) and recognized in all other high-resolution datasets. The bowl-shaped main negative CIE has a magnitude of -5.3‰ locally, and the first two steps are essential in its development, with drops of -4.2‰ and -3.2‰, respectively. The onset of black shale deposition follows the second carbon isotope step, after which $\delta^{13}C$ values remain very negative but are cyclically fluctuating. The recovery interval of the CIE with rising but still fluctuating values precedes the termination of black shale deposition. FTIR analyses suggest that only the amount but not the main source of the organic matter changed cyclically during the CIE. The $\delta^{13}C$ and FTIR data, together with elemental abundances (primarily Ca and Ti) measured by the XRF method, are the basis for cyclostratigraphy. Interval 2 of the main negative CIE is shown to comprise 10 cycles. Assuming these to represent a Milankovitch cyclicity, new astrochronologic estimates can be made for the duration of the CIE as 200 kyr, 350 kyr or 1.0 Myr, based on precession, obliquity, or short eccentricity forcing, respectively. These values are within the range of previously proposed durations. Enhanced weathering in the hinterland is supported by the elemental analyses, indicative of kaolinite dominance in the terrigenous clay fraction. The most intense period of weathering is recorded in the lower part of the section, below and at the onset of black shale sedimentation. The expanded stratigraphic record of the Jenkyns Event in black shale facies in the Réka Valley holds promise for subsequent more diverse studies.

ACKNOWLEDGEMENTS

We are grateful for the inspiration of Hugh Jenkyns for research on the T-OAE in Hungary and for the insights of Helmut Weissert during a field trip to Réka Valley. Thanks are due to the organizers of the 2015 Monte Verità “Climates of the past –

lessons for the future" workshop in honour of Hugh and Helmut, and the editors of this special volume for the opportunity to present and discuss this research. We are grateful to Mathieu Martinez who provided the Matlab codes for running the spectral analyses. Zs. Dallos, M. Temes, D. Komlósi and G. Cári helped during the field work. The constructive reviews by D. Kemp, M. Ruhl and an anonymous reviewer, and the helpful criticism of thematic issue editor S. Hesselbo greatly improved the manuscript. Research permit for the study site was granted by the Southern Transdanubian Environmental and Nature Protection Office. Financial support for student research from MOL Plc. is acknowledged. This is MTA-MTM-ELTE Paleo contribution No. 229.

REFERENCES

Al-Suwaidi, A.H., Angelozzi, G.N., Baudin, F., Damborenea, S.E., Hesselbo, S.P., Jenkyns, H.C., Mancenido, M.O. and Riccardi, A.C. (2010) First record of the Early Toarcian Oceanic Anoxic Event from the Southern Hemisphere, Neuquen Basin, Argentina. *Journal of the Geological Society*, **167,** 633-636.

Al-Suwaidi, A.H., Hesselbo, S.P., Damborenea, S.E., Manceñido, M.O., Jenkyns, H.C., Riccardi, A.C., Angelozzi, G.N. and Baudin, F. (2016) The Toarcian Oceanic Anoxic Event (Early Jurassic) in the Neuquén Basin, Argentina: A Reassessment of Age and Carbon Isotope Stratigraphy. *The Journal of Geology*, **124,** 171-193.

Bailey, T.R., Rosenthal, Y., McArthur, J.M., van de Schootbrugge, B. and Thirlwall, M.F. (2003) Paleoceanographic changes of the Late Pliensbachian-Early Toarcian interval: a possible link to the genesis of an Oceanic Anoxic Event. *Earth and Planetary Science Letters*, **212,** 307-320.

Baldanza, A., Bucefalo Palliani, R. and Mattioli, E. (1995) Lower Jurassic calcareous nannofossils and dinoflagellate cysts of Hungary and their comparison with assemblages from Central Italy. *Paleopelagos*, **5,** 161-174.

Baranyi, V. (2012) *A Réka-völgyi felső-pliensbachi–alsó-toarci szelvény palinológiai vizsgálata: a kora-toarci óceáni anoxikus esemény hatása a szerves vázú mikroplankton közösségekre (Palynological investigation of the Upper Pliensbachian–Lower Toarcian Réka Valley section: the impact of the Early Toarcian Oceanic Anoxic Event (ETOAE) on microplankton assemblages)*. MSc thesis, Eötvös Loránd University, Budapest, 130 pp.

Bassoulet, J.P., Elmi, S., Poisson, A., Cecca, F., Bellion, Y., Guiraud, R. and Baudin, F. (1993) Mid Toarcian. In: *Atlas Tethys Paleoenvironmental Maps* (Eds J. Dercourt, L.E. Ricou and B. Vrielynck), pp. 63-80. Beicip-Franlab, Rueil-Malmaison, France.

Beerling, D.J. and Brentnall, S.J. (2007) Numerical evaluation of mechanism driving Early Jurassic changes in global carbon cycling. *Geology*, **35,** 247-250.

Boulila, S., Galbrun, B., Huret, E., Hinnov, L.A., Rouget, I., Gardin, S. and Bartolini, A. (2014) Astronomical calibration of the Toarcian Stage: implications for sequence stratigraphy and duration of the early Toarcian OAE. *Earth and Planetary Science Letters*, **386,** 98-111.

Bown, P. (1998) *Calcareous nannofossil biostratigraphy*. Springer Science+Business Media, New York.

Brański, P. (2010) Kaolinite peaks in early Toarcian profiles from the Polish Basin - an inferred record of global warming. *Geological Quarterly*, **54,** 15-24.

Brazier, J.M., Suan, G., Tacail, T., Simon, L., Martin, J.E., Mattioli, E. and Baiter, V. (2015) Calcium isotope evidence for dramatic increase of continental weathering during the Toarcian oceanic anoxic event (Early Jurassic). *Earth and Planetary Science Letters*, **411,** 164-176.

Bruno, T.J. (1999) Sampling Accessories for Infrared Spectrometry. *Applied Spectroscopy Reviews*, **34,** 91-120.

Caruthers, A.H., Gröcke, D.R. and Smith, P.L. (2011) The significance of an Early Jurassic (Toarcian) carbon-isotope excursion in Haida Gwaii (Queen Charlotte Islands), British Columbia, Canada. *Earth and Planetary Science Letters*, **307,** 19-26.

Chester, R. and Elderfield, H. (1967) The application of infra-red absorption spectroscopy to carbonate mineralogy. *Sedimentology*, **9,** 5-21.

Cohen, A.S., Coe, A.L., Harding, S.M. and Schwark, L. (2004) Osmium isotope evidence for the regulation of atmospheric CO_2 by continental weathering. *Geology*, **32,** 157-160.

Cooley, J.W. and Tukey, J.W. (1965) An algorithm for the machine calculation of complex Fourier series. *Mathematics of Computation*, **19,** 297-301.

Csontos, L., Benkovics, L., Bergerat, F., Mansy, J.-L. and Wórum, G. (2002) Tertiary deformation history from seismic section study and fault analysis in a former European Tethyan margin (the Mecsek–Villány area, SW Hungary). *Tectonophysics*, **357,** 81-102.

Csontos, L. and Vörös, A. (2004) Mesozoic plate tectonic reconstruction of the Carpathian region. *Palaeogeography Palaeoclimatology Palaeoecology*, **210,** 1-56.

Deconinck, J.F. and Bernoulli, D. (1991) Clay mineral assemblages of Mesozoic pelagic and flysch sediments of the Lombardian Basin (Southern Alps): implications for palaeotectonics, palaeoclimate and diagenesis. *Geologische Rundschau*, **80,** 1-17.

Dera, G., Pellenard, P., Neige, P., Deconinck, J.F., Puceat, E. and Dommergues, J.L. (2009) Distribution of clay minerals in Early Jurassic Peritethyan seas: Palaeoclimatic significance inferred from multiproxy comparisons. *Palaeogeography Palaeoclimatology Palaeoecology*, **271,** 39-51.

Di Leo, P., Dinelli, E., Mongelli, G. and Schiattarella, M. (2002) Geology and geochemistry of Jurassic pelagic sediments, Scisti silicei Formation, southern Apennines, Italy. *Sedimentary Geology*, **150,** 229-246.

Duarte, L.V. (1998) Clay minerals and geochemical evolution in the Toarcian-lower Aalenian of the Lusitanian basin (Portugal). *Cuadernos de Geología Ibérica*, **24,** 69-98.

Dulai, A., Suba, Z. and Szarka, A. (1992) Toarci (alsójura) szervesanyagdús fekete pala a mecseki Réka-völgyben (Toarcian (Lower Jurassic) organic-rich black shale in the Réka Valley (Mecsek Hills, Hungary)). *Földtani Közlöny*, **122,** 67-87.

Erba, E., Bartolini, A. and Larson, R.L. (2004) Valanginian Weissert oceanic anoxic event. *Geology*, **32,** 149-152.

Farmer, V.C. (1974) *The Infrared Spectra of Minerals*. Mineralogical Society of Great Britain and Ireland, 536 pp.

Ferreira, J., Mattioli, E., Pittet, B., Cachão, M. and Spangenberg, J.E. (2015) Palaeoecological insights on Toarcian and lower Aalenian calcareous nannofossils from the Lusitanian Basin (Portugal). *Palaeogeography, Palaeoclimatology, Palaeoecology*, **436,** 245-262.

Főzy, I. (Ed),2012) *Magyarország litosztratigráfiai alapegységei. Jura [Lithostratigraphic Units of Hungary. Jurassic]*. Hungarian Geological Society, Budapest, 235 pp.

French, K. L., Sepulveda, J., Trabucho-Alexandre, J., Gröcke, D. R., & Summons, R. E. (2014). Organic geochemistry of the early Toarcian oceanic anoxic event in Hawsker Bottoms, Yorkshire, England. *Earth and Planetary Science Letters*, **390,** 116-127.

Galácz, A. (1991) *Palaeontological investigation of the Toarcian black shale in the Mecsek Mts. – Unpublished Manuscript*. Department of Palaeontology, Eötvös Loránd University, Budapest, 32 pp.

Gill, B.C., Lyons, T.W. and Jenkyns, H.C. (2011) A global perturbation to the sulfur cycle during the Toarcian Oceanic Anoxic Event. *Earth and Planetary Science Letters*, **312,** 484-496.

Griffiths, P. (1983) Fourier transform infrared spectrometry. *Science*, **222,** 297-302.

Gröcke, D.R., Hori, R.S., Trabucho-Alexandre, J., Kemp, D.B. and Schwark, L. (2011) An open ocean record of the Toarcian oceanic anoxic event. *Solid Earth*, **2,** 245-257.

Haas, J. and Péró, C. (2004) Mesozoic evolution of the Tisza Mega-unit. *International Journal of Earth Sciences*, **93,** 297-313.

Hallam, A. (1967) An Environmental Study of the Upper Domerian and Lower Toarcian in Great Britain. *Philosophical Transactions of the Royal Society B: Biological Sciences*, **252,** 393-445.

Hermoso, M., Minoletti, F., Le Callonnec, L., Jenkyns, H.C., Hesselbo, S.P., Rickaby, R.E.M., Renard, M., de Rafelis, M. and Emmanuel, L. (2009) Global and local forcing of Early Toarcian seawater chemistry: A comparative study of different paleoceanographic settings (Paris and Lusitanian basins). *Paleoceanography*, **24**.

Hermoso, M., Minoletti, F., Rickaby, R.E.M., Hesselbo, S.P., Baudin, F. and Jenkyns, H.C. (2012) Dynamics of a stepped carbon-isotope excursion: Ultra high-resolution study of Early Toarcian environmental change. *Earth and Planetary Science Letters*, **319-320,** 45-54.

Hesselbo, S.P., Gröcke, D.R., Jenkyns, H.C., Bjerrum, C.J., Farrimond, P., Morgans Bell, H.S. and Green, O.R. (2000) Massive dissociation of gas hydrate during a Jurassic oceanic anoxic event. *Nature*, **406,** 392-395.

Hesselbo, S.P., Jenkyns, H.C., Duarte, L.V. and Oliveira, L.C.V. (2007) Carbon-isotope record of the Early Jurassic (Toarcian) Oceanic Anoxic Event from fossil wood and marine carbonate (Lusitanian Basin, Portugal). *Earth and Planetary Science Letters*, **253,** 455-470.

Horváth, F. and Galácz, A. (2006) *The Carpathian-Pannonian Region. A Review of Mesozoic-Cenozoic Stratigraphy and Tectonics*. Hantken Press, Budapest, 624 pp.

Huang, C. and Hesselbo, S.P. (2014) Pacing of the Toarcian Oceanic Anoxic Event (Early Jurassic) from astronomical correlation of marine sections. *Gondwana Research*, **25,** 1348-1356.

Hutcheon, I., Bloch, J., De Caritat, P., Shevalier, M., Abercombie, H. and Longstaffe, F. (1998) What is the cause of potassium enrichment in shales? In: *Shales and Mudstones* (Eds J. Schieber, W. Zimmerle and P.S. Sethi), pp. 107-128. Schweizerbart'sche Verlagbuchhandlung, Stuttgart, Germany.

Izumi, K., Miyaji, T. and Tanabe, K. (2012) Early Toarcian (Early Jurassic) oceanic anoxic event recorded in the shelf deposits in the northwestern Panthalassa: Evidence from the Nishinakayama Formation in the Toyora area, west Japan. *Palaeogeography Palaeoclimatology Palaeoecology*, **315,** 100-108.

Jenkyns, H.C. (1985) The Early Toarcian and Cenomanian-Turonian anoxic events in Europe: comparisons and contrasts. *Geologische Rundschau*, **74,** 505-518.

Jenkyns, H.C. (1988) The early Toarcian (Jurassic) anoxic event: Stratigraphic, sedimentary, and geochemical evidence. *American Journal of Science*, **288,** 101-151.

Jenkyns, H.C. (2003) Evidence for rapid climate change in the Mesozoic{Palaeogene greenhouse world. *Philosophical Transactions of the Royal Society of London A.*, **361,** 1885-1916.

Jenkyns, H.C. (2010) Geochemistry of oceanic anoxic events. *Geochemistry Geophysics Geosystems*, **11,** 1-30.

Jenkyns, H.C. and Clayton, C.J. (1986) Black Shales and Carbon Isotopes in Pelagic Sediments from the Tethyan Lower Jurassic. *Sedimentology*, **33,** 87-106.

Jenkyns, H.C. and Clayton, C.J. (1997) Lower Jurassic epicontinental carbonates and mudstones from England and Wales: chemostratigraphic signals and the early Toarcian anoxic event. *Sedimentology*, **44,** 687-706.

Jenkyns, H.C., Géczy, B. and Marshall, J.D. (1991) Jurassic manganese carbonates of Central Europe and the Early Toarcian anoxic event. *Journal of Geology*, **99,** 137-149.

Jenkyns, H.C., Gröcke, D.R. and Hesselbo, S.P. (2001) Nitrogen isotope evidence for water mass denitrification during the early Toarcian (Jurassic) oceanic anoxic event. *Paleoceanography*, **16,** 593-603.

Jenkyns, H.C., Jones, C.E., Gröcke, D.R., Hesselbo, S.P. and Parkinson, D.N. (2002) Chemostratigraphy of the Jurassic System: applications, limitations and implications for palaeoceanography. *Journal of the Geological Society*, **159,** 351-378.

Jones, C.E., Jenkyns, H.C., Coe, A.L. and Hesselbo, S.P. (1994) Strontium Isotopic Variations in Jurassic and Cretaceous Seawater. *Geochimica et Cosmochimica Acta*, **58,** 3061-3074.

Kafousia, N., Karakitsios, V., Jenkyns, H.C. and Mattioli, E. (2011) A global event with a regional character: the Early Toarcian Oceanic Anoxic Event in the Pindos Ocean (northern Peloponnese, Greece). *Geological Magazine*, **148,** 619-631.

Kemp, D.B., Coe, A.L., Cohen, A.S. and Schwark, L. (2005) Astronomical pacing of methane release in the Early Jurassic period. *Nature*, **437,** 396-399.

Kemp, D.B., Coe, A.L., Cohen, A.S. and Weedon, G.P. (2011) Astronomical forcing and chronology of the early Toarcian (Early Jurassic) oceanic anoxic event in Yorkshire, UK. *Paleoceanography*, **26,** 1-17.

Kemp, D.B. and Izumi, K. (2014) Multiproxy geochemical analysis of a Panthalassic margin record of the early Toarcian oceanic anoxic event (Toyora area, Japan). *Palaeogeography Palaeoclimatology Palaeoecology*, **414,** 332-341.

Küspert, W. (1982) Environmental changes during oil shale deposition as deduced from stable isotope ratios. In: *Cyclic and Event Stratification* (Eds G. Einsele and A. Seilacher), pp. 482-501. Springer, Berlin.

Laskar, J., Robutel, P., Joutel, F., Gastineau, M., Correia, A.C.M. and Levrard, B. (2004) A long-term numerical solution for the insolation quantities of the Earth. *Astronomy & Astrophysics*, **428,** 261-285.

Madejova, J. and Komadel, P. (2001) Baseline studies of the clay minerals society source clays: infrared methods. *Clays and Clay Minerals*, **49,** 410-432.

Mann, M.E. and Lees, J.M. (1996) Robust estimation of background noise and signal detection in climatic time series. *Climatic Change*, **33,** 409-445.

Mattioli, E., Pittet, B., Palliani, R.B., Rohl, H.J., Schmid-Rohl, A. and Morettini, E. (2004) Phytoplankton evidence for the timing and correlation of palaeoceanographical changes during the early Toarcian oceanic anoxic event (Early Jurassic). *Journal of the Geological Society*, **161,** 685-693.

Mattioli, E., Pittet, B., Suan, G. and Mailliot, S. (2008) Calcareous nannoplankton changes across the early Toarcian oceanic anoxic event in the western Tethys. *Paleoceanography*, **23**.

McArthur, J.M., Donovan, D.T., Thirlwall, M.F., Fouke, B.W. and Mattey, D. (2000) Strontium isotope profile of the Early Toarcian (Jurassic) Oceanic Anoxic Event, the duration of ammonite biozones, and belemnite paleotemperatures. *Earth and Planetary Science Letters*, **179,** 269-285.

McElwain, J.C., Wade-Murphy, J. and Hesselbo, S.P. (2005) Changes in carbon dioxide during an oceanic anoxic event linked to intrusion into Gondwana coals. *Nature*, **435,** 479-482.

Meyers, S. R. (2014) Astrochron: An R Package for Astrochronology (0.6). (http://cran.r-project.org/package=astrochron)

Moore, D.M. and Reynolds, R.C. (1997) *X-Ray Diffraction and the Identification and Analysis of Clay Minerals*. Oxford University Press, Oxford, 378 pp.

Movasaghi, Z., Rehman, S. and ur Rehman, I. (2008) Fourier Transform Infrared (FTIR) Spectroscopy of Biological Tissues. *Applied Spectroscopy Reviews*, **43,** 134-179.

Müller, C.M., Pejcic, B., Esteban, L., Delle Piane, C., Raven, M. and Mizaikoff, B. (2014) Infrared attenuated total reflectance spectroscopy: an innovative strategy for analyzing mineral components in energy relevant systems. *Scientific Reports*, **4,** 6764.

Nesbitt, H.W., Markovics, G. and Price, R.C. (1980) Chemical processes affecting alkalis and alkaline earths during continental weathering. *Geochimica et Cosmochimica Acta*, **44,** 1659-1666.

Pálfy, J. and Smith, P.L. (2000) Synchrony between Early Jurassic extinction, oceanic anoxic event, and the Karoo-Ferrar flood basalt volcanism. *Geology*, **28,** 747-750.

Pistorius, A.M.A., DeGrip, W.J. and Egorova-Zachernyuk, T.A. (2009) Monitoring of biomass composition from microbiological sources by means of FT-IR spectroscopy. *Biotechnology and Bioengineering*, **103,** 123-129.

Plank, T. and Langmuir, C.H. (1998) The chemical composition of subducting sediment and its consequences for the crust and mantle. *Chemical Geology*, **145,** 325-394.

Rachold, V. and Brumsack, H.J. (2001) Inorganic geochemistry of Albian sediments from the Lower Saxony Basin NW Germany: palaeoenvironmental constraints and orbital cycles. *Palaeogeography Palaeoclimatology Palaeoecology*, **174,** 121-143.

Raucsik, B. and Merényi, L. (2000) Origin and environmental significance of clay minerals in the Lower Jurassic formations of the Mecsek Mts, Hungary. *Acta Geologica Hungarica*, **43,** 405-429.

Raucsik, B. and Varga, A. (2008) Climato-environmental controls on clay mineralogy of the Hettangian-Bajocian successions of the Mecsek Mountains, Hungary: An evidence for extreme continental weathering during the early Toarcian oceanic anoxic event. *Palaeogeography Palaeoclimatology Palaeoecology*, **265,** 1-13.

Röhl, H.-J., Schmid-Röhl, A., Oschmann, W., Frimmel, A. and Schwark, L. (2001) The Posidonia Shale (Lower Toarcian) of SW-Germany: an oxygen-depleted ecosystem controlled by sea level and palaeoclimate. *Palaeogeography, Palaeoclimatology, Palaeoecology*, **165,** 27-52.

Ruebsam, W., Münzberger, P. and Schwark, L. (2014) Chronology of the Early Toarcian environmental crisis in the Lorraine Sub-Basin (NE Paris Basin). *Earth and Planetary Science Letters*, **404,** 273-282.

Ruhl, M., Deenen, M.H.L., Abels, H.A., Bonis, N.R., Krijgsman, W. and Kürschner, W.M. (2010) Astronomical constraints on the duration of the early Jurassic Hettangian stage and recovery rates following the end-Triassic mass extinction (St Audrie's Bay/East Quantoxhead, UK). *Earth and Planetary Science Letters*, **295,** 262-276.

Sabatino, N., Neri, R., Bellanca, A., Jenkyns, H.C., Baudin, F., Parisi, G. and Masetti, D. (2009) Carbon-isotope records of the Early Jurassic (Toarcian) oceanic anoxic event from the Valdorbia (Umbria-Marche Apennines) and Monte Mangart (Julian Alps) sections: palaeoceanographic and stratigraphic implications. *Sedimentology*, **56,** 1307-1328.

Schlanger, S.O. and Jenkyns, H.C. (1976) Cretaceous Oceanic Anoxic Events: Causes and Consequences. *Geologie en Mijnbouw*, **55,** 179-184.

Schmid-Rohl, A., Rohl, H.J., Oschmann, W., Frimmel, A. and Schwark, L. (2002) Palaeoenvironmental reconstruction of Lower Toarcian epicontinental black shales (Posidonia Shale, SW Germany): global versus regional control. *Geobios*, **35,** 13-20.

Schouten, S., Van Kaam-Peters, H.M.E., Rijpstra, W.I.C., Schoell, M. and Damste, J.S.S. (2000) Effects of an oceanic anoxic event on the stable carbon isotopic composition of Early Toarcian carbon. *American Journal of Science*, **300,** 1-22.

Stuart, B. (2004) *Infrared Spectroscopy: Fundamentals and Applications*. Wiley, 244 pp.

Suan, G., Mattioli, E., Pittet, B., Lecuyer, C., Sucheras-Marx, B., Duarte, L.V., Philippe, M., Reggiani, L. and Martineau, F. (2010) Secular environmental precursors to Early Toarcian (Jurassic) extreme climate changes. *Earth and Planetary Science Letters*, **290,** 448-458.

Suan, G., Mattioli, E., Pittet, B., Mailliot, S. and Lecuyer, C. (2008a) Evidence for major environmental perturbation prior to and during the Toarcian (Early Jurassic) oceanic anoxic event from the Lusitanian Basin, Portugal. *Paleoceanography*, **23,** 1-14.

Suan, G., Pittet, B., Bour, I., Mattioli, E., Duarte, L.V. and Mailliot, S. (2008b) Duration of the Early Toarcian carbon isotope excursion deduced from spectral analysis: Consequence for its possible causes. *Earth and Planetary Science Letters*, **267,** 666-679.

Suan, G., van de Schootbrugge, B., Adatte, T., Fiebig, J. and Oschmann, W. (2015) Calibrating the magnitude of the Toarcian carbon cycle perturbation. *Paleoceanography*, **30,** 495-509.

Svensen, H., Planke, S., Chevallier, L., Malthe-Sorenssen, A., Corfu, F. and Jamtveit, B. (2007) Hydrothermal venting of greenhouse gases triggering Early Jurassic global warming. *Earth and Planetary Science Letters*, **256,** 554-566.

Tanaka, K. and Watanabe, N. (2015) Size distribution of alkali elements in riverbed sediment and its relevance to fractionation of alkali elements during chemical weathering. *Chemical Geology*, **411,** 12-18.

Taner, M.T. (2003) Attributes Revisited. Rock Solid Images, Houston, Texas http://www.rocksolidimages.com/attributes-revisited

Thomson, D.J. (1982) Spectrum Estimation and Harmonic Analysis. *Proceedings of the IEEE*, **70,** 1055-1096.

Trecalli, A., Spangenberg, J., Adatte, T., Follmi, K.B. and Parente, M. (2012) Carbonate platform evidence of ocean acidification at the onset of the early Toarcian oceanic anoxic event. *Earth and Planetary Science Letters*, **357,** 214-225.

Tremolada, F., Van de Schootbrugge, B. and Erba, E. (2005) Early Jurassic schizosphaerellid crisis in Cantabria, Spain: Implications for calcification rates and phytoplankton evolution across the Toarcian oceanic anoxic event. *Paleoceanography*, **20,** 1-11.

Tukey, J.W. (1977) *Exploratory Data Analysis*. Addison-Wesley Publishing Company, 688 pp.

Ullmann, C.V., Thibault, N., Ruhl, M., Hesselbo, S.P. and Korte, C. (2014) Effect of a Jurassic oceanic anoxic event on belemnite ecology and evolution. *Proceedings of the National Academy of Sciences*, **111,** 1-4.

van de Schootbrugge, B., Bachan, A., Suan, G., Richoz, S. and Payne, J.L. (2013) Microbes, mud and methane: cause and consequence of recurrent Early Jurassic anoxia following the end-Triassic mass extinction. *Palaeontology*, **56,** 685-709.

Varga, A., Mikes, T. and Raucsik, B. (2009) A mecseki toarci feketepala Réka-völgyi szelvényének előzetes petrográfiai és nehézásvány-vizsgálati eredményei (The petrography and heavy minerals of the Toarcian black shale of the Réka Valley section of the Mecsek Hills: a pilot study). *Földtani Közlöny*, **139,** 33-54.

Varga, A., Raucsik, B., Hámoriné Vidó, M. and Rostási, Á. (2007) Az Óbányai Aleurolit Formáció fekete palájának izotóp- geokémiai és szénhidrogén-genetikai jellemzése (Isotope geochemistry and characterization of hydrocarbon potential of black shale from Óbánya Siltstone Formation). *Földtani Közlöny*, **137,** 449-472.

Weaver, C.E. (1989) *Clays, Muds, and Shales*. Elsevier, Amsterdam, Oxford, New York, Tokyo, 819 pp.

Wedepohl, K.H. (1991) Chemical composition and fractionation of the continental crust. *Geologische Rundschau*, **80,** 207-223.

Woodfine, R.G., Jenkyns, H.C., Sarti, M., Baroncini, F. and Violante, C. (2008) The response of two Tethyan carbonate platforms to the early Toarcian (Jurassic) oceanic anoxic event: environmental change and differential subsidence. *Sedimentology*, **55,** 1011-1028.

FIGURE CAPTIONS

Fig. 1. (A) Location of the Réka Valley section (orange star) in southern Hungary. (B) Global palaeogeographic setting of the western Tethys (boxed area enlarged in (C)) during the Early Jurassic (after Woodfine et al., 2008). (C) Early Jurassic palaeogeographic configuration of the western Tethys (after Bassoulet et al. 1993 and Mattioli et al. 2008), showing the location of the Réka Valley section in the Mecsek basin (orange star) and other localities with $\delta^{13}C$ record of the Jenkyns Event discussed in the text: 1– Peniche (Lusitanian Basin), 2 – Yorkshire, 3 – Denkingen, Dotternhausen (SW German Basin), 4 – Sancerre, Lorraine (Paris Basin), 5 – Valdorbia (Umbria-Marche

Basin), 6 – Trento Platform. (D) Outcrop view of the naturally exposed part of the Lower Toarcian black shale in the Réka Valley. (E) Close-up view of slabs of the laminated black shale in the Réka Valley section.

Fig. 2. Stratigraphic distribution of $\delta^{13}C_{org}$ data, nannofossil abundance counts, $CaCO_3$ content, K_2O/Rb ratios, and $CH2_{FTIR}$ measurements along the Réka Valley section. On the lithology log black colour denotes the black shale, i.e. the Rékavölgy Formation, and brown denotes the spotted marl, i.e. the underlying Hosszúhetény Formation and the overlying Komló Formation. Turbiditic sandstone interbeds are coloured green. First occurrence (FO) and last occurrence (LO) of nannofossils are from this study.

Fig. 3. 2π-MTM power spectra of the detrended $\delta^{13}C_{org,}$ $CaCO_3$, and $CH2_{FTIR}$ signals. The blue shaded areas show the range of the filters corresponding to the prominent ~2 m cyclicity. The frequency domains of the filters are set as 0–1.13 cycles/m, 0–1.25 cycles/m, and 0–1.1 m in the case of the $\delta^{13}C$ signal, the $CaCO_3$ signal, and the $CH2_{FTIR}$ signal, respectively. The thick blue lines superimposed on the detrended signals are the filter output signals. The thick dashed lines show the lower and upper boundary of Interval 2 (see Fig. 4).

Fig. 4. Chemostratigraphic correlation of several well-known Lower Toarcian sections with the Réka Valley section. The $\delta^{13}C$ curves are from Hesselbo et al. (2007, Peniche), Kemp et al. (2011, Yorkshire), Suan et al. (2015, Denkingen), Hermoso et al. (2012,

Sancerre), Ruebsam et al. (2014, Lorraine), Sabatino et al. (2009, Valdorbia), Woodfine et al. (2008, Trento).

Fig. 5. (A) Al-Si-Ca ternary diagram (Rachold & Brumsack, 2001) of black shale samples from the Réka Valley section. (B) Al-K-Ca ternary diagram (Hutcheon et al., 1998) of black shale samples from the Réka Valley section.

Fig. 6. K_2O/Rb diagram (Plank & Langmuir, 1998; Di Leo et al., 2002) of black shale samples from the Réka Valley section.

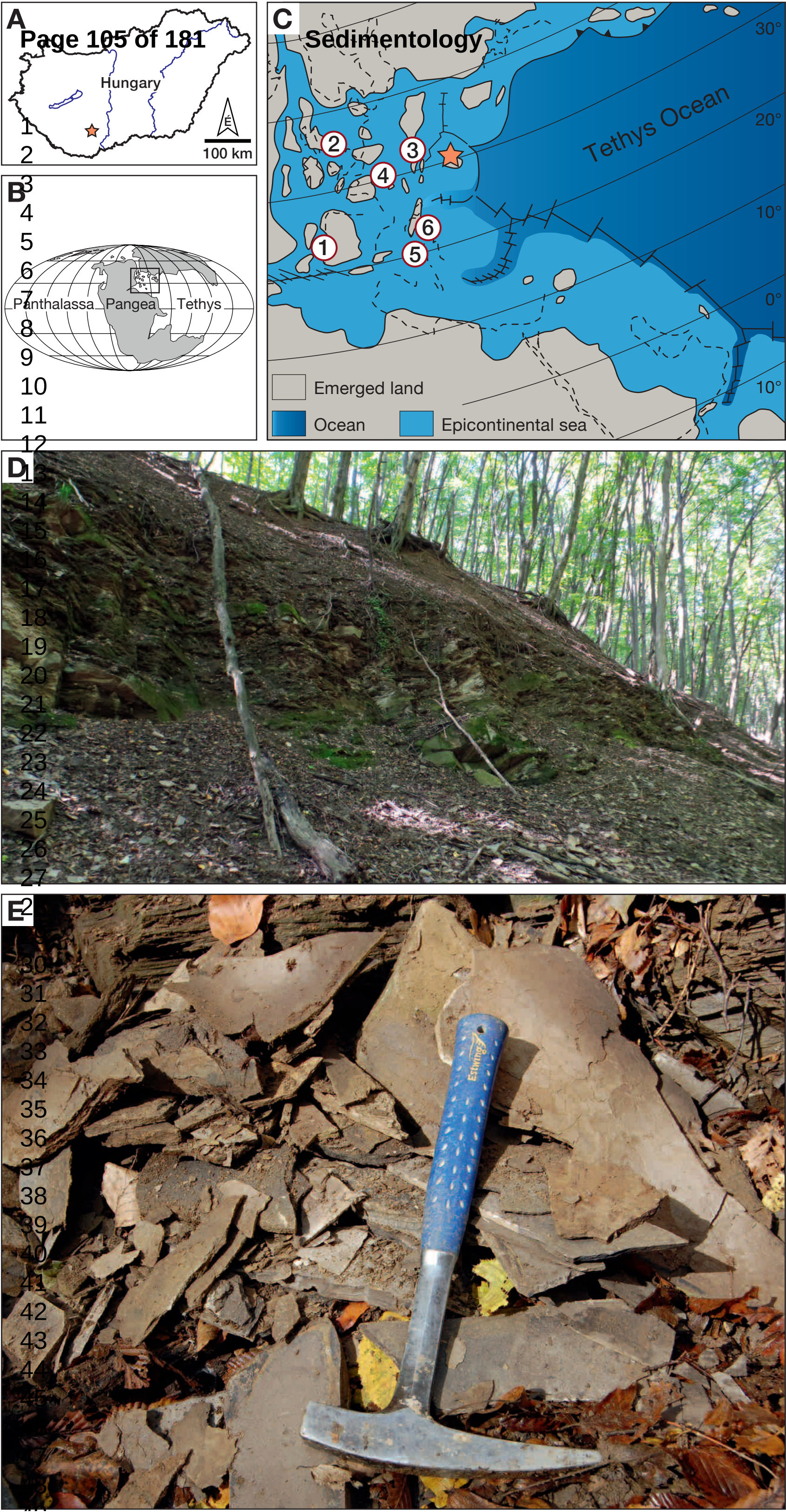
A
Hungary
É
100 km
B
Panthalassa
Pangea
Tethys
C
Tethys Ocean
30°
20°
10°
0°
10°
1
2
3
4
5
6
Emerged land
Ocean
Epicontinental sea
D
E
Estwing

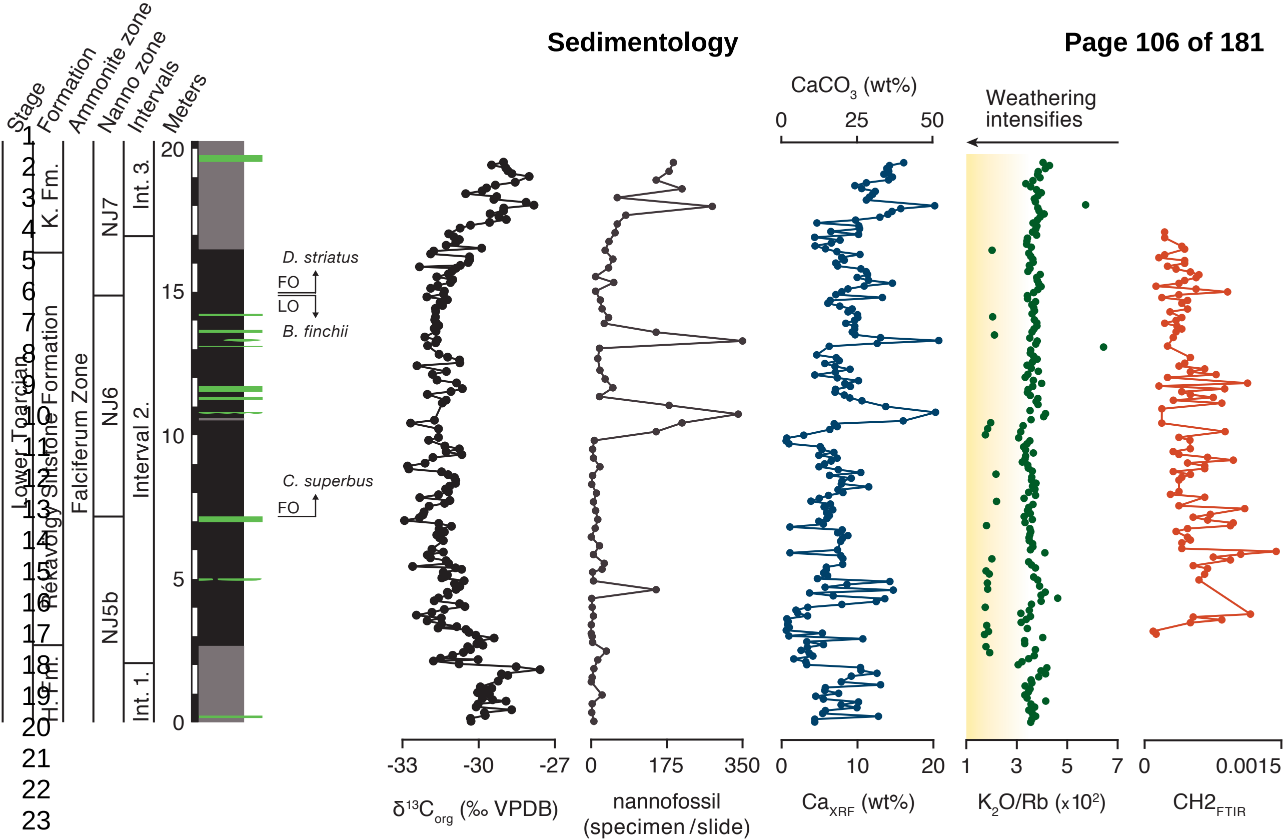
Stage
Formation
Ammonite zone
Nanno zone
Intervals
Meters
Lower Toarcian
K. Fm.
Rékavölgy Siltstone Formation
H. Fm.
Falciferum Zone
NJ7
NJ6
NJ5b
Int. 3.
Interval 2.
Int. 1.
20
15
10
5
0
D. striatus
FO
LO
B. finchii
C. superbus
FO
-33
-30
-27
δ13Corg (‰ VPDB)
0
175
350
nannofossil (specimen / slide)
CaCO3 (wt%)
0
25
50
0
10
20
CaXRF (wt%)
Weathering intensifies
1
3
5
7
K2O/Rb (x10²)
0
0.0015
CH2FTIR

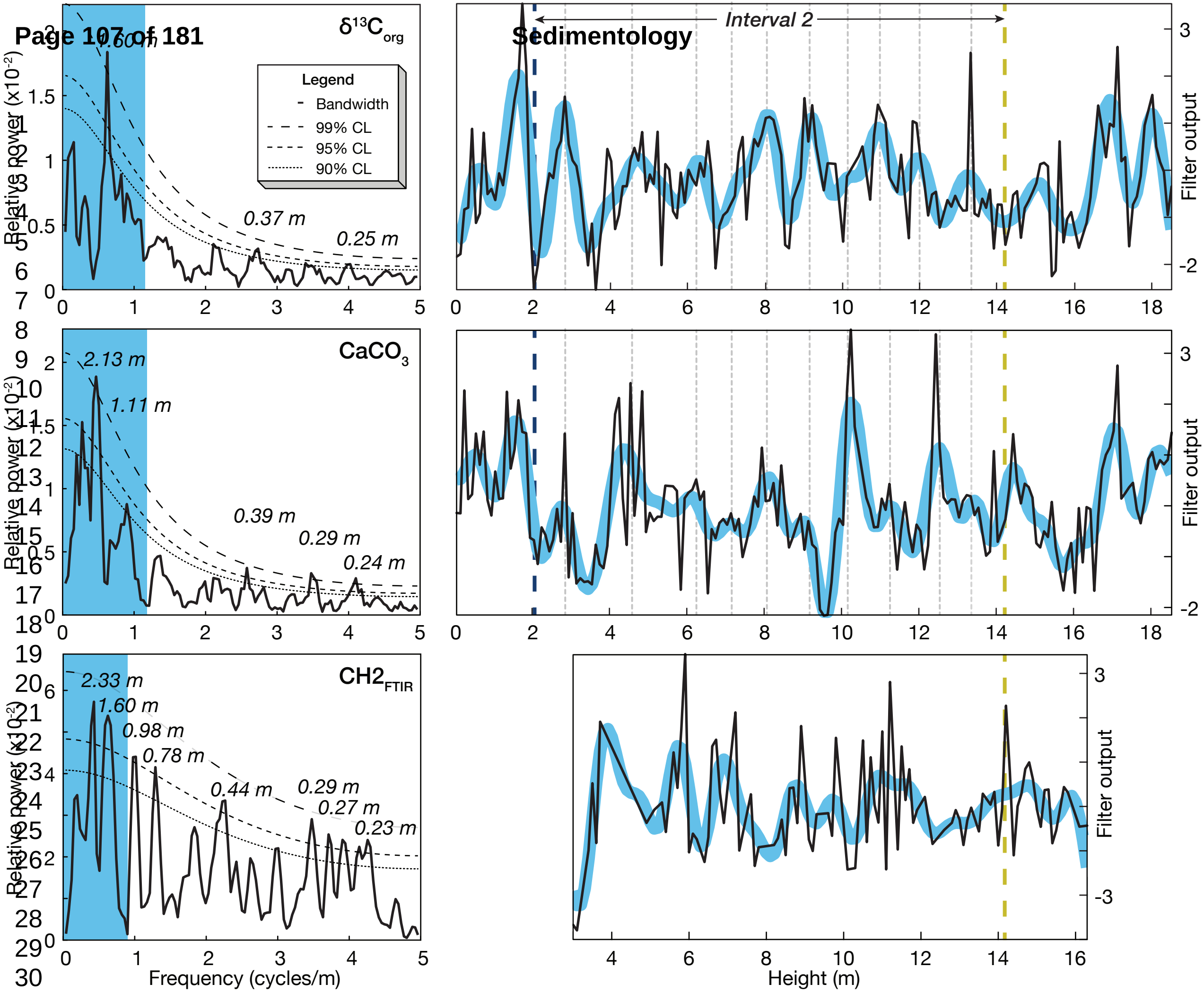
δ13C org
Legend
Bandwidth
99% CL
95% CL
90% CL
1.60 m
0.37 m
0.25 m
Relative power (x10-2)
Interval 2
Filter output
CaCO3
2.13 m
1.11 m
0.39 m
0.29 m
0.24 m
CH2 FTIR
2.33 m
1.60 m
0.98 m
0.78 m
0.44 m
0.29 m
0.27 m
0.23 m
Frequency (cycles/m)
Height (m)

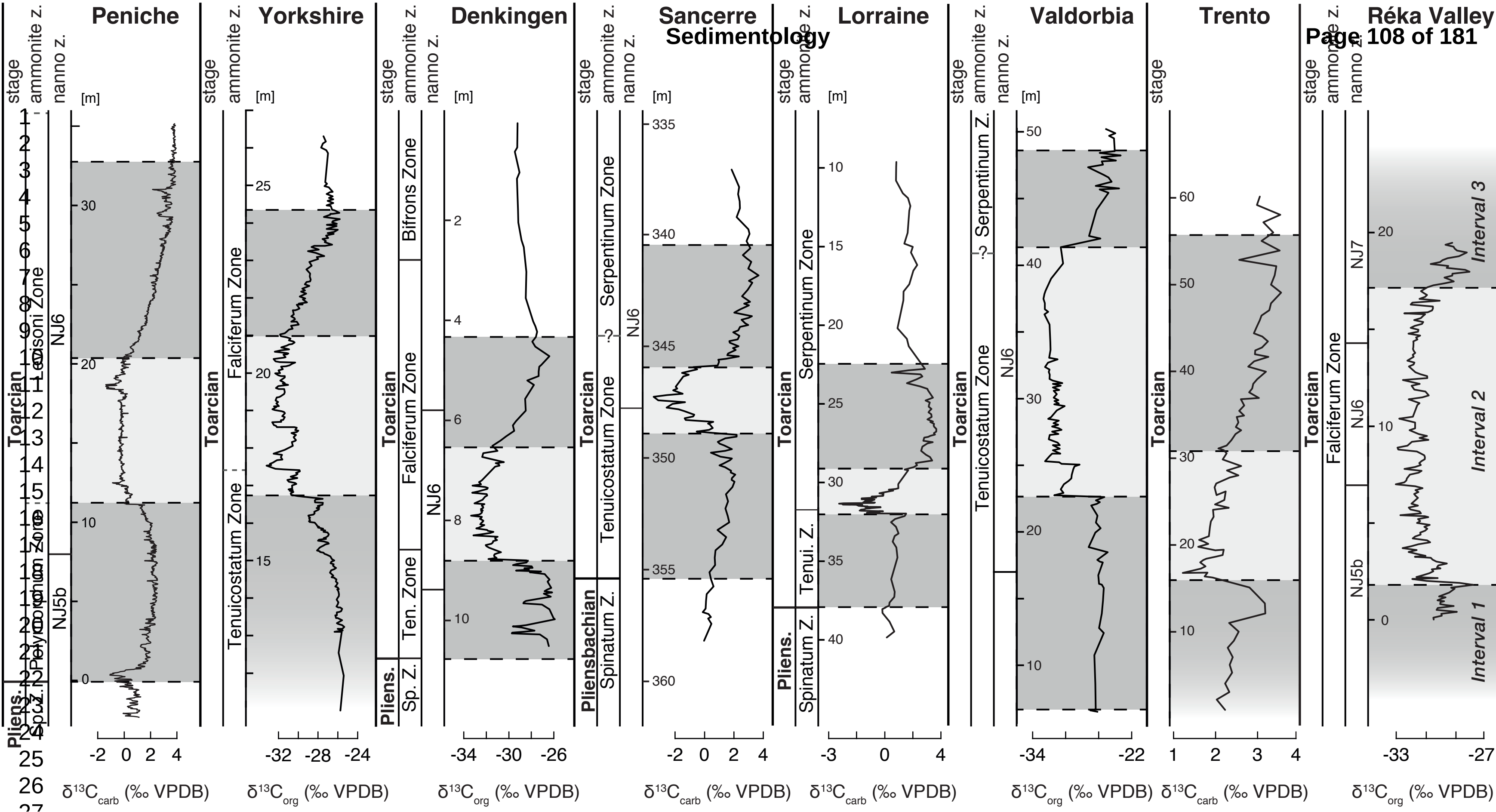
Peniche
Yorkshire
Denkingen
Sancerre
Lorraine
Valdorbia
Trento
Réka Valley
stage
ammonite z.
nanno z.
[m]
Toarcian
Pliens.
Pliensbachian
Levisoni Zone
Polymorphum Zone
NJ6
NJ5b
NJ7
Falciferum Zone
Tenuicostatum Zone
Bifrons Zone
Ten. Zone
Sp. Z.
Serpentinum Zone
Spinatum Z.
Tenui. Z.
Serpentinum Z.
Interval 1
Interval 2
Interval 3
δ13Ccarb (‰ VPDB)
δ13Corg (‰ VPDB)

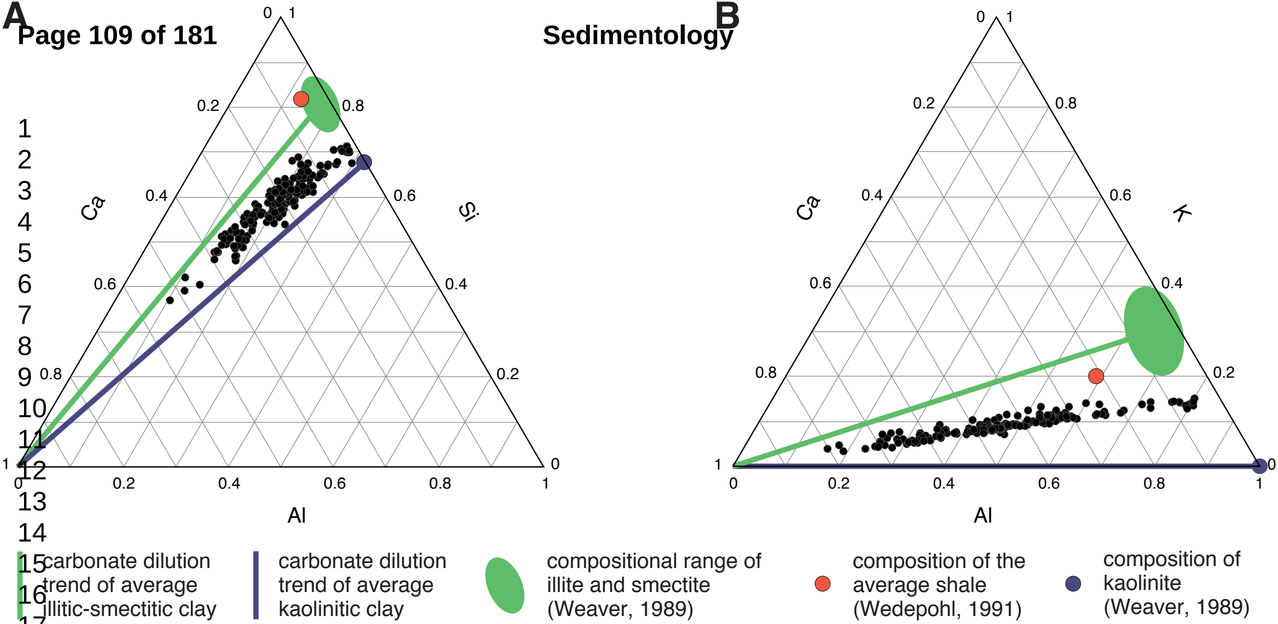
A
B
Ca
Si
Al
Ca
K
Al
0
1
0.2
0.4
0.6
0.8
carbonate dilution trend of average illitic-smectitic clay
carbonate dilution trend of average kaolinitic clay
compositional range of illite and smectite (Weaver, 1989)
composition of the average shale (Wedepohl, 1991)
composition of kaolinite (Weaver, 1989)

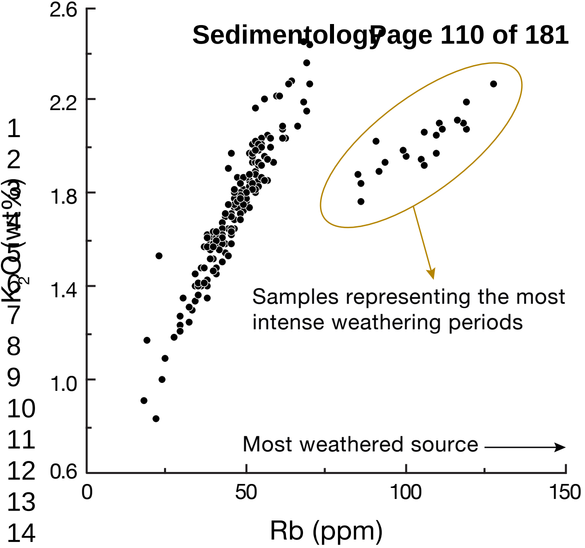

2.6
2.2
1.8
1.4
1.0
0.6
K_2O (wt%)
Samples representing the most intense weathering periods
Most weathered source
0
50
100
150
Rb (ppm)

Supplementary Material

Fig. S1. Photomicrographs of diagnostic calcareous nannofossil taxa from the Réka Valley section. Photos taken under polarized light using crossed Nicols. Scale bar is 5 μm to A–J and 10 μm to K–L. *(A, B) Lotharingius hauffi, (C) Biscutum finchii, (D) Crepidolithus impontus, (E) Lotharingius sigillatus, (F) Carinolithus superbus, (G) Discorhabdus striatus, (H) Bussonius prinsii, (I) Zeugrhabdotus erectus, (J) Watznaueria sp. (K) Schizosphaerella sp., (L) Orthogonoides hamiltoniae.*

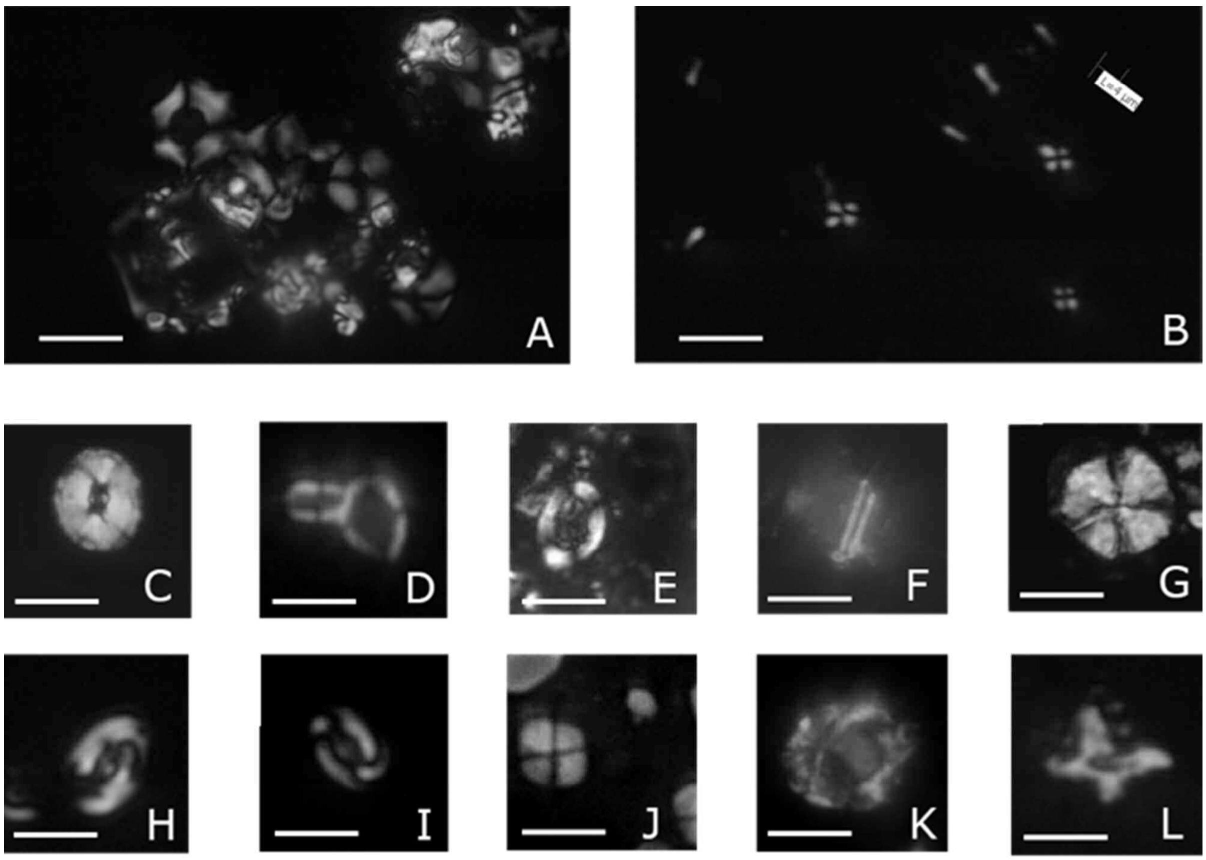

Fig. S2. FTIR spectra of the Réka Valley section with characteristic wavenumbers used to identify the mineral phases and organic matter present in the samples: 3690 cm^{-1}, 3620 cm^{-1}, 1032 cm^{-1} – kaolinite; 2923 cm^{-1} – CH stretching of organic matter; 2850 cm^{-1} – CH2 stretching of organic matter; 1420 cm^{-1}, 876 cm^{-1}, 711 cm^{-1} – carbonate; 789 cm^{-1}, 779 cm^{-1} – quartz (Vaculikova & Plevova, 2005; Movasaghi et al., 2008).

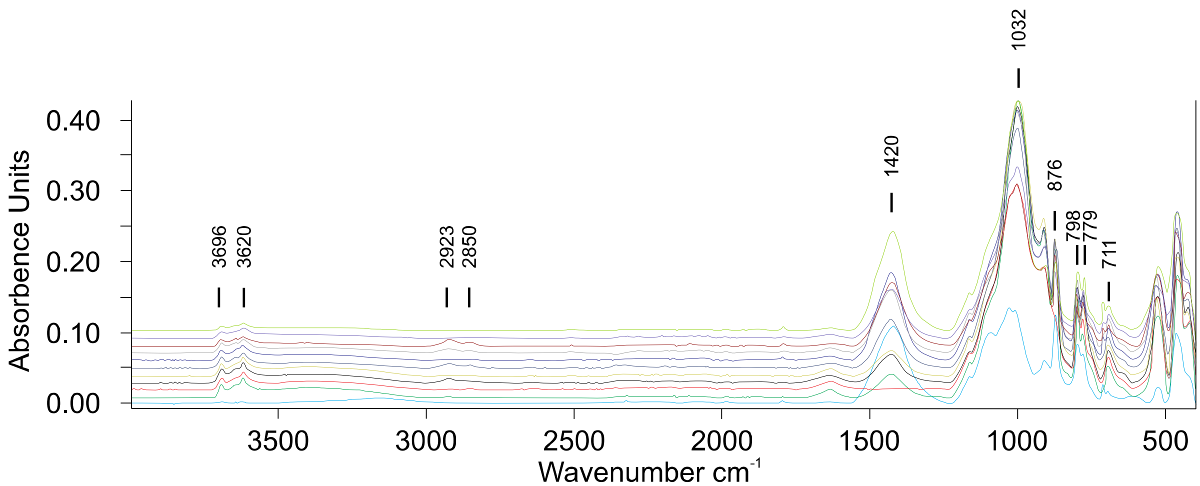

Fig. S3. 2π-MTM power spectrum and filter output signal of the Ti/Al dataset. Taner bandwith filter is set as 0-1.48 cycles/m (blue shading).

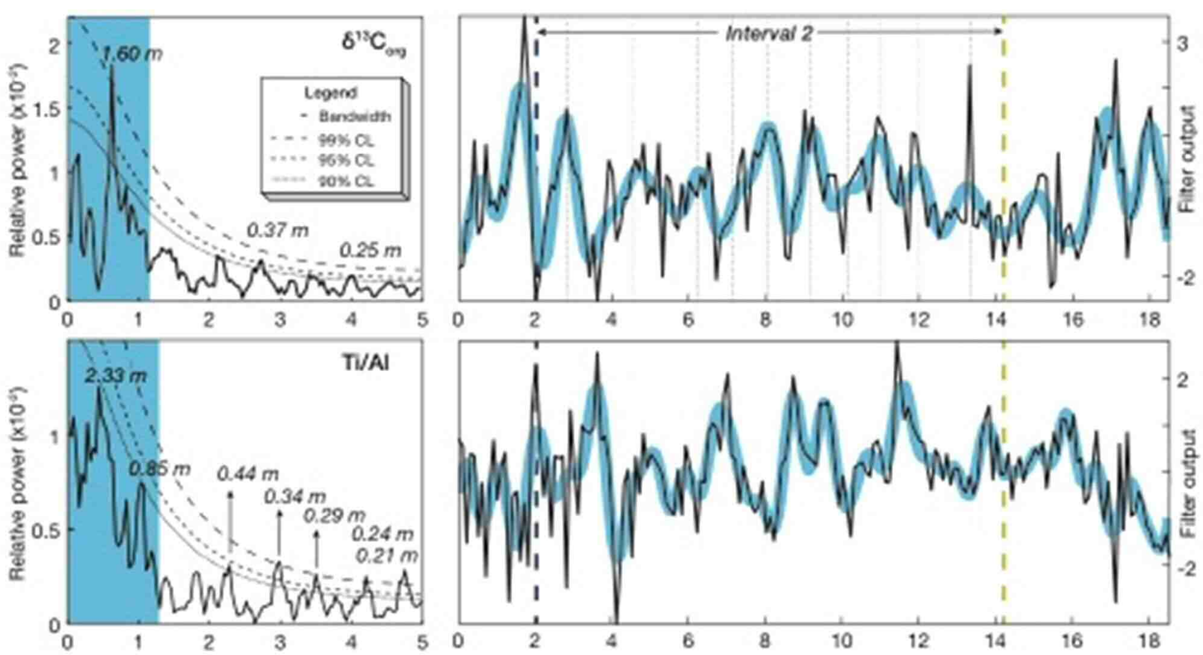

References

Vaculikova, L. and Plevova, E. (2005) Identification of clay minerals and micas in sedimentary rocks. *Acta Geodynamica et Geomaterialia*, **2,** 163.

Movasaghi, Z., Rehman, S. and ur Rehman, I. (2008) Fourier Transform Infrared (FTIR) Spectroscopy of Biological Tissues. *Applied Spectroscopy Reviews*, **43,** 134-179.

Uncertanity of XRF analzyes in case of particular elements
For main components:
RSD(%): Fe 1.10, Mn 4.73, Ti 2.99, Ca 1.59, K 2.18, S 4.47, Al 2.10, P 16.31, Si 0.57, Mg 17.67

For minor components:
RSD(%): Mo 29.36, Zr 3.77, Sr 1.72, Rb 4.64, Th 25.50, Pb 17.73, As 26.73, Zn 11.85, Cu 26.74, Cr 15.41, Ba 5.

Turbidite levels are marked green

Sample	Height (m)	Ti	Mo	Zr	Sr	Rb	Th	Pb	As	Zn	Cu
RA 00	0,0	4422,55	3,22	175,31	317,65	57,39	14,46	44,91	23,59	92,27	49,00
RA 10	0,1	4308,17	< LOD	148,78	288,30	53,47	14,25	40,65	63,54	92,41	48,18
RA 20	0,2	2241,57	< LOD	66,78	567,04	37,16	< LOD	18,43	38,61	70,15	< LOD
RA 30	0,3	5225,65	< LOD	190,94	368,16	60,97	12,93	48,00	27,79	94,38	45,22
RA 40	0,4	5005,35	< LOD	193,79	338,52	65,32	15,83	46,60	22,14	80,95	31,46
RA 50	0,5	2869,54	< LOD	111,63	653,38	43,18	< LOD	27,89	38,73	82,96	< LOD
RA 60	0,6	3831,33	4,00	127,28	279,98	53,85	< LOD	31,19	52,37	100,66	28,15
RA 70	0,7	1669,01	< LOD	62,34	333,35	30,63	< LOD	15,54	39,64	84,93	35,49
RA 80	0,8	4907,60	3,11	209,87	479,04	71,01	15,94	37,89	18,51	99,15	37,22
RA 90	0,9	3644,88	< LOD	162,88	522,01	62,38	13,86	33,30	40,08	83,56	57,88
RA 100	1,0	2621,87	< LOD	94,79	301,82	41,85	< LOD	19,37	65,32	83,38	45,41
RA 110	1,1	4985,91	3,48	226,96	491,37	69,35	16,89	52,69	20,92	89,28	38,84
RA 120	1,2	4841,38	3,63	230,28	426,97	70,38	16,92	41,64	23,37	94,69	38,56
RA 130	1,3	1029,14	< LOD	42,40	330,12	22,91	< LOD	< LOD	39,57	66,09	< LOD
RA 140	1,4	4517,09	4,37	213,61	474,81	62,01	14,21	39,09	14,58	87,70	44,24
	1,5										
RA 160	1,6	4280,69	< LOD	203,46	432,41	56,78	13,67	30,99	15,11	89,88	27,81
RA 170	1,7	2260,24	< LOD	105,04	605,38	38,98	< LOD	20,24	< LOD	68,38	56,60
RA 180	1,8	4028,16	< LOD	169,19	480,09	54,51	15,96	35,54	11,91	96,13	55,96
RA 190	1,9	3470,40	4,83	107,95	350,79	46,65	< LOD	18,45	29,99	92,95	< LOD
RA 200	2,0	4599,73	< LOD	191,22	303,97	70,24	12,13	26,69	18,13	101,16	59,65
RA 210	2,1	5831,07	4,96	276,95	328,16	70,61	18,27	22,23	11,90	118,15	45,37
RA 220	2,2	4678,11	3,69	230,42	222,24	58,35	15,05	99,72	45,18	108,13	57,08
RA 230	2,3	3727,61	3,38	118,28	168,29	47,74	< LOD	42,44	75,55	87,81	40,35
RA 240	2,4	4649,00	< LOD	192,67	269,55	#####	17,95	52,92	34,48	94,42	49,62
RA 250	2,5	3277,73	3,86	118,17	150,93	52,37	< LOD	46,00	88,64	88,10	47,56
RA 260	2,6	4846,51	< LOD	196,06	261,85	#####	14,46	56,47	80,15	96,13	39,53
RA 270	2,7	4071,58	< LOD	197,16	333,25	54,99	15,79	49,90	44,63	88,01	38,28
RA 280	2,8	4698,70	4,29	193,47	266,84	62,77	15,37	77,92	34,98	138,39	58,36
RA 290	2,9	1381,67	< LOD	53,17	340,91	24,50	< LOD	< LOD	73,26	66,90	53,94
RA 300	3,0	5675,97	3,69	201,53	201,30	#####	19,82	37,73	38,17	105,88	47,61
RA 310	3,1	4580,93	< LOD	189,23	361,22	#####	17,87	25,55	33,20	91,74	55,43
RA 320	3,2	3708,94	< LOD	126,12	121,15	57,10	< LOD	69,50	97,65	94,54	73,06
RB 90	3,3	5589,42	8,04	221,14	233,59	#####	15,69	62,40	22,92	116,80	83,57
RB 100	3,4	5439,81	3,72	219,14	237,97	63,69	18,52	55,22	29,30	139,11	74,01
RB 110	3,5	5397,78	8,04	220,87	234,81	58,88	18,41	56,14	30,89	126,56	90,54
RB 120	3,6	5552,35	5,55	208,63	230,84	55,97	14,98	53,45	34,68	99,18	56,46
RB 130	3,7	4686,31	8,45	207,46	310,41	58,17	15,40	43,89	20,80	166,25	#####
RB 140	3,8	5288,93	4,37	218,68	258,59	64,48	16,57	56,61	29,34	109,94	76,18
RB 150	3,9	5356,30	4,91	230,21	262,63	#####	18,94	52,90	21,94	90,90	85,93

SUPLEMENTARY DATA_REVISED XRF

RB 160	4,0	4660,11	3,38	202,13	306,31	55,52	14,86	50,34	43,07	108,68	47,71
RB 170	4,1	2668,61	3,41	87,63	323,17	39,59	< LOD	< LOD	66,06	74,14	44,51
RB 180	4,2	1061,37	3,80	39,23	346,60	19,43	< LOD	< LOD	49,89	180,55	< LOD
RB 190	4,3	2454,36	< LOD	123,56	848,71	40,46	12,82	35,45	17,29	65,18	24,17
RB 200	4,4	4098,70	4,26	163,48	595,32	45,97	17,18	33,15	20,13	77,33	33,05
RB 210	4,5	4578,81	< LOD	198,46	332,78	#####	16,95	39,61	42,12	74,03	67,82
RB 220	4,6	2520,41	3,90	149,70	781,77	39,68	10,25	22,48	11,38	160,76	< LOD
RB 230	4,7	4622,08	< LOD	210,38	439,97	#####	12,48	44,55	39,98	106,17	31,02
RB 240	4,8	3804,24	4,44	121,93	361,48	48,38	< LOD	20,00	79,62	75,90	26,18
RB 250	4,9	4131,65	4,04	292,20	534,65	38,71	10,51	33,38	14,07	84,99	< LOD
RB 260	5,0	4630,63	< LOD	206,40	344,07	#####	16,47	46,32	62,05	95,09	54,19
RB 270	5,1	4749,93	3,48	210,43	408,96	#####	13,68	42,98	30,99	80,31	49,48
RB 280	5,2	4721,18	3,46	192,83	397,91	53,32	15,79	47,56	23,37	79,58	35,86
RB 290	5,3	4444,31	< LOD	204,47	506,50	55,07	15,75	45,73	30,01	104,31	58,46
RB 300	5,4	4166,84	11,97	179,01	509,86	54,27	15,97	39,79	27,70	96,63	49,16
RC 110	5,5	3580,05	4,72	141,71	497,22	87,37	12,44	32,27	30,50	121,70	53,12
RC 120	5,6										
RC 130	5,7	3421,31	5,06	141,41	472,13	38,99	13,44	35,99	28,59	63,84	42,56
RC 140	5,8	3793,34	7,36	150,20	392,26	48,83	12,50	27,77	15,62	113,33	85,34
RC 150	5,9	3660,75	7,52	110,99	162,38	55,74	16,78	39,84	#####	86,68	71,43
RC 160	6,0	3669,29	5,48	168,74	376,65	47,60	11,28	27,63	17,13	100,93	60,73
	6,1										
	6,2										
RC 190	6,3	4175,44	3,47	175,86	440,44	54,62	12,51	38,83	16,37	192,74	62,68
RC 200	6,4	3977,33	5,51	165,47	450,78	54,99	13,69	38,56	23,71	88,28	42,78
RC 210	6,5	3164,53	< LOD	138,68	490,01	49,74	13,50	36,05	16,11	86,22	47,35
RC 220	6,6	4103,19	6,21	157,47	423,94	56,12	10,53	39,97	55,46	83,18	43,25
RC 230	6,7	3794,49	7,08	166,48	450,73	54,63	15,44	36,19	16,08	95,49	47,66
RC 240	6,8	5177,18	5,88	187,88	253,08	#####	18,98	39,00	51,48	107,86	71,64
RC 250	6,9	3814,56	6,52	157,08	336,92	55,42	14,11	43,57	15,20	72,46	89,95
RC 260	7,0	4055,04	16,98	173,22	337,50	49,98	15,37	39,74	19,97	118,34	83,76
RC 270	7,1	4207,35	12,17	194,93	392,75	55,38	10,97	40,78	18,83	107,64	#####
RC 280	7,2	3224,24	7,33	153,01	406,43	44,41	13,71	36,70	18,11	90,72	97,45
RC 290	7,3	4040,28	9,52	160,09	449,82	51,16	12,55	34,28	35,73	142,47	#####
RC 300	7,4	3759,29	9,58	183,47	483,12	51,05	14,29	42,35	45,75	99,50	94,13
RC 310	7,5	4180,01	8,95	157,55	373,81	53,54	14,09	39,70	21,41	101,78	82,74
RC 320	7,6	3832,98	4,70	152,45	403,44	91,47	14,80	36,52	29,18	79,85	63,22
RC 330	7,7	3287,22	5,16	103,59	205,29	54,53	< LOD	29,30	72,79	74,38	62,53
RC 340	7,8	3762,92	3,72	155,20	338,55	53,77	17,95	38,52	26,13	82,78	49,46
RC 350	7,9	3474,57	3,32	148,89	390,54	54,01	11,76	34,27	20,59	72,78	72,44
RC 360	8,0	3453,71	5,01	152,32	587,47	52,80	17,43	35,48	19,84	68,48	26,50
RC 370	8,1	3766,49	< LOD	168,74	491,92	55,23	10,55	34,26	21,67	67,27	43,23
RC 380	8,2	2810,05	< LOD	124,97	787,33	44,93	10,66	30,28	20,27	65,44	42,33
RC 390	8,3	2579,50	< LOD	131,62	665,81	48,35	12,85	31,33	15,70	70,49	62,00
RC 400	8,4	1992,46	< LOD	89,52	466,26	43,80	< LOD	20,08	34,81	55,75	51,86
RC 410	8,5	3082,61	< LOD	135,74	707,31	86,07	13,80	27,19	21,40	65,14	57,98
RC 420	8,6	3385,21	4,51	154,25	358,16	51,82	11,08	29,46	77,55	68,39	52,96
RC 430	8,7	2240,18	< LOD	157,69	770,44	43,29	11,14	24,05	13,58	75,24	58,75
RC 440	8,8	3336,61	8,95	173,45	526,56	50,12	11,51	33,87	24,36	132,99	59,93
RC 450	8,9	4122,88	11,66	179,68	444,58	59,74	16,34	44,17	24,61	83,51	75,78

RC 460	9,0	4112,33	15,64	191,45	430,79	55,75	14,48	41,70	19,04	109,29	96,20
RC 470	9,1	3954,30	14,93	178,27	449,39	54,11	14,05	44,64	22,47	109,30	79,56
RC 480	9,2	3547,39	12,70	149,23	505,92	46,42	14,02	37,76	20,85	88,53	70,75
RC 490	9,3	4162,85	8,18	168,59	370,23	57,83	11,48	48,53	69,56	122,94	70,75
RC 500	9,4	4092,94	10,03	152,94	536,26	56,43	14,22	41,52	21,19	87,99	65,63
RC 510	9,5	3934,13	6,21	166,61	482,34	56,16	13,09	39,24	22,31	99,18	59,62
RC 520	9,6	4041,01	9,16	151,25	440,06	51,88	14,12	42,89	38,20	81,53	68,33
RC 530	9,7	6594,24	19,11	270,13	212,37	67,49	19,88	54,12	26,57	126,09	57,35
RC 540	9,8	6080,99	16,51	255,22	214,05	#####	19,31	50,19	20,75	101,84	59,59
RC 550	9,9	6305,94	16,98	242,70	211,72	68,94	17,74	61,94	16,83	109,26	86,08
RC 560	10,0	5543,44	12,89	226,57	301,82	#####	13,95	50,00	15,87	122,14	59,22
	10,1										
RC 580	10,2	4300,39	15,26	189,13	401,38	62,26	16,13	43,67	18,34	119,23	49,01
RC 590	10,3	3960,54	12,59	134,45	478,57	#####	10,77	39,53	12,13	115,42	57,23
RC 600	10,4	3728,74	26,19	162,47	372,40	48,52	11,67	34,01	24,34	110,67	57,05
RC 610	10,5	2373,22	10,68	122,55	590,38	30,19	9,17	29,13	11,65	50,95	39,25
	10,6										
	10,7										
RC 640	10,8	1860,44	13,55	106,16	729,89	26,10	7,17	20,05	13,03	68,78	40,02
	10,9										
RC 660	11,0	3433,77	12,30	129,10	551,95	39,39	8,99	36,97	13,37	105,12	53,85
RC 670	11,1										
RC 680	11,2	3343,88	15,36	154,30	489,76	41,03	10,93	28,76	16,51	118,04	44,82
RC 690	11,3	3722,66	16,20	151,86	461,20	44,07	14,01	30,68	21,74	82,40	56,07
RC 700	11,4	3153,50	20,27	162,79	435,15	42,55	11,09	30,49	21,38	74,41	39,67
RC 710	11,5	4450,42	34,82	186,48	407,93	52,10	12,84	36,64	21,44	176,21	97,97
RC 720	11,6	4285,60	31,47	187,04	402,10	51,48	13,74	46,34	15,25	181,84	#####
RC 730	11,7	3678,66	21,96	169,50	461,49	47,54	10,82	39,28	12,85	168,91	#####
RC 740	11,8	3889,13	11,06	174,88	412,23	49,20	14,69	26,21	14,95	90,10	#####
RC 750	11,9	3432,62	15,93	161,07	962,23	40,90	11,32	29,65	22,17	113,64	#####
RC 760	12,0	4117,02	9,36	175,77	424,37	47,55	11,90	38,91	8,61	129,70	#####
RC 770	12,1	4215,18	14,39	171,51	343,45	51,86	14,57	40,67	16,74	147,06	#####
RC 780	12,2	4309,40	11,23	177,50	433,95	53,23	12,61	37,09	16,67	130,00	90,31
RC 790	12,3	3434,68	19,39	201,74	487,93	40,74	10,36	36,08	15,47	213,99	82,89
RC 800	12,4	4003,24	14,33	184,88	380,84	45,94	14,43	37,69	15,39	167,18	72,54
RD 10	12,5	4283,93	7,75	175,97	374,21	52,95	12,28	39,51	15,43	88,47	#####
RD 20	12,6	3871,32	8,90	155,53	398,21	45,42	8,90	34,75	8,67	94,38	#####
RD 30	12,7	3709,91	10,23	195,20	436,87	41,88	12,86	30,47	12,98	103,01	95,16
RD 40	12,8	4448,97	6,92	160,14	331,37	50,90	11,01	38,98	11,81	118,73	#####
	12,9										
	13,0										
RD 70	13,1	4330,85	8,14	187,03	358,84	56,01	12,09	30,98	17,45	99,24	68,07
RD 80	13,2	3328,54	9,86	200,19	542,70	41,37	12,27	28,58	15,20	105,11	29,45
RD 90	13,3	2499,96	7,73	221,41	845,67	23,71	8,02	14,18	11,20	44,15	< LOD
RD 100	13,4	3214,05	11,96	186,40	555,26	34,48	12,20	25,47	18,08	81,87	33,93
RD 110	13,5	3047,35	19,61	149,63	492,54	39,80	10,64	38,54	19,38	99,96	61,92
RD 120	13,6	4234,74	11,89	196,53	507,04	51,15	12,28	35,08	18,05	86,29	42,03
RD 130	13,7	4076,80	11,44	168,93	501,29	86,78	10,17	35,64	17,35	112,32	53,61
RD 140	13,8	4043,73	11,26	163,07	478,15	49,47	11,02	30,98	20,73	107,22	43,90
RD 150	13,9	4328,69	12,53	166,71	437,71	50,53	13,93	35,13	15,89	92,30	46,79

RD 160	14,0	3730,04	15,35	154,72	491,52	47,23	13,97	34,86	22,18	122,89	55,35
RD 170	14,1	3859,43	13,31	163,81	498,75	47,51	13,58	30,19	17,57	103,19	47,95
RD 180	14,2	3921,63	13,19	169,77	494,64	49,50	13,79	37,32	48,32	84,47	42,75
RD 190	14,3	3965,84	14,03	167,16	478,09	94,41	14,55	39,43	14,87	125,09	60,59
RD 200	14,4	3831,08	12,49	156,32	496,70	51,94	9,76	37,08	20,26	126,23	44,92
RD 210	14,5	4174,79	23,70	190,84	499,81	44,09	12,71	33,93	24,23	196,15	#####
RD 220	14,6	3921,25	16,39	164,12	450,73	43,00	41,15	39,64	21,97	115,37	87,64
RD 230	14,7	3932,92	32,78	168,35	394,65	43,60	9,88	39,29	17,13	192,86	#####
RD 240	14,8	2330,91	18,18	130,91	988,90	33,19	7,12	31,22	17,52	158,13	#####
RD 250	14,9	4135,53	24,02	181,87	499,17	46,93	14,45	30,95	19,50	129,13	#####
RD 260	15,0	3676,34	20,74	156,62	543,84	49,76	12,96	31,72	31,04	99,01	#####
RD 270	15,1	2727,36	17,62	164,57	643,84	41,20	9,56	31,07	57,90	74,70	89,28
RD 280	15,2	2987,61	23,12	174,92	652,71	34,76	9,53	31,05	21,27	138,34	#####
RD 290	15,3	2450,72	16,63	157,37	906,75	30,34	8,73	23,38	15,77	78,89	59,25
RD 300	15,4	2560,51	16,49	146,23	621,89	33,64	9,24	30,04	12,96	103,95	71,28
RD 310	15,5	2679,83	14,49	127,02	643,54	35,66	11,14	29,47	13,00	201,41	#####
RD 320	15,6	3374,61	20,16	145,97	836,45	39,67	9,67	38,48	12,95	90,09	78,21
RD 330	15,7	3086,57	16,14	148,63	534,64	35,41	9,84	30,02	10,23	107,19	69,32
RD 340	15,8	3037,18	18,45	163,29	506,51	38,88	11,42	28,45	16,57	140,27	83,01
RD 350	15,9	3848,16	16,42	174,83	422,98	46,59	12,65	33,33	11,52	128,94	#####
RD 360	16,0	3840,40	17,11	176,62	403,88	46,35	11,37	41,48	17,10	131,72	88,33
RD 370	16,1	3714,82	13,85	167,09	442,15	44,06	12,03	34,66	48,39	116,03	85,66
RD 380	16,2	3596,06	8,27	156,46	432,46	48,25	10,50	36,12	15,81	87,61	56,66
RD 390	16,3	3325,42	19,69	148,41	516,72	41,03	8,32	30,92	52,45	162,38	64,35
RD 400	16,4	3968,63	13,98	167,54	407,55	44,34	11,36	39,84	41,91	124,06	91,57
RD 410	16,5	4723,91	9,67	180,61	426,96	93,16	15,41	33,57	23,35	122,05	68,67
RD 420	16,6	4192,62	21,36	199,50	343,40	47,06	11,95	33,67	55,87	165,48	83,51
RD 430	16,7	4233,85	12,69	198,84	389,88	49,50	12,61	31,41	18,99	130,31	95,28
RD 440	16,8	3781,54	15,05	173,86	408,52	46,45	11,43	31,55	20,79	141,92	76,48
RD 450	16,9	4036,51	5,95	180,59	340,02	50,73	10,53	33,64	16,08	114,22	#####
RD 460	17,0	2833,92	13,06	149,71	460,29	36,68	9,97	26,24	18,00	183,19	79,58
RD 470	17,1	4080,35	9,07	173,48	353,66	46,74	12,84	35,73	22,80	80,60	57,85
RD 480	17,2	2791,18	4,54	156,25	440,59	42,55	12,28	25,23	21,87	70,73	56,72
RD 490	17,3	3221,48	3,92	169,51	509,69	45,84	12,06	29,82	25,46	115,40	66,83
RD 500	17,4	4294,41	7,53	164,11	328,54	54,26	17,57	39,24	30,81	92,73	48,10
RD 510	17,5	3340,04	3,74	143,10	529,24	44,63	11,04	35,92	22,16	105,02	56,57
RD 520	17,6	2262,55	4,38	78,64	434,10	37,53	< LOD	17,47	63,10	43,70	< LOD
RD 530	17,7	2368,23	< LOD	118,00	596,29	38,14	11,74	25,92	17,49	73,67	48,45
RD 540	17,8	2488,37	< LOD	146,32	660,63	35,88	11,97	21,16	65,26	83,32	34,35
RD 550	17,9	2174,19	< LOD	124,30	701,77	36,55	11,85	25,70	23,98	73,65	55,65
RD 560	18,0	988,57	< LOD	41,34	470,08	20,35	< LOD	11,24	23,10	45,03	< LOD
	18,1										
RD 580	18,2	2202,48	< LOD	71,25	339,31	37,73	< LOD	19,35	49,56	50,42	41,17
RD 590	18,3	2664,28	4,06	132,06	514,23	43,37	12,23	35,86	19,61	76,67	39,93
RD 600	18,4	2658,46	< LOD	110,18	533,72	42,23	11,35	25,53	19,40	80,87	53,21
RD 610	18,5	2707,49	< LOD	133,54	529,38	39,32	12,28	27,82	47,56	72,88	37,93
RD 620	18,6	3096,76	3,19	140,00	538,95	45,96	14,97	42,34	19,80	97,37	46,09
RD 630	18,7	3922,52	3,24	170,49	458,36	49,67	15,33	35,06	17,57	94,21	50,33
RD 640	18,8	3038,72	< LOD	166,27	659,38	45,44	14,32	33,76	20,97	53,50	46,72
RD 650	18,9	2861,68	< LOD	146,83	821,66	42,59	11,96	32,86	20,35	66,57	31,73

RD 660	19,0	2645,83	< LOD	126,31	######	37,56	11,21	26,27	15,01	86,12	24,72
RD 670	19,1	2713,68	< LOD	120,80	910,99	41,47	11,85	29,99	19,40	75,78	27,99
RD 680	19,2	2736,20	3,12	121,54	791,64	40,54	12,33	32,20	16,59	78,89	33,38
RD 690	19,3	2404,05	3,78	112,70	692,97	34,95	12,35	38,99	18,50	74,28	< LOD
RD 700	19,4	2317,95	< LOD	107,24	674,33	31,20	11,42	24,44	19,47	53,98	34,29
RD 710	19,5	1934,04	3,90	70,55	472,01	29,00	< LOD	20,61	52,26	62,80	34,55

86, Nb 13.36

Fe	Mn	Cr	Ca	K	S	Ba	Nb	Al	P
61851,85	23309,74	221,66	43694,46	16921,05	462,18	942,21	14,35	80878,30	< LOD
68742,30	42780,98	240,07	43773,40	15976,77	< LOD	1028,67	13,51	80692,16	711,17
96491,84	29071,32	< LOD	127595,72	11565,28	< LOD	1281,76	15,40	62935,44	2457,41
56357,14	18670,96	227,73	54135,44	18277,43	651,51	885,86	15,99	100486,77	879,20
44064,93	13501,85	212,23	57659,30	18856,28	< LOD	915,10	16,28	96943,40	497,35
71398,13	25054,01	234,00	99356,70	13295,60	< LOD	1111,98	29,98	77858,46	11023,77
68628,59	36116,58	204,56	78439,38	15933,42	< LOD	800,06	15,28	82046,82	703,88
129634,36	39566,11	342,30	101367,91	10547,65	369,46	665,33	12,21	56668,94	2059,12
53887,52	4933,10	231,69	55091,48	20088,17	< LOD	849,67	15,41	106646,21	532,80
43112,60	2571,76	159,36	44990,30	17182,62	< LOD	709,74	12,39	66759,58	463,95
98527,00	37007,91	< LOD	75237,09	12015,04	< LOD	1328,55	9,32	60070,49	415,86
51422,04	4100,19	240,30	56934,67	20297,27	< LOD	823,46	16,87	100335,45	1371,76
44163,38	3568,69	177,65	57699,05	19456,16	301,86	799,51	15,37	92692,33	614,08
199521,59	21995,52	457,48	130452,85	6846,37	462,41	1477,63	7,40	41556,50	554,64
41395,99	5624,95	186,28	78603,78	18358,94	< LOD	797,14	15,81	102106,57	766,72
45348,45	2622,05	193,37	91897,38	18240,22	459,85	775,57	13,82	94736,98	451,64
91864,92	5241,76	305,37	125716,72	13400,54	< LOD	1025,09	31,12	69914,16	19136,98
46561,94	3213,84	221,95	104538,90	17926,70	< LOD	754,73	12,97	93502,92	597,95
86316,81	4665,83	305,03	103964,41	16235,15	< LOD	850,82	14,19	110548,66	1816,89
41730,77	3426,58	169,66	33232,50	17807,93	< LOD	674,32	14,92	76318,77	646,29
46136,59	2434,15	231,98	31985,13	18793,24	< LOD	702,22	18,37	84979,02	684,34
90142,44	4239,44	300,98	16075,70	16816,77	415,60	1020,56	15,57	84786,60	305,59
93809,89	19845,61	298,90	41319,89	14636,23	365,41	1024,26	14,33	84161,19	703,35
85896,80	8663,36	313,67	36431,67	16124,03	373,14	827,39	14,90	90365,49	661,03
102959,65	9083,49	349,26	25708,44	16246,63	422,09	572,85	13,92	88956,27	866,57
78375,20	5372,94	305,92	33969,08	16300,37	< LOD	830,44	13,19	93819,65	439,65
66276,69	13418,89	257,87	55238,44	15129,29	< LOD	781,57	15,30	79549,61	405,16
79366,22	14967,92	350,06	33259,47	17241,78	433,85	708,48	13,86	91015,51	595,18
166084,59	15342,90	344,87	107083,48	8195,20	315,15	562,34	9,28	50581,79	1456,84
69613,05	17810,13	239,03	9697,67	17165,86	286,86	727,54	15,70	94525,71	477,19
48378,51	12261,04	214,38	53712,29	17391,56	376,30	693,74	16,67	92958,40	884,84
102065,91	13038,42	296,83	6215,92	16200,10	311,24	490,59	14,63	90309,22	464,20
67290,95	1073,76	281,28	10141,45	18071,90	789,31	645,37	16,06	97523,97	641,19
74814,11	2046,96	278,22	7913,86	16777,07	743,73	758,25	19,23	96738,19	958,82
81004,52	1896,76	308,01	8750,42	16492,21	1027,00	686,75	18,01	96598,28	872,98
83916,78	2775,75	318,85	6992,09	16458,35	< LOD	762,06	16,21	97640,63	523,97
55377,81	1244,49	241,63	34292,75	15269,32	1204,16	568,66	19,86	66249,86	1029,28
69390,76	1915,31	282,91	21295,20	18713,31	701,28	661,03	17,51	96851,03	654,41
72017,59	1404,03	284,93	18983,57	17365,15	720,12	717,94	17,36	96821,95	789,55

69720,63	12522,25	300,10	34532,54	16507,75	390,74	897,48	14,27	91924,62	518,38
110484,03	19831,65	372,30	79428,50	13032,72	337,45	564,05	14,54	71445,34	1016,96
186483,59	17355,29	451,06	124707,88	7455,84	360,06	584,01	7,60	51726,64	788,69
57664,69	6581,51	195,05	136032,19	13307,10	421,94	828,42	16,78	76299,00	2567,69
69236,69	11677,57	263,20	68061,23	15751,75	< LOD	808,35	14,49	88045,04	1082,81
72157,33	5076,05	255,28	36872,58	16971,65	< LOD	679,29	14,46	93170,51	736,00
53690,84	3828,49	216,17	147144,50	12860,84	470,03	881,52	14,71	76158,30	1958,45
73747,80	3992,50	237,69	57361,02	16094,91	375,25	789,42	12,80	89804,16	1119,37
65350,64	30013,69	243,06	86226,76	15376,65	445,38	915,09	12,57	84791,43	561,32
47026,35	4056,64	210,11	142676,94	11789,03	431,03	918,54	11,90	74063,64	937,99
64456,53	4712,58	257,55	47276,20	17000,19	863,29	623,83	17,11	93258,23	975,56
58398,48	5920,09	207,79	60664,54	15871,16	531,62	704,63	15,36	91355,49	1052,67
56266,13	6903,49	242,53	55478,69	16552,80	2184,56	719,15	12,98	92585,80	1055,13
60605,31	11319,42	247,61	58719,26	16384,46	< LOD	689,61	15,91	89444,18	1372,70
61971,86	3168,63	242,99	58991,79	15629,10	837,21	709,25	16,85	86723,39	745,81
56180,77	5203,71	201,13	80508,15	14595,89	11138,12	682,19	10,18	83230,71	1061,45
62672,87	3107,05	204,44	80770,83	13315,96	10709,63	741,07	11,81	83852,86	1090,29
48004,69	1271,56	196,44	77996,71	14354,64	2074,81	523,68	13,24	77191,80	750,25
105731,03	3399,77	355,78	11124,15	16837,12	1405,71	735,03	14,87	89417,37	720,01
54471,16	2121,99	249,47	73685,17	14338,17	1905,07	544,41	13,75	68556,80	1115,89
51483,79	3973,33	244,02	77826,18	15848,96	746,70	732,71	14,08	83141,12	761,19
51533,99	4155,30	202,48	80144,83	15908,86	732,97	740,84	14,91	86224,79	621,89
40444,69	1664,27	< LOD	87400,02	14521,93	9433,86	686,72	12,15	84131,75	599,70
52369,50	2727,27	229,31	73888,15	16561,12	827,94	729,53	15,79	86955,81	710,56
48293,44	2379,68	235,09	79885,46	15955,43	742,21	729,59	12,09	80953,20	511,93
96621,65	3428,59	343,64	11042,91	17445,26	811,30	766,08	16,00	92299,12	1110,54
47416,19	1545,62	209,06	55032,89	15305,83	978,58	542,44	13,40	66062,19	480,90
59142,89	937,10	226,61	49136,11	15001,42	1901,72	476,05	14,61	71182,32	1039,19
42594,27	1431,68	213,57	59887,35	15136,66	1145,94	581,52	15,03	79823,10	532,78
39376,43	1127,33	170,86	62931,78	13027,54	891,85	539,80	9,66	51222,79	560,92
40036,34	1229,62	183,39	59353,12	14548,01	1148,18	432,85	12,89	60515,54	701,29
47009,82	1446,03	186,99	67484,12	14720,01	1375,22	579,89	15,03	72586,17	884,02
52483,24	1119,78	278,29	56088,93	16189,78	1504,10	575,25	14,76	82082,46	736,27
64887,34	3315,20	253,60	64350,67	16676,96	1016,89	723,80	12,54	88866,54	741,07
78583,09	8446,88	235,35	38740,53	14886,36	576,37	797,82	12,47	65862,55	603,16
71147,47	6373,09	253,30	49660,05	16706,38	736,07	812,86	14,55	80661,12	1075,93
56506,95	2052,59	192,71	61842,63	15558,87	913,80	686,65	14,89	80446,05	584,97
54777,63	8067,86	209,32	80884,75	16301,71	724,16	713,34	13,96	83332,89	792,44
51825,01	2655,32	207,50	74377,19	16613,69	764,50	691,27	15,11	88493,41	721,09
45161,61	7440,53	< LOD	114819,38	14031,97	538,33	689,82	10,68	59767,78	708,09
51560,49	7171,08	< LOD	78793,77	14384,68	453,33	893,76	11,38	68657,48	520,37
41082,34	3919,88	189,71	79667,66	13068,42	529,62	925,51	9,26	49207,60	530,32
54763,24	2790,70	209,17	91786,80	15538,65	660,89	835,76	12,94	85345,88	812,45
67241,79	2042,78	227,44	63254,30	15547,85	1174,85	912,85	13,49	81188,43	682,89
32269,81	1604,55	< LOD	104396,38	12421,40	606,93	770,07	10,58	44671,72	504,94
47783,96	971,96	203,21	74684,21	14290,70	863,87	649,51	14,33	65247,06	386,45
53281,73	850,63	249,52	49333,05	15964,12	785,80	532,00	16,81	72003,71	477,78

49619,88	1034,26	228,09	56671,34	15392,61	1277,07	584,96	15,61	62035,71	466,04
49892,58	1563,39	227,00	65322,59	15046,86	1143,07	681,35	14,31	64412,70	689,09
51882,06	4712,64	246,67	73162,07	14091,21	1375,74	608,51	13,58	65409,93	863,26
64322,01	1789,97	245,72	49126,46	16079,76	989,26	674,40	15,60	79489,48	622,21
47585,86	3602,21	237,57	68960,94	15322,68	936,83	680,80	16,04	79415,36	626,45
59390,23	5475,30	239,42	53312,20	15858,16	666,34	732,55	14,98	77531,59	517,10
49022,44	999,48	211,91	50999,63	15150,93	1243,65	661,63	14,09	80891,94	754,43
56268,14	666,21	254,98	9834,46	17223,11	537,18	669,59	18,00	107441,94	422,29
48036,07	881,74	248,68	6025,46	18736,64	697,54	574,41	16,52	99522,45	547,11
48356,97	892,50	199,26	6881,42	18064,94	725,12	716,29	17,62	102143,19	488,03
44585,49	1300,32	205,07	29235,88	17186,72	861,62	1052,63	15,94	96983,43	571,57
42694,17	1258,01	206,83	63539,03	16802,48	875,40	735,51	15,17	86758,51	563,99
37880,69	1646,84	176,24	73287,45	16412,63	994,34	1315,34	14,80	92741,22	800,38
49580,64	2022,99	210,10	69397,79	14364,11	2090,04	605,44	14,91	77560,09	1006,22
28072,68	2994,05	< LOD	160187,30	10189,09	1534,33	722,13	10,57	55741,64	862,46
27184,68	2295,33	< LOD	202792,85	8966,56	1681,01	699,92	8,08	50331,68	1013,34
37153,81	1881,10	170,52	137216,96	11529,61	1678,58	637,66	10,66	69133,41	1089,99
43632,98	1149,24	223,25	105924,47	13086,92	2605,05	545,71	12,52	66106,20	1302,89
48507,20	1405,11	184,50	89968,60	13780,92	2013,78	646,63	13,56	76173,45	1714,85
55618,71	900,71	207,97	82606,94	13547,21	2066,96	648,88	14,48	65699,46	1491,82
49211,39	1080,53	214,11	70443,20	15287,12	1634,80	623,28	14,86	82484,83	1070,06
44152,25	1160,55	181,05	71050,00	14629,07	1816,81	568,66	15,28	78457,68	999,28
34787,71	811,76	153,35	90616,43	13611,63	1900,04	703,55	15,02	71220,64	955,06
31238,34	694,70	186,70	83361,80	14837,71	1398,15	599,04	13,81	82780,74	836,96
43498,73	1291,34	187,66	101331,51	13533,44	2064,75	608,29	14,28	73225,14	1025,24
34161,49	1006,51	153,98	73420,98	14439,15	1735,97	592,24	13,32	75991,95	1171,35
44817,60	1995,87	173,93	43771,55	14350,56	1420,56	600,77	15,73	57716,54	555,39
39216,21	1476,12	199,69	70911,35	15205,95	1268,86	643,95	15,70	65743,39	905,34
40664,98	1319,84	144,66	90244,65	13036,72	2071,09	749,11	13,40	58727,66	1261,89
39637,55	618,49	178,91	70428,64	13626,85	1558,74	611,50	15,44	65889,99	823,79
34516,54	552,01	180,56	56989,06	14983,01	1596,96	497,51	15,62	74501,54	1004,86
29972,65	693,10	168,07	75989,79	13636,26	1861,52	518,86	12,78	69202,46	751,72
37160,22	753,27	185,02	72047,73	13237,59	1528,38	495,17	11,48	68104,37	1049,02
35948,28	528,78	182,45	46284,49	15473,07	1612,90	472,79	13,83	82100,97	1015,57
34696,86	792,29	184,42	62808,19	16444,05	1268,93	579,05	13,35	87631,54	669,77
34064,76	957,20	145,42	126033,86	12194,45	912,85	621,92	11,64	73125,44	891,36
25145,36	2491,99	< LOD	207088,75	12678,50	582,19	847,02	10,53	47270,76	833,36
45157,63	1180,92	< LOD	130447,55	10739,58	982,31	741,26	12,90	62247,19	804,49
60382,61	1615,39	224,70	96882,34	12584,01	1827,77	862,36	13,74	64248,28	1311,03
43528,16	1510,98	200,70	93131,65	14926,19	1061,53	646,61	14,37	81297,69	883,71
39164,34	825,39	195,75	96329,60	15227,99	1302,45	902,24	13,98	87505,66	834,05
39673,43	991,86	175,05	96429,73	14810,46	1219,09	595,23	13,99	81541,44	816,01
43230,38	958,07	196,60	84619,34	15455,32	1270,88	599,23	14,89	87749,43	914,13

41805,18	1049,48	173,22	96092,03	14896,93	1211,65	638,00	13,28	81173,92	644,92
40712,07	1042,98	213,07	100471,35	14962,25	1286,08	628,43	14,32	85539,85	798,45
41778,21	1020,82	206,03	100028,79	15191,24	1165,05	565,09	14,74	81392,99	904,77
42806,05	940,69	205,70	87588,66	16003,71	1188,73	601,32	16,22	88590,66	812,86
43276,29	1039,08	202,72	92976,12	15548,70	993,33	617,44	14,01	80735,99	856,73
41977,82	1051,70	198,14	76711,06	13552,32	2140,88	518,28	15,28	75687,91	857,68
51060,39	1642,39	229,95	60994,38	13109,20	2195,87	641,67	17,39	66733,50	1178,75
44004,13	1154,50	187,18	64095,13	13027,55	2905,04	573,23	14,05	64532,14	983,65
30774,34	801,34	< LOD	132787,27	10314,97	2922,43	573,83	11,76	49054,34	940,90
44337,53	816,04	190,90	71460,19	13349,21	1503,76	635,17	14,99	74309,53	750,67
46837,54	860,25	213,70	79362,77	14128,83	1867,83	554,33	13,95	75807,66	761,63
35683,87	692,50	< LOD	87488,77	12544,62	6042,95	954,69	14,95	56327,16	1278,37
43484,02	1125,34	187,36	108868,29	11063,14	2161,79	661,54	14,08	57263,34	1227,85
30909,68	1773,32	< LOD	145991,50	9983,47	1218,03	687,32	11,13	55824,90	777,60
34309,04	1334,51	182,37	114482,74	10801,76	1924,81	599,14	14,62	51741,82	1007,13
29552,79	990,77	< LOD	99602,09	11286,51	2858,39	572,97	12,16	52018,93	1236,62
37672,43	1049,26	176,42	113302,66	12482,13	1314,05	667,73	12,69	71554,68	990,71
33961,90	1528,62	158,25	111451,05	11548,58	2279,21	604,46	12,76	61626,64	885,53
33181,94	1122,83	173,21	104550,13	11108,71	2047,50	573,69	14,00	59290,29	1117,92
38683,86	1074,63	202,57	73860,69	13629,55	1470,39	598,40	12,98	72467,18	919,90
42476,41	1367,82	207,60	71364,12	13465,35	1213,84	587,21	15,97	73928,81	807,77
39899,70	1010,28	212,26	82565,94	13347,56	1114,67	523,22	14,26	68405,14	870,34
49562,79	1605,94	196,37	79126,86	14569,37	1088,22	1501,86	15,73	78279,88	580,11
44126,97	1506,59	219,82	103296,59	12102,04	1576,24	638,71	16,03	64705,99	1206,71
43238,00	1211,23	192,73	72987,17	12794,44	1402,29	616,24	14,85	70586,60	1073,05
49512,64	1991,24	239,73	57881,02	15621,50	724,35	658,84	14,09	90694,33	755,10
57119,26	811,32	231,27	44123,06	13966,22	1817,90	558,83	17,70	71459,53	1713,95
38874,34	868,61	237,04	65631,96	13925,71	1713,66	570,84	14,48	72452,15	1305,87
41806,36	1096,02	186,64	77069,39	13111,88	1626,17	570,41	14,18	69181,93	1163,33
43918,38	2275,65	212,85	43544,89	14409,98	1448,47	540,11	16,29	67968,44	1034,64
35519,09	1623,99	177,81	101491,66	11526,45	1959,76	590,20	11,99	55980,08	1047,40
56873,70	1828,91	218,44	64938,11	14066,97	1225,44	640,79	13,48	79469,15	976,25
45538,45	2108,87	193,66	102822,89	13248,97	1357,93	1529,65	13,09	64674,07	748,20
44587,96	2228,87	194,45	101787,65	14452,14	878,32	707,67	15,75	72777,52	1064,46
73570,21	2047,83	256,80	46644,76	16418,23	552,66	705,49	15,16	86195,72	525,86
49853,57	2189,92	196,25	97506,39	14137,46	452,74	674,74	13,38	59190,99	383,27
63604,68	6546,06	< LOD	129516,75	12232,56	386,96	828,59	11,77	50012,20	1004,01
40797,11	3162,39	174,69	140045,71	12934,85	398,48	829,77	11,70	59595,69	900,43
46028,40	5062,65	< LOD	145453,55	11567,69	380,58	738,59	11,14	52802,43	378,84
51167,11	4468,09	< LOD	157020,53	11628,93	389,15	843,67	11,45	56958,62	502,84
28989,16	6249,43	< LOD	201730,41	9679,78	< LOD	960,55	4,31	39940,24	507,62
47988,50	7188,17	< LOD	111693,84	11705,74	274,26	822,57	10,48	40767,20	524,05
51724,56	4056,33	191,52	115668,14	13307,01	499,29	779,63	11,97	69681,46	667,17
41715,23	2075,97	185,30	119988,14	13455,73	646,38	617,76	12,46	47337,50	820,33
40490,74	2117,85	178,43	123369,52	12962,56	770,74	732,00	13,31	66328,17	557,34
52027,25	2963,31	226,94	105555,31	14429,63	498,96	756,82	13,26	74650,87	514,63
39347,68	2775,97	190,31	96577,32	14646,98	458,38	639,18	15,78	86673,87	472,75
48381,10	5347,85	< LOD	111707,03	12666,74	350,21	925,24	12,99	70181,56	509,30
47273,86	5497,91	< LOD	140994,52	12865,80	372,96	727,98	14,45	73292,00	813,44

37740,38	5612,24	< LOD	146011,20	12226,57	381,54	826,85	11,98	69853,25	692,93
45986,98	7463,26	< LOD	134823,98	13166,98	< LOD	784,19	12,35	77524,98	862,59
43605,71	5860,40	< LOD	141197,81	12956,74	396,39	716,11	11,86	77027,09	751,85
45689,69	10143,87	< LOD	138658,88	11988,70	< LOD	771,05	12,06	70115,97	939,04
42607,64	3829,42	< LOD	142188,65	11126,67	596,26	681,62	10,39	62039,48	1034,45
47466,04	23415,79	< LOD	160940,72	9731,10	476,06	2049,69	11,32	58067,68	946,77

Si	Mg
234400,17	< LOD
220559,84	11174,19
179598,94	13880,00
260504,16	8016,98
250857,36	8619,03
211571,41	8860,20
214636,92	9870,94
160030,00	< LOD
255380,11	12111,91
194563,47	< LOD
171414,72	10719,54
254603,13	7032,91
241774,30	11322,73
117508,99	< LOD
249870,03	18172,05
244687,09	< LOD
186264,95	< LOD
234490,09	10703,90
250287,70	13633,10
196802,66	6102,25
236904,65	10693,27
239995,83	13644,00
232341,02	16381,47
236364,03	14290,60
235843,61	14483,04
238951,22	13425,20
221417,10	12220,05
234517,47	11807,02
170471,87	11945,99
247567,03	15681,47
238413,74	13801,60
239984,89	12336,30
254536,24	12939,89
251510,85	13569,52
245484,26	14857,81
244233,81	14825,88
208231,66	11321,93
243271,52	13245,31
243404,82	14451,91

238739,52	15406,57
213651,37	11730,40
172688,26	11550,45
201645,98	12636,35
227597,88	14564,50
240882,48	13477,03
188998,02	16046,66
231144,74	15000,50
221067,34	12101,79
191389,31	14263,40
233675,68	14802,45
232163,60	15357,14
232175,21	13868,38
234068,67	14765,72
231473,02	13483,69
214229,77	14880,84
212528,39	14828,27
224369,62	12314,87
243215,86	14345,13
223176,06	10830,93
227756,36	12889,45
234213,69	11105,43
213818,09	16801,24
234338,21	11715,30
225388,47	12217,68
243487,84	14068,00
206314,14	8071,46
218726,42	9264,44
222669,26	12765,39
180520,46	7299,33
200873,94	7660,67
222083,95	9988,52
232319,53	12347,82
235942,82	13432,61
206450,79	11209,29
231362,21	12495,77
229338,78	13380,56
228825,81	13825,94
233522,34	14569,48
188505,92	7187,37
200604,12	12080,60
181180,65	7511,52
230535,64	14614,30
227776,28	12968,35
165421,47	8154,91
198880,00	8939,55
222403,54	10226,63

211384,24	8920,07
211231,66	8123,70
222422,04	9840,94
235412,32	10878,81
222856,28	8309,10
237702,70	10774,77
251311,87	12009,51
243964,39	11987,95
263140,03	12802,48
258841,61	12213,99
254719,87	12789,39
232635,58	11087,19
238463,31	13033,78
226584,33	10961,88
196717,08	9289,17
162629,76	12409,87
181565,04	11454,31
199655,67	11049,47
217325,40	8732,12
225760,21	10912,03
239328,99	11904,23
239166,28	11504,79
229702,89	11989,13
240883,49	12430,88
227572,96	10333,17
237059,12	10746,78
216540,80	8244,04
214377,91	8737,44
203033,62	9415,44
210769,48	8236,70
235785,08	10164,11
229958,40	10412,87
243104,08	10040,66
256464,19	9870,76
242918,41	11483,48
210048,03	11388,92
184901,53	8937,38
211966,71	10273,98
222205,53	8843,05
226216,47	11553,26
233658,20	13422,68
227368,22	11330,62
240448,30	11256,58

225202,11	11392,79
232047,61	12463,33
224941,60	12082,51
236314,39	12786,67
229668,19	12010,40
228996,09	10758,09
213171,28	11088,74
203400,03	8688,85
165765,63	8205,98
220595,69	9351,72
219520,51	9697,48
190078,45	9267,85
197619,83	7786,65
196618,46	7309,44
190830,18	8879,44
188691,62	9410,81
218762,36	9009,18
203562,92	10891,88
206518,40	9013,83
227303,19	10131,37
229127,21	10418,85
223624,06	11172,38
230749,89	10964,27
213045,61	7991,49
233057,26	9691,37
247953,67	12714,90
236868,85	9095,33
231497,68	9948,24
228959,59	10312,48
245878,50	8989,01
203061,01	9141,53
233064,69	10808,47
209583,99	8092,53
227470,05	11978,94
253067,68	12089,80
200045,80	7660,59
193385,54	8749,17
201831,60	7254,34
181785,85	10415,91
183613,84	10783,72
141752,45	8546,88
159893,43	6715,28
223969,77	8089,91
171435,39	8735,73
222331,31	10686,71
229353,22	12157,99
238660,72	10651,63
201990,63	9414,06
209306,65	10700,01

207941,18	9563,39
215706,96	10172,39
222598,89	11000,18
215208,22	11611,69
210905,79	11138,65
202802,83	8250,38

Turbidite levels are marked green

Sample	Height (m)	d13Corg
RA 00	0,00	-30,30
	0,05	
RA 10	0,10	-30,32
	0,15	
RA 20	0,20	-29,74
	0,25	
RA 30	0,30	-29,77
	0,35	
RA 40	0,40	-28,70
	0,45	
RA 50	0,50	-30,10
	0,55	
RA 60	0,60	-30,02
	0,65	
RA 70	0,70	-28,92
RA 75	0,75	-29,45
RA 80	0,80	-29,85
	0,85	
RA 90	0,90	-29,83
RA 95	0,95	-29,58
RA 100	1,00	-30,04
	1,05	
RA 110	1,10	-29,71
RA 115	1,15	-29,48
RA 120	1,20	-29,93
	1,25	
RA 130	1,30	
	1,35	
RA 140	1,40	-29,23
	1,45	
	1,50	
	1,55	
RA 160	1,60	-28,85
RA 165	1,65	-29,10
RA 170	1,70	
	1,75	
RA 180	1,80	-27,58
	1,85	
RA 190	1,90	-28,52
	1,95	
RA 200	2,00	-30,77
	2,05	
RA 210	2,10	-31,78
RA 215	2,15	-30,02
RA 220	2,20	-31,50
	2,25	
RA 230	2,30	-31,02

	2,35	
RA 240	2,40	-30,60
	2,45	
RA 250	2,50	-30,32
	2,55	
RA 260	2,60	-30,43
RA 265	2,65	-29,83
RA 270	2,70	-30,07
	2,75	
RA 280	2,80	-29,98
	2,85	
RA 290	2,90	-29,39
	2,95	
RA 300	3,00	-30,11
	3,05	
RA 310	3,10	-30,38
	3,15	
RA 320	3,20	-30,50
RB 85	3,25	-31,60
RB 90	3,30	-30,86
	3,35	
RB 100	3,40	-31,46
	3,45	
RB 110	3,50	-32,03
	3,55	
RB 120	3,60	-31,47
	3,65	
RB 130	3,70	-32,45
	3,75	
RB 140	3,80	-31,84
	3,85	
RB 150	3,90	-31,35
	3,95	
RB 160	4,00	-30,54
	4,05	
RB 170	4,10	-30,75
	4,15	
RB 180	4,20	-31,75
	4,25	
RB 190	4,30	-31,58
	4,35	
RB 200	4,40	-31,20
	4,45	
RB 210	4,50	-31,23
	4,55	
RB 220	4,60	-30,89
	4,65	
RB 230	4,70	-30,74
	4,75	
RB 240	4,80	-30,95

	4,85	
RB 250	4,90	-30,57
	4,95	
RB 260	5,00	-31,45
RB 265	5,05	-31,32
RB 270	5,10	-31,23
	5,15	
RB 280	5,20	-31,39
	5,25	
RB 290	5,30	-30,67
RB 295	5,35	-30,91
RB 300	5,40	-32,60
	5,45	
RC 110	5,50	-31,18
	5,55	
RC 120	5,60	-31,28
	5,65	
RC 130	5,70	-31,90
	5,75	
RC 140	5,80	-32,02
	5,85	
RC 150	5,90	-31,39
	5,95	
RC 160	6,00	-31,84
	6,05	
	6,10	
	6,15	
	6,20	
	6,25	
RC 190	6,30	-31,39
	6,35	
RC 200	6,40	-31,54
	6,45	
RC 210	6,50	-31,65
	6,55	
RC 220	6,60	-31,35
	6,65	
RC 230	6,70	-31,56
	6,75	
RC 240	6,80	-31,07
	6,85	
RC 250	6,90	-31,57
	6,95	
RC 260	7,00	-32,92
	7,05	
RC 270	7,10	-32,33
	7,15	
RC 280	7,20	-32,19
	7,25	
RC 290	7,30	-32,15

	7,35	
RC 300	7,40	
	7,45	
RC 310	7,50	-31,95
	7,55	
RC 320	7,60	-31,34
	7,65	
RC 330	7,70	-31,13
	7,75	
RC 340	7,80	-32,32
	7,85	
RC 350	7,90	-31,58
	7,95	
RC 360	8,00	-31,19
	8,05	
RC 370	8,10	-31,30
	8,15	
RC 380	8,20	-31,14
	8,25	
RC 390	8,30	-30,91
	8,35	
RC 400	8,40	-30,90
	8,45	
RC 410	8,50	-30,95
	8,55	
RC 420	8,60	-31,20
	8,65	
RC 430	8,70	-31,46
	8,75	
RC 440	8,80	-32,75
	8,85	
RC 450	8,90	-32,80
	8,95	
RC 460	9,00	-32,11
	9,05	
RC 470	9,10	
	9,15	
RC 480	9,20	-31,80
	9,25	
RC 490	9,30	-30,66
	9,35	
RC 500	9,40	-31,28
	9,45	
RC 510	9,50	-30,76
	9,55	
RC 520	9,60	-31,33
	9,65	
RC 530	9,70	
	9,75	
RC 540	9,80	-31,97

	9,85	
RC 550	9,90	-31,58
	9,95	
RC 560	10,00	
	10,05	
	10,10	
	10,15	
RC 580	10,20	-31,58
	10,25	
RC 590	10,30	
	10,35	
RC 600	10,40	-32,68
	10,45	
RC 610	10,50	-31,74
	10,55	
	10,60	
	10,65	
	10,70	
	10,75	
RC 640	10,80	
	10,85	
	10,90	
	10,95	
RC 660	11,00	
	11,05	
RC 670	11,10	-31,43
	11,15	
RC 680	11,20	-31,28
	11,25	
RC 690	11,30	
	11,35	
RC 700	11,40	-32,02
	11,45	
RC 710	11,50	-31,09
	11,55	
RC 720	11,60	-30,64
	11,65	
RC 730	11,70	
	11,75	
RC 740	11,80	-30,87
	11,85	
RC 750	11,90	-31,64
	11,95	
RC 760	12,00	
	12,05	
RC 770	12,10	-31,82
	12,15	
RC 780	12,20	-31,27
	12,25	
RC 790	12,30	

	12,35	
RC 800	12,40	-32,43
	12,45	
RD 10	12,50	-30,74
	12,55	
RD 20	12,60	-30,75
	12,65	
RD 30	12,70	-31,22
	12,75	
RD 40	12,80	-31,56
	12,85	
	12,90	
	12,95	
	13,00	
	13,05	
RD 70	13,10	-32,01
	13,15	
RD 80	13,20	-31,69
	13,25	
RD 90	13,30	-31,63
	13,35	
RD 100	13,40	-32,12
	13,45	
RD 110	13,50	-24,77 outlier
	13,55	
RD 120	13,60	-31,68
	13,65	
RD 130	13,70	-31,75
	13,75	
RD 140	13,80	-31,57
	13,85	
RD 150	13,90	-31,67
	13,95	
RD 160	14,00	-31,73
	14,05	
RD 170	14,10	-31,70
	14,15	
RD 180	14,20	-29,42
	14,25	
RD 190	14,30	-31,69
	14,35	
RD 200	14,40	-31,70
	14,45	
RD 210	14,50	-31,42
	14,55	
RD 220	14,60	-31,52
	14,65	
RD 230	14,70	-31,23
	14,75	
RD 240	14,80	-32,04

	14,85	
RD 250	14,90	-31,38
	14,95	
RD 260	15,00	-31,35
	15,05	
RD 270	15,10	-31,89
	15,15	
RD 280	15,20	-31,61
	15,25	
RD 290	15,30	-31,11
	15,35	
RD 300	15,40	-31,02
	15,45	
RD 310	15,50	-31,65
	15,55	
RD 320	15,60	-31,19
	15,65	
RD 330	15,70	-31,05
	15,75	
RD 340	15,80	-30,89
RD 345	15,85	-32,33
RD 350	15,90	-30,72
	15,95	
RD 360	16,00	-30,41
	16,05	
RD 370	16,10	-30,35
	16,15	
RD 380	16,20	-30,36
	16,25	
RD 390	16,30	-31,89
	16,35	
RD 400	16,40	-31,77
	16,45	
RD 410	16,50	-29,88
	16,55	
RD 420	16,60	-31,28
	16,65	
RD 430	16,70	-30,90
	16,75	
RD 440	16,80	-30,76
	16,85	
RD 450	16,90	-30,98
	16,95	
RD 460	17,00	-31,18
	17,05	
RD 470	17,10	
	17,15	
RD 480	17,20	-30,73
	17,25	
RD 490	17,30	-30,32

	17,35	
RD 500	17,40	-29,57
	17,45	
RD 510	17,50	-28,91
	17,55	
RD 520	17,60	-29,20
	17,65	
RD 530	17,70	-29,55
	17,75	
RD 540	17,80	-29,02
	17,85	
RD 550	17,90	-29,01
	17,95	
RD 560	18,00	-27,82
	18,05	
	18,10	-28,13
	18,15	
RD 580	18,20	-29,40
	18,25	
RD 590	18,30	-29,29
	18,35	
RD 600	18,40	-30,51
	18,45	
RD 610	18,50	-29,86
	18,55	
RD 620	18,60	-29,69
	18,65	
RD 630	18,70	-29,34
	18,75	
RD 640	18,80	-28,56
	18,85	
RD 650	18,90	
	18,95	
RD 660	19,00	-28,01
	19,05	
RD 670	19,10	-28,69
	19,15	
RD 680	19,20	-28,85
	19,25	
RD 690	19,30	-28,93
	19,35	
RD 700	19,40	-29,49
	19,45	
RD 710	19,50	-29,02

Turbidite levels are marked green

Sample	Height [m]	ORG C-H	ORG C-H2	CO3
RA 00	0,0			0,021393
RA 10	0,1			0,025900
RA 20	0,2			0,051570
RA 30	0,3			0,030420
RA 40	0,4			0,036340
RA 50	0,5			0,035730
RA 60	0,6			0,042460
RA 70	0,7			0,043870
RA 80	0,8			0,082200
RA 90	0,9			0,044270
RA 100	1,0			0,050590
RA 110	1,1			0,063110
RA 120	1,2			0,044770
RA 130	1,3			0,096170
RA 140	1,4			0,059030
	1,5			
RA 160	1,6			
RA 170	1,7			
RA 180	1,8			0,052100
RA 190	1,9			0,060360
RA 200	2,0			0,027000
RA 210	2,1			0,021079
RA 220	2,2			0,014554
RA 230	2,3			0,034630
RA 240	2,4			0,030716
RA 250	2,5			0,019949
RA 260	2,6			0,034404
RA 270	2,7			0,032070
RA 280	2,8	0,000408		0,031619
RA 290	2,9			0,071890
RA 300	3,0			0,001581
RA 310	3,1	0,000188	0,000126	0,045870
RA 320	3,2	0,000314	0,000094	0,001506
RB 90	3,3	0,003607		0,003462
RB 100	3,4	0,002855		0,002522
RB 110	3,5	0,003670	0,000502	0,002221
RB 120	3,6	0,002447	0,000847	0,002409
RB 130	3,7	0,004924	0,000533	0,038692
RB 140	3,8	0,003200	0,001161	0,023839
RB 150	3,9	0,002948		0,017252
RB 160	4,0	0,000722		0,033288
RB 170	4,1			0,080100
RB 180	4,2			0,067760
RB 190	4,3			0,123460
RB 200	4,4			0,081000
RB 210	4,5	0,001465		0,043560
RB 220	4,6			0,147930

RB 230	4,7			0,047200
RB 240	4,8	0,000501		0,074230
RB 250	4,9			0,056600
RB 260	5,0	0,001725	0,000596	0,039072
RB 270	5,1	0,001223		0,056310
RB 280	5,2	0,002133	0,000658	0,045000
RB 290	5,3			0,051900
RB 300	5,4	0,002854	0,000690	0,062610
RC 110	5,5	0,002196	0,000533	0,079270
RC 120	5,6			
RC 130	5,7	0,002540	0,000941	0,089050
RC 140	5,8	0,002980	0,000753	0,073030
RC 150	5,9	0,004532	0,001054	0,008055
RC 160	6,0	0,003670	0,001443	0,066120
	6,1		0,000408	
	6,2			
RC 190	6,3	0,002070	0,000408	0,072400
RC 200	6,4	0,001976	0,000502	0,073280
RC 210	6,5	0,001756	0,000470	0,082700
RC 220	6,6	0,002039		0,071970
RC 230	6,7	0,001287	0,000345	0,075140
RC 240	6,8	0,002573	0,000471	0,005684
RC 250	6,9	0,003419	0,000941	0,063870
RC 260	7,0	0,004517	0,000972	0,064620
RC 270	7,1	0,003325	0,000691	0,054710
RC 280	7,2	0,003168	0,000532	0,071640
RC 290	7,3	0,003419	0,000721	0,060470
RC 300	7,4	0,003074		0,069580
RC 310	7,5	0,004297	0,001098	0,065370
RC 320	7,6	0,002478	0,000376	0,072520
RC 330	7,7	0,001694		0,049310
RC 340	7,8	0,001349		0,049810
RC 350	7,9	0,002196	0,000659	0,060480
RC 360	8,0	0,001035	0,000283	0,087760
RC 370	8,1	0,002415	0,000377	0,089960
RC 380	8,2			0,086120
RC 390	8,3			0,100640
RC 400	8,4			0,115940
RC 410	8,5	0,001161	0,000376	0,110290
RC 420	8,6	0,003701	0,000408	0,073780
RC 430	8,7	0,002478	0,000502	0,129190
RC 440	8,8	0,001600	0,000314	0,070920
RC 450	8,9	0,002416	0,000659	0,061730
RC 460	9,0	0,003576	0,000659	0,062030
RC 470	9,1	0,002447	0,000471	0,054050
RC 480	9,2	0,003983	0,000973	0,083110
RC 490	9,3	0,003168	0,000690	0,043910
RC 500	9,4	0,003106	0,000376	0,079050
RC 510	9,5	0,001349	0,000313	0,053460
RC 520	9,6	0,003293	0,000501	0,051950

RC 530	9,7	0,000533		0,005195	
RC 540	9,8	0,000628		0,001280	
RC 550	9,9	0,001345	0,000497	0,001280	
RC 560	10,0	0,001882	0,000376	0,015621	
	10,1				
RC 580	10,2	0,001711	0,000883	0,054900	
RC 590	10,3	0,002290		0,072570	
RC 600	10,4	0,002227	0,004130	0,084820	outlier
RC 610	10,5	0,002227	0,000188	0,128480	
	10,6				
	10,7				
RC 640	10,8	0,001694		0,239400	
	10,9				
RC 660	11,0	0,001568	0,000189	0,168630	
RC 670	11,1				
RC 680	11,2	0,004109	0,000847	0,123590	
RC 690	11,3	0,003576	0,000315	0,107650	
RC 700	11,4	0,003105	0,000753	0,111420	
RC 710	11,5	0,002635	0,000502	0,090900	
RC 720	11,6	0,002886	0,000407	0,090530	
RC 730	11,7	0,003701	0,000878	0,121950	
RC 740	11,8	0,002164	0,000157	0,106370	
RC 750	11,9	0,003858	0,001129	0,046170	
RC 760	12,0	0,002980		0,071660	
RC 770	12,1	0,003607	0,000251	0,034630	
RC 780	12,2	0,003043	0,000784	0,063240	
RC 790	12,3	0,002321	0,000502	0,086290	
RC 800	12,4	0,002635	0,000659	0,065500	
RD 10	12,5	0,002353	0,000377	0,059720	
RD 20	12,6	0,003639	0,000440	0,089440	
RD 30	12,7				
RD 40	12,8	0,002541	0,000502	0,045170	
	12,9				
	13,0				
RD 70	13,1	0,002760		0,064750	
RD 80	13,2	0,001192	0,000251	0,074160	
RD 90	13,3			0,092350	
RD 100	13,4			0,071360	
RD 110	13,5	0,000753	0,000314	0,090330	
RD 120	13,6	0,001003		0,075730	
RD 130	13,7	0,002541	0,000345	0,059970	
RD 140	13,8	0,001318	0,000408	0,066850	
RD 150	13,9	0,001380	0,000355	0,057910	
RD 160	14,0	0,000910	0,000220	0,060680	
RD 170	14,1	0,001662	0,000345	0,082510	
RD 180	14,2	0,002509	0,000408	0,084310	
RD 190	14,3	0,002823		0,088980	
RD 200	14,4	0,000878	0,000278	0,072420	
RD 210	14,5	0,002416	0,000471	0,058420	
RD 220	14,6			0,036010	

RD 230	14,7	0,002729	0,000408	0,052700
RD 240	14,8	0,003513	0,000471	0,090340
RD 250	14,9	0,002227	0,000189	0,045270
RD 260	15,0	0,001599	0,000376	0,061610
RD 270	15,1	0,004611	0,000910	0,083840
RD 280	15,2	0,002698	0,000564	0,086010
RD 290	15,3	0,001349	0,000125	0,111660
RD 300	15,4	0,001286	0,000377	0,080180
RD 310	15,5	0,002917	0,000439	0,068360
RD 320	15,6	0,001003	0,000565	0,085070
RD 330	15,7	0,002321	0,000596	0,094290
RD 340	15,8	0,002416	0,000502	0,128050
RD 350	15,9	0,001600	0,000345	0,043290
RD 360	16,0	0,000941	0,000251	0,063610
RD 370	16,1	0,001599	0,000439	0,074160
RD 380	16,2	0,000847	0,000439	0,065410
RD 390	16,3	0,001004	0,000156	0,089970
RD 400	16,4	0,000659	0,000220	0,057850
RD 410	16,5			0,030803
RD 420	16,6	0,001600	0,000439	0,029285
RD 430	16,7	0,000784	0,000408	0,064120
RD 440	16,8			
RD 450	16,9	0,002666		0,029611
RD 460	17,0	0,001668	0,000220	0,112920
RD 470	17,1	0,001286		0,055960
RD 480	17,2	0,000596	0,000219	0,100370
RD 490	17,3	0,001537		0,086280
RD 500	17,4			0,038950
RD 510	17,5			0,059980
RD 520	17,6			0,113170
RD 530	17,7			0,143040
RD 540	17,8			0,107400
RD 550	17,9			0,130490
RD 560	18,0			0,125970
	18,1			
RD 580	18,2			0,125980
RD 590	18,3			0,145550
RD 600	18,4			0,125720
RD 610	18,5			0,109410
RD 620	18,6			0,097340
RD 630	18,7			0,061920
RD 640	18,8			0,090150
RD 650	18,9			0,102390
RD 660	19,0			0,104830
RD 670	19,1			0,099870
RD 680	19,2			0,116940
RD 690	19,3			0,141530
RD 700	19,4			0,115750
RD 710	19,5			0,130990

Sample	Height (m)	sum/sample
RA 00	0,0	12
RA 30	0,3	6
RA 60	0,6	1
RA 90	0,9	2
RA 120	1,2	25
RA 165	1,7	0
RA 180	1,8	2
RA 210	2,1	6
RA 240	2,4	15
RA 270	2,7	35
RA 300	3,0	3
RA 320	3,2	2
RB 90	3,3	0
RB 120	3,6	0
RB 150	3,9	5
RB 180	4,2	2
RB 210	4,5	1
RB 240	4,8	150
RB 270	5,1	5
RB 300	5,4	3
RC 110	5,5	25
RC 130	5,7	30
RC 160	6,0	5
RC 190	6,3	19
RC 220	6,6	0
RC 250	6,9	9
RC 280	7,2	15
RC 310	7,5	10
RC 340	7,8	5
RC 370	8,1	12
RC 400	8,4	1
RC 430	8,7	3
RC 460	9,0	20
RC 490	9,3	5
RC 520	9,6	3
RC 550	9,9	7
RC 580	10,2	150
RC 610	10,5	210
RC 640	10,8	340
RC 670	11,1	180
RC 700	11,4	19
RC 730	11,7	50
RC 760	12,0	32
RC 790	12,3	20
RD 30	12,7	15
RD 65	13,1	19
RD 90	13,3	350
RD 120	13,6	150
RD 150	13,9	30

RD 170	14,1	40
RD 200	14,4	25
RD 230	14,7	21
RD 260	15,0	10
RD 290	15,3	52
RD 310	15,5	10
RD 340	15,8	40
RD 370	16,1	50
RD 400	16,4	32
RD 430	16,7	41
RD 460	17,0	55
RD 490	17,3	60
RD 520	17,6	80
RD 550	17,9	280
RD 580	18,2	60
RD 610	18,5	210
RD 640	18,8	150
RD 670	19,1	180
RD 700	19,4	190

The datasets in this sheet are used for the cyclostratigraphy.
Outliers were removed.
Turbidites were taken out of stratigraphy.

Height (m)	$CaCO_3$ (wt%)	Height (m)	$\delta^{13}C_{org}$ (‰ VPDB)	Height (m)
0,0	10,92	0,00	-30,30	3,0
0,1	10,94	0,10	-30,32	3,1
0,2	31,90	0,20	-29,74	3,4
0,3	13,53	0,30	-29,77	3,5
0,4	14,41	0,40	-28,70	3,6
0,5	24,84	0,50	-30,10	3,7
0,6	19,61	0,60	-30,02	4,9
0,7	25,34	0,70	-28,92	5,1
0,8	13,77	0,75	-29,45	5,3
0,9	11,25	0,80	-29,85	5,4
1,0	18,81	0,90	-29,83	5,6
1,1	14,23	0,95	-29,58	5,7
1,2	14,42	1,00	-30,04	5,8
1,3	32,61	1,10	-29,71	5,9
1,4	19,65	1,15	-29,48	6,0
1,5	22,97	1,20	-29,93	6,1
1,6	31,43	1,40	-29,23	6,2
1,7	26,13	1,50	-28,85	6,4
1,8	25,99	1,55	-29,10	6,5
1,9	8,31	1,70	-27,58	6,6
2,0	8,00	1,80	-28,52	6,7
2,1	4,02	1,90	-30,77	6,8
2,2	10,33	2,00	-31,78	6,9
2,3	9,11	2,05	-30,02	7,0
2,4	6,43	2,10	-31,50	7,2
2,5	8,49	2,20	-31,02	7,3
2,6	13,81	2,30	-30,60	7,6
2,7	8,31	2,40	-30,32	7,7
2,8	26,77	2,50	-30,43	7,8
2,9	2,42	2,55	-29,83	8,2
3,0	13,43	2,60	-30,07	8,3
3,1	1,55	2,70	-29,98	8,4
3,2	2,54	2,80	-29,39	8,5
3,3	1,98	2,90	-30,11	8,6
3,4	2,19	3,00	-30,38	8,7
3,5	1,75	3,10	-30,50	8,8
3,6	8,57	3,15	-31,60	8,9
3,7	5,32	3,20	-30,86	9,0
3,8	4,75	3,30	-31,46	9,1
3,9	8,63	3,40	-32,03	9,2
4,0	19,86	3,50	-31,47	9,3
4,1	31,18	3,60	-32,45	9,6
4,2	34,01	3,70	-31,84	9,7
4,3	17,02	3,80	-31,35	9,8

4,4	9,22	3,90	-30,54	10,1
4,5	36,79	4,00	-30,75	10,3
4,6	14,34	4,10	-31,75	10,5
4,7	21,56	4,20	-31,58	10,6
4,8	35,67	4,30	-31,20	10,7
4,9	11,82	4,40	-31,23	10,8
5,0	15,17	4,50	-30,89	10,9
5,1	13,87	4,60	-30,74	11,0
5,2	14,68	4,70	-30,95	11,1
5,3	14,75	4,80	-30,57	11,2
5,4	20,13	4,90	-31,45	11,4
5,6	20,19	4,95	-31,32	11,5
5,7	19,50	5,00	-31,23	11,6
5,8	2,78	5,10	-31,39	11,7
5,9	18,42	5,20	-30,67	11,8
6,0	19,46	5,25	-30,91	11,9
6,1	20,04	5,30	-32,60	12,1
6,2	21,85	5,40	-31,18	12,3
6,3	18,47	5,50	-31,28	12,6
6,4	19,97	5,60	-31,90	12,8
6,5	2,76	5,70	-32,02	12,9
6,6	13,76	5,80	-31,39	13,0
6,7	12,28	5,90	-31,84	13,1
6,8	14,97	6,00	-31,39	13,2
6,9	15,73	6,10	-31,54	13,3
7,0	14,84	6,20	-31,65	13,5
7,1	16,87	6,30	-31,35	13,6
7,2	14,02	6,40	-31,56	13,8
7,3	16,09	6,50	-31,07	13,9
7,4	9,69	6,60	-31,57	14,0
7,5	12,42	6,70	-32,92	14,1
7,6	15,46	6,80	-32,33	14,2
7,7	20,22	6,90	-32,19	14,3
7,8	18,59	7,00	-32,15	14,4
7,9	28,70	7,20	-31,95	14,5
8,0	19,70	7,30	-31,34	14,6
8,1	19,92	7,40	-31,13	14,7
8,2	22,95	7,50	-32,32	14,8
8,3	15,81	7,60	-31,58	14,9
8,4	26,10	7,70	-31,19	15,0
8,5	18,67	7,80	-31,30	15,1
8,6	12,33	7,90	-31,14	15,2
8,7	14,17	8,00	-30,91	15,3
8,8	16,33	8,10	-30,90	15,4
8,9	18,29	8,20	-30,95	15,5
9,0	12,28	8,30	-31,20	15,7
9,1	17,24	8,40	-31,46	15,8
9,2	13,33	8,50	-32,75	16,1
9,3	12,75	8,60	-32,80	16,3
9,4	2,46	8,70	-32,11	16,3

9,5	1,51	8,90	-31,80
9,6	1,72	9,00	-30,66
9,7	7,31	9,10	-31,28
9,8	15,88	9,20	-30,76
9,9	18,32	9,30	-31,33
10,0	17,35	9,50	-31,97
10,1	40,05	9,60	-31,58
10,2	50,70	9,80	-31,58
10,3	34,30	10,00	-32,68
10,5	26,48	10,10	-31,74
10,6	22,49	10,40	-31,43
10,7	20,65	10,50	-31,28
10,8	17,61	10,70	-32,02
10,9	17,76	10,80	-31,09
11,0	22,65	10,90	-30,64
11,1	20,84	11,10	-30,87
11,2	25,33	11,20	-31,64
11,3	18,36	11,40	-31,82
11,4	10,94	11,50	-31,27
11,5	17,73	11,70	-32,43
11,6	22,56	11,80	-30,74
11,7	17,61	11,90	-30,75
11,8	14,25	12,00	-31,22
11,9	19,00	12,10	-31,56
12,0	18,01	12,20	-32,01
12,1	11,57	12,30	-31,69
12,2	15,70	12,40	-31,63
12,3	31,51	12,50	-32,12
12,4	51,77	12,70	-31,68
12,5	32,61	12,80	-31,75
12,6	24,22	12,90	-31,57
12,7	23,28	13,00	-31,67
12,8	24,08	13,10	-31,73
12,9	24,11	13,20	-31,70
13,0	21,15	13,30	-29,42
13,1	24,02	13,40	-31,69
13,2	25,12	13,50	-31,70
13,3	25,01	13,60	-31,42
13,4	21,90	13,70	-31,52
13,5	23,24	13,80	-31,23
13,6	19,18	13,90	-32,04
13,7	15,25	14,00	-31,38
13,8	16,02	14,10	-31,35
13,9	33,20	14,20	-31,89
14,0	17,87	14,30	-31,61
14,1	19,84	14,40	-31,11
14,2	21,87	14,50	-31,02
14,3	27,22	14,60	-31,65
14,4	36,50	14,70	-31,19
14,5	28,62	14,80	-31,05

14,6	24,90	14,90	-30,89	
14,7	28,33	14,95	-32,33	
14,8	27,86	15,00	-30,72	
14,9	26,14	15,10	-30,41	
15,0	18,47	15,20	-30,35	
15,1	17,84	15,30	-30,36	
15,2	20,64	15,40	-31,89	
15,3	19,78	15,50	-31,77	
15,4	25,82	15,60	-29,88	
15,5	18,25	15,70	-31,28	
15,6	14,47	15,80	-30,90	
15,7	11,03	15,90	-30,76	
15,8	16,41	16,00	-30,98	
15,9	19,27	16,10	-31,18	
16,0	10,89	16,30	-30,73	
16,1	25,37	16,40	-30,32	
16,2	16,23	16,50	-29,57	
16,3	25,71	16,60	-28,91	
16,4	25,45	16,70	-29,20	
16,5	11,66	16,80	-29,55	
16,6	24,38	16,90	-29,02	
16,7	32,38	17,00	-29,01	
16,8	35,01	17,10	-27,82	
16,9	36,36	17,20	-29,40	
17,0	39,26	17,30	-29,29	
17,1	50,43	17,40	-30,51	
17,2	27,92	17,50	-29,86	
17,3	28,92	17,60	-29,69	
17,4	30,00	17,70	-29,34	
17,5	30,84	17,80	-28,56	
17,6	26,39	18,00	-28,01	
17,7	24,14	18,10	-28,69	
17,8	27,93	18,20	-28,85	
17,9	35,25	18,30	-28,93	
18,0	36,50	18,40	-29,49	
18,1	33,71	18,50	-29,02	
18,2	35,30			
18,3	34,66			
18,4	35,55			
18,5	40,24			
Total # 184		**Total #** 180		**Total #**

FTIR CH2
0,000126
0,000094
0,000502
0,000847
0,000533
0,001161
0,000596
0,000658
0,000690
0,000533
0,000941
0,000753
0,001054
0,001443
0,000408
0,000502
0,000470
0,000345
0,000471
0,000941
0,000972
0,000691
0,000532
0,000721
0,001098
0,000376
0,000659
0,000283
0,000377
0,000376
0,000408
0,000502
0,000314
0,000659
0,000659
0,000471
0,000973
0,000690
0,000376
0,000313
0,000501
0,000497
0,000376
0,000883

0,000188
0,000189
0,000847
0,000315
0,000753
0,000502
0,000407
0,000878
0,000157
0,001129
0,000251
0,000784
0,000502
0,000659
0,000377
0,000440
0,000502
0,000251
0,000314
0,000345
0,000408
0,000355
0,000220
0,000345
0,000408
0,000278
0,000471
0,000408
0,000471
0,000189
0,000376
0,000910
0,000564
0,000125
0,000377
0,000439
0,000565
0,000596
0,000502
0,000345
0,000251
0,000439
0,000439
0,000156
0,000220
0,000439
0,000408
0,000220
0,000219
0,000219

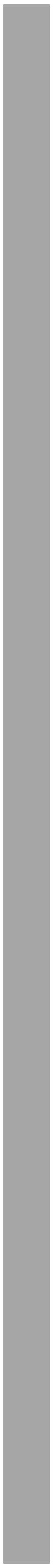

94

Sample	Height (m)	Si/Al	Ti/Al	Fe/Al	Mn/Al	Ca/Al	Mg/Al	K/Al
RA 00	0,0	2,8982	0,0547	0,7648	0,2882	0,5402		0,2092
RA 10	0,1	2,7333	0,0534	0,8519	0,5302	0,5425	0,1385	0,1980
RA 20	0,2	2,8537	0,0356	1,5332	0,4619	2,0274	0,2205	0,1838
RA 30	0,3	2,5924	0,0520	0,5608	0,1858	0,5387	0,0798	0,1819
RA 40	0,4	2,5877	0,0516	0,4545	0,1393	0,5948	0,0889	0,1945
RA 50	0,5	2,7174	0,0369	0,9170	0,3218	1,2761	0,1138	0,1708
RA 60	0,6	2,6160	0,0467	0,8365	0,4402	0,9560	0,1203	0,1942
RA 70	0,7	2,8239	0,0295	2,2876	0,6982	1,7888		0,1861
RA 80	0,8	2,3946	0,0460	0,5053	0,0463	0,5166	0,1136	0,1884
RA 90	0,9	2,9144	0,0546	0,6458	0,0385	0,6739		0,2574
RA 100	1,0	2,8536	0,0436	1,6402	0,6161	1,2525	0,1784	0,2000
RA 110	1,1	2,5375	0,0497	0,5125	0,0409	0,5674	0,0701	0,2023
RA 120	1,2	2,6084	0,0522	0,4765	0,0385	0,6225	0,1222	0,2099
RA 130	1,3	2,8277	0,0248	4,8012	0,5293	3,1392		0,1647
RA 140	1,4	2,4471	0,0442	0,4054	0,0551	0,7698	0,1780	0,1798
	1,5							
RA 160	1,6	2,5828	0,0452	0,4787	0,0277	0,9700		0,1925
RA 170	1,7	2,6642	0,0323	1,3140	0,0750	1,7982		0,1917
RA 180	1,8	2,5078	0,0431	0,4980	0,0344	1,1180	0,1145	0,1917
RA 190	1,9	2,2641	0,0314	0,7808	0,0422	0,9404	0,1233	0,1469
RA 200	2,0	2,5787	0,0603	0,5468	0,0449	0,4354	0,0800	0,2333
RA 210	2,1	2,7878	0,0686	0,5429	0,0286	0,3764	0,1258	0,2212
RA 220	2,2	2,8306	0,0552	1,0632	0,0500	0,1896	0,1609	0,1983
RA 230	2,3	2,7607	0,0443	1,1146	0,2358	0,4910	0,1946	0,1739
RA 240	2,4	2,6156	0,0514	0,9505	0,0959	0,4032	0,1581	0,1784
RA 250	2,5	2,6512	0,0368	1,1574	0,1021	0,2890	0,1628	0,1826
RA 260	2,6	2,5469	0,0517	0,8354	0,0573	0,3621	0,1431	0,1737
RA 270	2,7	2,7834	0,0512	0,8331	0,1687	0,6944	0,1536	0,1902
RA 280	2,8	2,5767	0,0516	0,8720	0,1645	0,3654	0,1297	0,1894
RA 290	2,9	3,3702	0,0273	3,2835	0,3033	2,1170	0,2362	0,1620
RA 300	3,0	2,6190	0,0600	0,7364	0,1884	0,1026	0,1659	0,1816
RA 310	3,1	2,5647	0,0493	0,5204	0,1319	0,5778	0,1485	0,1871
RA 320	3,2	2,6574	0,0411	1,1302	0,1444	0,0688	0,1366	0,1794
RB 90	3,3	2,6100	0,0573	0,6900	0,0110	0,1040	0,1327	0,1853
RB 100	3,4	2,5999	0,0562	0,7734	0,0212	0,0818	0,1403	0,1734
RB 110	3,5	2,5413	0,0559	0,8386	0,0196	0,0906	0,1538	0,1707
RB 120	3,6	2,5014	0,0569	0,8594	0,0284	0,0716	0,1518	0,1686
RB 130	3,7	3,1431	0,0707	0,8359	0,0188	0,5176	0,1709	0,2305
RB 140	3,8	2,5118	0,0546	0,7165	0,0198	0,2199	0,1368	0,1932
RB 150	3,9	2,5139	0,0553	0,7438	0,0145	0,1961	0,1493	0,1794
RB 160	4,0	2,5971	0,0507	0,7585	0,1362	0,3757	0,1676	0,1796
RB 170	4,1	2,9904	0,0374	1,5464	0,2776	1,1117	0,1642	0,1824
RB 180	4,2	3,3385	0,0205	3,6052	0,3355	2,4109	0,2233	0,1441
RB 190	4,3	2,6428	0,0322	0,7558	0,0863	1,7829	0,1656	0,1744
RB 200	4,4	2,5850	0,0466	0,7864	0,1326	0,7730	0,1654	0,1789
RB 210	4,5	2,5854	0,0491	0,7745	0,0545	0,3958	0,1446	0,1822
RB 220	4,6	2,4816	0,0331	0,7050	0,0503	1,9321	0,2107	0,1689
RB 230	4,7	2,5739	0,0515	0,8212	0,0445	0,6387	0,1670	0,1792
RB 240	4,8	2,6072	0,0449	0,7707	0,3540	1,0169	0,1427	0,1813

RB 250	4,9	2,5841	0,0558	0,6349	0,0548	1,9264	0,1926	0,1592
RB 260	5,0	2,5057	0,0497	0,6912	0,0505	0,5069	0,1587	0,1823
RB 270	5,1	2,5413	0,0520	0,6392	0,0648	0,6640	0,1681	0,1737
RB 280	5,2	2,5077	0,0510	0,6077	0,0746	0,5992	0,1498	0,1788
RB 290	5,3	2,6169	0,0497	0,6776	0,1266	0,6565	0,1651	0,1832
RB 300	5,4	2,6691	0,0480	0,7146	0,0365	0,6802	0,1555	0,1802
RC 110	5,5	2,5739	0,0430	0,6750	0,0625	0,9673	0,1788	0,1754
	5,6							
RC 130	5,7	2,5345	0,0408	0,7474	0,0371	0,9632	0,1768	0,1588
RC 140	5,8	2,9067	0,0491	0,6219	0,0165	1,0104	0,1595	0,1860
RC 150	5,9	2,7200	0,0409	1,1824	0,0380	0,1244	0,1604	0,1883
RC 160	6,0	3,2553	0,0535	0,7945	0,0310	1,0748	0,1580	0,2091
	6,1							
	6,2							
RC 190	6,3	2,7394	0,0502	0,6192	0,0478	0,9361	0,1550	0,1906
RC 200	6,4	2,7163	0,0461	0,5977	0,0482	0,9295	0,1288	0,1845
RC 210	6,5	2,5415	0,0376	0,4807	0,0198	1,0388	0,1997	0,1726
RC 220	6,6	2,6949	0,0472	0,6023	0,0314	0,8497	0,1347	0,1905
RC 230	6,7	2,7842	0,0469	0,5966	0,0294	0,9868	0,1509	0,1971
RC 240	6,8	2,6380	0,0561	1,0468	0,0371	0,1196	0,1524	0,1890
RC 250	6,9	3,1230	0,0577	0,7178	0,0234	0,8330	0,1222	0,2317
RC 260	7,0	3,0728	0,0570	0,8309	0,0132	0,6903	0,1302	0,2107
RC 270	7,1	2,7895	0,0527	0,5336	0,0179	0,7503	0,1599	0,1896
RC 280	7,2	3,5242	0,0629	0,7687	0,0220	1,2286	0,1425	0,2543
RC 290	7,3	3,3194	0,0668	0,6616	0,0203	0,9808	0,1266	0,2404
RC 300	7,4	3,0596	0,0518	0,6476	0,0199	0,9297	0,1376	0,2028
RC 310	7,5	2,8303	0,0509	0,6394	0,0136	0,6833	0,1504	0,1972
RC 320	7,6	2,6550	0,0431	0,7302	0,0373	0,7241	0,1512	0,1877
RC 330	7,7	3,1346	0,0499	1,1931	0,1283	0,5882	0,1702	0,2260
RC 340	7,8	2,8683	0,0467	0,8821	0,0790	0,6157	0,1549	0,2071
RC 350	7,9	2,8508	0,0432	0,7024	0,0255	0,7687	0,1663	0,1934
RC 360	8,0	2,7459	0,0414	0,6573	0,0968	0,9706	0,1659	0,1956
RC 370	8,1	2,6389	0,0426	0,5856	0,0300	0,8405	0,1646	0,1877
RC 380	8,2	3,1540	0,0470	0,7556	0,1245	1,9211	0,1203	0,2348
RC 390	8,3	2,9218	0,0376	0,7510	0,1044	1,1476	0,1760	0,2095
RC 400	8,4	3,6820	0,0405	0,8349	0,0797	1,6190	0,1526	0,2656
RC 410	8,5	2,7012	0,0361	0,6417	0,0327	1,0755	0,1712	0,1821
RC 420	8,6	2,8055	0,0417	0,8282	0,0252	0,7791	0,1597	0,1915
RC 430	8,7	3,7030	0,0501	0,7224	0,0359	2,3370	0,1826	0,2781
RC 440	8,8	3,0481	0,0511	0,7324	0,0149	1,1446	0,1370	0,2190
RC 450	8,9	3,0888	0,0573	0,7400	0,0118	0,6851	0,1420	0,2217
RC 460	9,0	3,4075	0,0663	0,7999	0,0167	0,9135	0,1438	0,2481
RC 470	9,1	3,2793	0,0614	0,7746	0,0243	1,0141	0,1261	0,2336
RC 480	9,2	3,4004	0,0542	0,7932	0,0720	1,1185	0,1505	0,2154
RC 490	9,3	2,9616	0,0524	0,8092	0,0225	0,6180	0,1369	0,2023
RC 500	9,4	2,8062	0,0515	0,5992	0,0454	0,8684	0,1046	0,1929
RC 510	9,5	3,0659	0,0507	0,7660	0,0706	0,6876	0,1390	0,2045
RC 520	9,6	3,1068	0,0500	0,6060	0,0124	0,6305	0,1485	0,1873
RC 530	9,7	2,2707	0,0614	0,5237	0,0062	0,0915	0,1116	0,1603
RC 540	9,8	2,6440	0,0611	0,4827	0,0089	0,0605	0,1286	0,1883

RC 550	9,9	2,5341	0,0617	0,4734	0,0087	0,0674	0,1196	0,1769
RC 560	10,0	2,6264	0,0572	0,4597	0,0134	0,3015	0,1319	0,1772
	10,1							
RC 580	10,2	2,6814	0,0496	0,4921	0,0145	0,7324	0,1278	0,1937
RC 590	10,3	2,5713	0,0427	0,4085	0,0178	0,7902	0,1405	0,1770
RC 600	10,4	2,9214	0,0481	0,6393	0,0261	0,8948	0,1413	0,1852
RC 610	10,5	3,5291	0,0426	0,5036	0,0537	2,8737	0,1666	0,1828
	10,6							
	10,7							
RC 640	10,8	3,2312	0,0370	0,5401	0,0456	4,0291	0,2466	0,1781
	10,9							
RC 660	11,0	2,6263	0,0497	0,5374	0,0272	1,9848	0,1657	0,1668
	11,1							
RC 680	11,2	3,0202	0,0506	0,6600	0,0174	1,6023	0,1671	0,1980
RC 690	11,3	2,8530	0,0489	0,6368	0,0184	1,1811	0,1146	0,1809
RC 700	11,4	3,4363	0,0480	0,8466	0,0137	1,2573	0,1661	0,2062
RC 710	11,5	2,9015	0,0540	0,5966	0,0131	0,8540	0,1443	0,1853
RC 720	11,6	3,0483	0,0546	0,5628	0,0148	0,9056	0,1466	0,1865
RC 730	11,7	3,2252	0,0517	0,4884	0,0114	1,2723	0,1683	0,1911
RC 740	11,8	2,9099	0,0470	0,3774	0,0084	1,0070	0,1502	0,1792
RC 750	11,9	3,1079	0,0469	0,5940	0,0176	1,3838	0,1411	0,1848
RC 760	12,0	3,1195	0,0542	0,4495	0,0132	0,9662	0,1414	0,1900
RC 770	12,1	3,7518	0,0730	0,7765	0,0346	0,7584	0,1428	0,2486
RC 780	12,2	3,2608	0,0655	0,5965	0,0225	1,0786	0,1329	0,2313
RC 790	12,3	3,4572	0,0585	0,6924	0,0225	1,5367	0,1603	0,2220
RC 800	12,4	3,1988	0,0608	0,6016	0,0094	1,0689	0,1250	0,2068
RD 10	12,5	3,1648	0,0575	0,4633	0,0074	0,7649	0,1364	0,2011
RD 20	12,6	3,3230	0,0559	0,4331	0,0100	1,0981	0,1505	0,1970
RD 30	12,7	3,5696	0,0545	0,5456	0,0111	1,0579	0,1474	0,1944
RD 40	12,8	3,1238	0,0542	0,4379	0,0064	0,5638	0,1202	0,1885
	12,9							
	13,0							
RD 70	13,1	2,7720	0,0494	0,3959	0,0090	0,7167	0,1310	0,1876
RD 80	13,2	2,8724	0,0455	0,4658	0,0131	1,7235	0,1557	0,1668
RD 90	13,3	3,9115	0,0529	0,5319	0,0527	4,3809	0,1891	0,2682
RD 100	13,4	3,4052	0,0516	0,7255	0,0190	2,0956	0,1651	0,1725
RD 110	13,5	3,4585	0,0474	0,9398	0,0251	1,5079	0,1376	0,1959
RD 120	13,6	2,7826	0,0521	0,5354	0,0186	1,1456	0,1421	0,1836
RD 130	13,7	2,6702	0,0466	0,4476	0,0094	1,1008	0,1534	0,1740
RD 140	13,8	2,7884	0,0496	0,4865	0,0122	1,1826	0,1390	0,1816
RD 150	13,9	2,7402	0,0493	0,4927	0,0109	0,9643	0,1283	0,1761
RD 160	14,0	2,7743	0,0460	0,5150	0,0129	1,1838	0,1404	0,1835
RD 170	14,1	2,7127	0,0451	0,4759	0,0122	1,1746	0,1457	0,1749
RD 180	14,2	2,7636	0,0482	0,5133	0,0125	1,2290	0,1484	0,1866
RD 190	14,3	2,6675	0,0448	0,4832	0,0106	0,9887	0,1443	0,1806
RD 200	14,4	2,8447	0,0475	0,5360	0,0129	1,1516	0,1488	0,1926
RD 210	14,5	3,0255	0,0552	0,5546	0,0139	1,0135	0,1421	0,1791
RD 220	14,6	3,1944	0,0588	0,7651	0,0246	0,9140	0,1662	0,1964
RD 230	14,7	3,1519	0,0609	0,6819	0,0179	0,9932	0,1346	0,2019
RD 240	14,8	3,3792	0,0475	0,6274	0,0163	2,7069	0,1673	0,2103

RD 250	14,9	2,9686	0,0557	0,5967	0,0110	0,9617	0,1258	0,1796
RD 260	15,0	2,8958	0,0485	0,6178	0,0113	1,0469	0,1279	0,1864
RD 270	15,1	3,3745	0,0484	0,6335	0,0123	1,5532	0,1645	0,2227
RD 280	15,2	3,4511	0,0522	0,7594	0,0197	1,9012	0,1360	0,1932
RD 290	15,3	3,5221	0,0439	0,5537	0,0318	2,6152	0,1309	0,1788
RD 300	15,4	3,6881	0,0495	0,6631	0,0258	2,2126	0,1716	0,2088
RD 310	15,5	3,6274	0,0515	0,5681	0,0190	1,9147	0,1809	0,2170
RD 320	15,6	3,0573	0,0472	0,5265	0,0147	1,5834	0,1259	0,1744
RD 330	15,7	3,3032	0,0501	0,5511	0,0248	1,8085	0,1767	0,1874
RD 340	15,8	3,4832	0,0512	0,5597	0,0189	1,7634	0,1520	0,1874
RD 350	15,9	3,1366	0,0531	0,5338	0,0148	1,0192	0,1398	0,1881
RD 360	16,0	3,0993	0,0519	0,5746	0,0185	0,9653	0,1409	0,1821
RD 370	16,1	3,2691	0,0543	0,5833	0,0148	1,2070	0,1633	0,1951
RD 380	16,2	2,9478	0,0459	0,6331	0,0205	1,0108	0,1401	0,1861
RD 390	16,3	3,2925	0,0514	0,6820	0,0233	1,5964	0,1235	0,1870
RD 400	16,4	3,3017	0,0562	0,6126	0,0172	1,0340	0,1373	0,1813
RD 410	16,5	2,7339	0,0521	0,5459	0,0220	0,6382	0,1402	0,1722
RD 420	16,6	3,3147	0,0587	0,7993	0,0114	0,6175	0,1273	0,1954
RD 430	16,7	3,1952	0,0584	0,5366	0,0120	0,9059	0,1373	0,1922
RD 440	16,8	3,3095	0,0547	0,6043	0,0158	1,1140	0,1491	0,1895
RD 450	16,9	3,6175	0,0594	0,6462	0,0335	0,6407	0,1323	0,2120
RD 460	17,0	3,6274	0,0506	0,6345	0,0290	1,8130	0,1633	0,2059
RD 470	17,1	2,9328	0,0513	0,7157	0,0230	0,8171	0,1360	0,1770
RD 480	17,2	3,2406	0,0432	0,7041	0,0326	1,5899	0,1251	0,2049
RD 490	17,3	3,1256	0,0443	0,6127	0,0306	1,3986	0,1646	0,1986
RD 500	17,4	2,9360	0,0498	0,8535	0,0238	0,5411	0,1403	0,1905
RD 510	17,5	3,3797	0,0564	0,8422	0,0370	1,6473	0,1294	0,2388
RD 520	17,6	3,8668	0,0452	1,2718	0,1309	2,5897	0,1749	0,2446
RD 530	17,7	3,3867	0,0397	0,6846	0,0531	2,3499	0,1217	0,2170
RD 540	17,8	3,4428	0,0471	0,8717	0,0959	2,7547	0,1973	0,2191
RD 550	17,9	3,2236	0,0382	0,8983	0,0784	2,7567	0,1893	0,2042
RD 560	18,0	3,5491	0,0248	0,7258	0,1565	5,0508	0,2140	0,2424
	18,1							
RD 580	18,2	3,9221	0,0540	1,1771	0,1763	2,7398	0,1647	0,2871
RD 590	18,3	3,2142	0,0382	0,7423	0,0582	1,6600	0,1161	0,1910
RD 600	18,4	3,6216	0,0562	0,8812	0,0439	2,5347	0,1845	0,2843
RD 610	18,5	3,3520	0,0408	0,6105	0,0319	1,8600	0,1611	0,1954
RD 620	18,6	3,0723	0,0415	0,6969	0,0397	1,4140	0,1629	0,1933
RD 630	18,7	2,7535	0,0453	0,4540	0,0320	1,1143	0,1229	0,1690
RD 640	18,8	2,8781	0,0433	0,6894	0,0762	1,5917	0,1341	0,1805
RD 650	18,9	2,8558	0,0390	0,6450	0,0750	1,9237	0,1460	0,1755
RD 660	19,0	2,9768	0,0379	0,5403	0,0803	2,0903	0,1369	0,1750
RD 670	19,1	2,7824	0,0350	0,5932	0,0963	1,7391	0,1312	0,1698
RD 680	19,2	2,8899	0,0355	0,5661	0,0761	1,8331	0,1428	0,1682
RD 690	19,3	3,0693	0,0343	0,6516	0,1447	1,9776	0,1656	0,1710
RD 700	19,4	3,3995	0,0374	0,6868	0,0617	2,2919	0,1795	0,1793
RD 710	19,5	3,4925	0,0333	0,8174	0,4032	2,7716	0,1421	0,1676
ASWedepohl		6,2302	0,1058	0,5454	0,0192	0,3560	0,3553	0,3382

P/Al	Zr/Al	Th/Al	Nb/Al	Sr/Al	Rb/Al	Pb/Al	Ba/Al
	0,0022	0,0002	0,0002	0,0039	0,0007	0,0006	0,0116
0,0088	0,0018	0,0002	0,0002	0,0036	0,0007	0,0005	0,0127
0,0390	0,0011		0,0002	0,0090	0,0006	0,0003	0,0204
0,0087	0,0019	0,0001	0,0002	0,0037	0,0006	0,0005	0,0088
0,0051	0,0020	0,0002	0,0002	0,0035	0,0007	0,0005	0,0094
0,1416	0,0014		0,0004	0,0084	0,0006	0,0004	0,0143
0,0086	0,0016		0,0002	0,0034	0,0007	0,0004	0,0098
0,0363	0,0011		0,0002	0,0059	0,0005	0,0003	0,0117
0,0050	0,0020	0,0001	0,0001	0,0045	0,0007	0,0004	0,0080
0,0069	0,0024	0,0002	0,0002	0,0078	0,0009	0,0005	0,0106
0,0069	0,0016		0,0002	0,0050	0,0007	0,0003	0,0221
0,0137	0,0023	0,0002	0,0002	0,0049	0,0007	0,0005	0,0082
0,0066	0,0025	0,0002	0,0002	0,0046	0,0008	0,0004	0,0086
0,0133	0,0010		0,0002	0,0079	0,0006		0,0356
0,0075	0,0021	0,0001	0,0002	0,0047	0,0006	0,0004	0,0078
0,0048	0,0021	0,0001	0,0001	0,0046	0,0006	0,0003	0,0082
0,2737	0,0015		0,0004	0,0087	0,0006	0,0003	0,0147
0,0064	0,0018	0,0002	0,0001	0,0051	0,0006	0,0004	0,0081
0,0164	0,0010		0,0001	0,0032	0,0004	0,0002	0,0077
0,0085	0,0025	0,0002	0,0002	0,0040	0,0009	0,0003	0,0088
0,0081	0,0033	0,0002	0,0002	0,0039	0,0008	0,0003	0,0083
0,0036	0,0027	0,0002	0,0002	0,0026	0,0007	0,0012	0,0120
0,0084	0,0014		0,0002	0,0020	0,0006	0,0005	0,0122
0,0073	0,0021	0,0002	0,0002	0,0030	0,0011	0,0006	0,0092
0,0097	0,0013		0,0002	0,0017	0,0006	0,0005	0,0064
0,0047	0,0021	0,0002	0,0001	0,0028	0,0012	0,0006	0,0089
0,0051	0,0025	0,0002	0,0002	0,0042	0,0007	0,0006	0,0098
0,0065	0,0021	0,0002	0,0002	0,0029	0,0007	0,0009	0,0078
0,0288	0,0011		0,0002	0,0067	0,0005		0,0111
0,0050	0,0021	0,0002	0,0002	0,0021	0,0013	0,0004	0,0077
0,0095	0,0020	0,0002	0,0002	0,0039	0,0012	0,0003	0,0075
0,0051	0,0014		0,0002	0,0013	0,0006	0,0008	0,0054
0,0066	0,0023	0,0002	0,0002	0,0024	0,0012	0,0006	0,0066
0,0099	0,0023	0,0002	0,0002	0,0025	0,0007	0,0006	0,0078
0,0090	0,0023	0,0002	0,0002	0,0024	0,0006	0,0006	0,0071
0,0054	0,0021	0,0002	0,0002	0,0024	0,0006	0,0005	0,0078
0,0155	0,0031	0,0002	0,0003	0,0047	0,0009	0,0007	0,0086
0,0068	0,0023	0,0002	0,0002	0,0027	0,0007	0,0006	0,0068
0,0082	0,0024	0,0002	0,0002	0,0027	0,0012	0,0005	0,0074
0,0056	0,0022	0,0002	0,0002	0,0033	0,0006	0,0005	0,0098
0,0142	0,0012		0,0002	0,0045	0,0006		0,0079
0,0152	0,0008		0,0001	0,0067	0,0004		0,0113
0,0337	0,0016	0,0002	0,0002	0,0111	0,0005	0,0005	0,0109
0,0123	0,0019	0,0002	0,0002	0,0068	0,0005	0,0004	0,0092
0,0079	0,0021	0,0002	0,0002	0,0036	0,0012	0,0004	0,0073
0,0257	0,0020	0,0001	0,0002	0,0103	0,0005	0,0003	0,0116
0,0125	0,0023	0,0001	0,0001	0,0049	0,0012	0,0005	0,0088
0,0066	0,0014		0,0001	0,0043	0,0006	0,0002	0,0108

0,0127	0,0039	0,0001	0,0002	0,0072	0,0005	0,0005	0,0124
0,0105	0,0022	0,0002	0,0002	0,0037	0,0012	0,0005	0,0067
0,0115	0,0023	0,0001	0,0002	0,0045	0,0012	0,0005	0,0077
0,0114	0,0021	0,0002	0,0001	0,0043	0,0006	0,0005	0,0078
0,0153	0,0023	0,0002	0,0002	0,0057	0,0006	0,0005	0,0077
0,0086	0,0021	0,0002	0,0002	0,0059	0,0006	0,0005	0,0082
0,0128	0,0017	0,0001	0,0001	0,0060	0,0010	0,0004	0,0082
0,0130	0,0017	0,0002	0,0001	0,0056	0,0005	0,0004	0,0088
0,0097	0,0019	0,0002	0,0002	0,0051	0,0006	0,0004	0,0068
0,0081	0,0012	0,0002	0,0002	0,0018	0,0006	0,0004	0,0082
0,0163	0,0025	0,0002	0,0002	0,0055	0,0007	0,0004	0,0079
0,0092	0,0021	0,0002	0,0002	0,0053	0,0007	0,0005	0,0088
0,0072	0,0019	0,0002	0,0002	0,0052	0,0006	0,0004	0,0086
0,0071	0,0016	0,0002	0,0001	0,0058	0,0006	0,0004	0,0082
0,0082	0,0018	0,0001	0,0002	0,0049	0,0006	0,0005	0,0084
0,0063	0,0021	0,0002	0,0001	0,0056	0,0007	0,0004	0,0090
0,0120	0,0020	0,0002	0,0002	0,0027	0,0013	0,0004	0,0083
0,0073	0,0024	0,0002	0,0002	0,0051	0,0008	0,0007	0,0082
0,0146	0,0024	0,0002	0,0002	0,0047	0,0007	0,0006	0,0067
0,0067	0,0024	0,0001	0,0002	0,0049	0,0007	0,0005	0,0073
0,0110	0,0030	0,0003	0,0002	0,0079	0,0009	0,0007	0,0105
0,0116	0,0026	0,0002	0,0002	0,0074	0,0008	0,0006	0,0072
0,0122	0,0025	0,0002	0,0002	0,0067	0,0007	0,0006	0,0080
0,0090	0,0019	0,0002	0,0002	0,0046	0,0007	0,0005	0,0070
0,0083	0,0017	0,0002	0,0001	0,0045	0,0010	0,0004	0,0081
0,0092	0,0016		0,0002	0,0031	0,0008	0,0004	0,0121
0,0133	0,0019	0,0002	0,0002	0,0042	0,0007	0,0005	0,0101
0,0073	0,0019	0,0001	0,0002	0,0049	0,0007	0,0004	0,0085
0,0095	0,0018	0,0002	0,0002	0,0070	0,0006	0,0004	0,0086
0,0081	0,0019	0,0001	0,0002	0,0056	0,0006	0,0004	0,0078
0,0118	0,0021	0,0002	0,0002	0,0132	0,0008	0,0005	0,0115
0,0076	0,0019	0,0002	0,0002	0,0097	0,0007	0,0005	0,0130
0,0108	0,0018		0,0002	0,0095	0,0009	0,0004	0,0188
0,0095	0,0016	0,0002	0,0002	0,0083	0,0010	0,0003	0,0098
0,0084	0,0019	0,0001	0,0002	0,0044	0,0006	0,0004	0,0112
0,0113	0,0035	0,0002	0,0002	0,0172	0,0010	0,0005	0,0172
0,0059	0,0027	0,0002	0,0002	0,0081	0,0008	0,0005	0,0100
0,0066	0,0025	0,0002	0,0002	0,0062	0,0008	0,0006	0,0074
0,0075	0,0031	0,0002	0,0003	0,0069	0,0009	0,0007	0,0094
0,0107	0,0028	0,0002	0,0002	0,0070	0,0008	0,0007	0,0106
0,0132	0,0023	0,0002	0,0002	0,0077	0,0007	0,0006	0,0093
0,0078	0,0021	0,0001	0,0002	0,0047	0,0007	0,0006	0,0085
0,0079	0,0019	0,0002	0,0002	0,0068	0,0007	0,0005	0,0086
0,0067	0,0021	0,0002	0,0002	0,0062	0,0007	0,0005	0,0094
0,0093	0,0019	0,0002	0,0002	0,0054	0,0006	0,0005	0,0082
0,0039	0,0025	0,0002	0,0002	0,0020	0,0006	0,0005	0,0062
0,0055	0,0026	0,0002	0,0002	0,0022	0,0013	0,0005	0,0058

0,0048	0,0024	0,0002	0,0002	0,0021	0,0007	0,0006	0,0070
0,0059	0,0023	0,0001	0,0002	0,0031	0,0012	0,0005	0,0109
0,0065	0,0022	0,0002	0,0002	0,0046	0,0007	0,0005	0,0085
0,0086	0,0014	0,0001	0,0002	0,0052	0,0011	0,0004	0,0142
0,0130	0,0021	0,0002	0,0002	0,0048	0,0006	0,0004	0,0078
0,0155	0,0022	0,0002	0,0002	0,0106	0,0005	0,0005	0,0130
0,0201	0,0021	0,0001	0,0002	0,0145	0,0005	0,0004	0,0139
0,0158	0,0019	0,0001	0,0002	0,0080	0,0006	0,0005	0,0092
0,0197	0,0023	0,0002	0,0002	0,0074	0,0006	0,0004	0,0083
0,0225	0,0020	0,0002	0,0002	0,0061	0,0006	0,0004	0,0085
0,0227	0,0025	0,0002	0,0002	0,0066	0,0006	0,0005	0,0099
0,0130	0,0023	0,0002	0,0002	0,0049	0,0006	0,0004	0,0076
0,0127	0,0024	0,0002	0,0002	0,0051	0,0007	0,0006	0,0072
0,0134	0,0024	0,0002	0,0002	0,0065	0,0007	0,0006	0,0099
0,0101	0,0021	0,0002	0,0002	0,0050	0,0006	0,0003	0,0072
0,0140	0,0022	0,0002	0,0002	0,0131	0,0006	0,0004	0,0083
0,0154	0,0023	0,0002	0,0002	0,0056	0,0006	0,0005	0,0078
0,0096	0,0030	0,0003	0,0003	0,0060	0,0009	0,0007	0,0104
0,0138	0,0027	0,0002	0,0002	0,0066	0,0008	0,0006	0,0098
0,0215	0,0034	0,0002	0,0002	0,0083	0,0007	0,0006	0,0128
0,0125	0,0028	0,0002	0,0002	0,0058	0,0007	0,0006	0,0093
0,0135	0,0024	0,0002	0,0002	0,0050	0,0007	0,0005	0,0067
0,0109	0,0022	0,0001	0,0002	0,0058	0,0007	0,0005	0,0075
0,0154	0,0029	0,0002	0,0002	0,0064	0,0006	0,0004	0,0073
0,0124	0,0020	0,0001	0,0002	0,0040	0,0006	0,0005	0,0058
0,0076	0,0021	0,0001	0,0002	0,0041	0,0006	0,0004	0,0066
0,0122	0,0027	0,0002	0,0002	0,0074	0,0006	0,0004	0,0085
0,0176	0,0047	0,0002	0,0002	0,0179	0,0005	0,0003	0,0179
0,0129	0,0030	0,0002	0,0002	0,0089	0,0006	0,0004	0,0119
0,0204	0,0023	0,0002	0,0002	0,0077	0,0006	0,0006	0,0134
0,0109	0,0024	0,0002	0,0002	0,0062	0,0006	0,0004	0,0080
0,0095	0,0019	0,0001	0,0002	0,0057	0,0010	0,0004	0,0103
0,0100	0,0020	0,0001	0,0002	0,0059	0,0006	0,0004	0,0073
0,0104	0,0019	0,0002	0,0002	0,0050	0,0006	0,0004	0,0068
0,0079	0,0019	0,0002	0,0002	0,0061	0,0006	0,0004	0,0079
0,0093	0,0019	0,0002	0,0002	0,0058	0,0006	0,0004	0,0073
0,0111	0,0021	0,0002	0,0002	0,0061	0,0006	0,0005	0,0069
0,0092	0,0019	0,0002	0,0002	0,0054	0,0011	0,0004	0,0068
0,0106	0,0019	0,0001	0,0002	0,0062	0,0006	0,0005	0,0076
0,0113	0,0025	0,0002	0,0002	0,0066	0,0006	0,0004	0,0068
0,0177	0,0025	0,0006	0,0003	0,0068	0,0006	0,0006	0,0096
0,0152	0,0026	0,0002	0,0002	0,0061	0,0007	0,0006	0,0089
0,0192	0,0027	0,0001	0,0002	0,0202	0,0007	0,0006	0,0117

0,0101	0,0024	0,0002	0,0002	0,0067	0,0006	0,0004	0,0085
0,0100	0,0021	0,0002	0,0002	0,0072	0,0007	0,0004	0,0073
0,0227	0,0029	0,0002	0,0003	0,0114	0,0007	0,0006	0,0169
0,0214	0,0031	0,0002	0,0002	0,0114	0,0006	0,0005	0,0116
0,0139	0,0028	0,0002	0,0002	0,0162	0,0005	0,0004	0,0123
0,0195	0,0028	0,0002	0,0003	0,0120	0,0007	0,0006	0,0116
0,0238	0,0024	0,0002	0,0002	0,0124	0,0007	0,0006	0,0110
0,0138	0,0020	0,0001	0,0002	0,0117	0,0006	0,0005	0,0093
0,0144	0,0024	0,0002	0,0002	0,0087	0,0006	0,0005	0,0098
0,0189	0,0028	0,0002	0,0002	0,0085	0,0007	0,0005	0,0097
0,0127	0,0024	0,0002	0,0002	0,0058	0,0006	0,0005	0,0083
0,0109	0,0024	0,0002	0,0002	0,0055	0,0006	0,0006	0,0079
0,0127	0,0024	0,0002	0,0002	0,0065	0,0006	0,0005	0,0076
0,0074	0,0020	0,0001	0,0002	0,0055	0,0006	0,0005	0,0192
0,0186	0,0023	0,0001	0,0002	0,0080	0,0006	0,0005	0,0099
0,0152	0,0024	0,0002	0,0002	0,0058	0,0006	0,0006	0,0087
0,0083	0,0020	0,0002	0,0002	0,0047	0,0010	0,0004	0,0073
0,0240	0,0028	0,0002	0,0002	0,0048	0,0007	0,0005	0,0078
0,0180	0,0027	0,0002	0,0002	0,0054	0,0007	0,0004	0,0079
0,0168	0,0025	0,0002	0,0002	0,0059	0,0007	0,0005	0,0082
0,0152	0,0027	0,0002	0,0002	0,0050	0,0007	0,0005	0,0079
0,0187	0,0027	0,0002	0,0002	0,0082	0,0007	0,0005	0,0105
0,0123	0,0022	0,0002	0,0002	0,0045	0,0006	0,0004	0,0081
0,0116	0,0024	0,0002	0,0002	0,0068	0,0007	0,0004	0,0237
0,0146	0,0023	0,0002	0,0002	0,0070	0,0006	0,0004	0,0097
0,0061	0,0019	0,0002	0,0002	0,0038	0,0006	0,0005	0,0082
0,0065	0,0024	0,0002	0,0002	0,0089	0,0008	0,0006	0,0114
0,0201	0,0016		0,0002	0,0087	0,0008	0,0003	0,0166
0,0151	0,0020	0,0002	0,0002	0,0100	0,0006	0,0004	0,0139
0,0072	0,0028	0,0002	0,0002	0,0125	0,0007	0,0004	0,0140
0,0088	0,0022	0,0002	0,0002	0,0123	0,0006	0,0005	0,0148
0,0127	0,0010		0,0001	0,0118	0,0005	0,0003	0,0240
0,0129	0,0017		0,0003	0,0083	0,0009	0,0005	0,0202
0,0096	0,0019	0,0002	0,0002	0,0074	0,0006	0,0005	0,0112
0,0173	0,0023	0,0002	0,0003	0,0113	0,0009	0,0005	0,0131
0,0084	0,0020	0,0002	0,0002	0,0080	0,0006	0,0004	0,0110
0,0069	0,0019	0,0002	0,0002	0,0072	0,0006	0,0006	0,0101
0,0055	0,0020	0,0002	0,0002	0,0053	0,0006	0,0004	0,0074
0,0073	0,0024	0,0002	0,0002	0,0094	0,0006	0,0005	0,0132
0,0111	0,0020	0,0002	0,0002	0,0112	0,0006	0,0004	0,0099
0,0099	0,0018	0,0002	0,0002	0,0146	0,0005	0,0004	0,0118
0,0111	0,0016	0,0002	0,0002	0,0118	0,0005	0,0004	0,0101
0,0098	0,0016	0,0002	0,0002	0,0103	0,0005	0,0004	0,0093
0,0134	0,0016	0,0002	0,0002	0,0099	0,0005	0,0006	0,0110
0,0167	0,0017	0,0002	0,0002	0,0109	0,0005	0,0004	0,0110
0,0163	0,0012		0,0002	0,0081	0,0005	0,0004	0,0353
0,0079	0,0036	0,0003	0,0004	0,0068	0,0032	0,0005	0,0131

Mo/Al	As/Al	Zn/Al	Cu/Al	Cr/Al	SiO2	Al2O3	CaO	CaCO3
0,0000	0,0003	0,0011	0,0006	0,0027	50,15	15,28	6,11	10,92
	0,0008	0,0011	0,0006	0,0030	47,19	15,25	6,12	10,94
	0,0006	0,0011			38,42	11,89	17,85	31,90
	0,0003	0,0009	0,0005	0,0023	55,73	18,99	7,57	13,53
	0,0002	0,0008	0,0003	0,0022	53,67	18,32	8,07	14,41
	0,0005	0,0011		0,0030	45,26	14,71	13,90	24,84
0,0000	0,0006	0,0012	0,0003	0,0025	45,92	15,50	10,98	19,61
	0,0007	0,0015	0,0006	0,0060	34,24	10,71	14,18	25,34
0,0000	0,0002	0,0009	0,0003	0,0022	54,63	20,15	7,71	13,77
	0,0006	0,0013	0,0009	0,0024	41,62	12,61	6,29	11,25
	0,0011	0,0014	0,0008		36,67	11,35	10,53	18,81
0,0000	0,0002	0,0009	0,0004	0,0024	54,47	18,96	7,97	14,23
0,0000	0,0003	0,0010	0,0004	0,0019	51,72	17,51	8,07	14,42
	0,0010	0,0016		0,0110	25,14	7,85	18,25	32,61
0,0000	0,0001	0,0009	0,0004	0,0018	53,46	19,29	11,00	19,65
	0,0002	0,0009	0,0003	0,0020	52,35	17,90	12,86	22,97
		0,0010	0,0008	0,0044	39,85	13,21	17,59	31,43
	0,0001	0,0010	0,0006	0,0024	50,17	17,67	14,63	26,13
0,0000	0,0003	0,0008		0,0028	53,55	20,89	14,55	25,99
	0,0002	0,0013	0,0008	0,0022	42,10	14,42	4,65	8,31
0,0001	0,0001	0,0014	0,0005	0,0027	50,68	16,06	4,48	8,00
0,0000	0,0005	0,0013	0,0007	0,0035	51,34	16,02	2,25	4,02
0,0000	0,0009	0,0010	0,0005	0,0036	49,71	15,90	5,78	10,33
	0,0004	0,0010	0,0005	0,0035	50,57	17,07	5,10	9,11
0,0000	0,0010	0,0010	0,0005	0,0039	50,46	16,81	3,60	6,43
	0,0009	0,0010	0,0004	0,0033	51,12	17,73	4,75	8,49
	0,0006	0,0011	0,0005	0,0032	47,37	15,03	7,73	13,81
0,0000	0,0004	0,0015	0,0006	0,0038	50,17	17,20	4,65	8,31
	0,0014	0,0013	0,0011	0,0068	36,47	9,56	14,98	26,77
0,0000	0,0004	0,0011	0,0005	0,0025	52,96	17,86	1,36	2,42
	0,0004	0,0010	0,0006	0,0023	51,01	17,56	7,52	13,43
	0,0011	0,0010	0,0008	0,0033	51,34	17,06	0,87	1,55
0,0001	0,0002	0,0012	0,0009	0,0029	54,45	18,43	1,42	2,54
0,0000	0,0003	0,0014	0,0008	0,0029	53,81	18,28	1,11	1,98
0,0001	0,0003	0,0013	0,0009	0,0032	52,52	18,25	1,22	2,19
0,0001	0,0004	0,0010	0,0006	0,0033	52,25	18,45	0,98	1,75
0,0001	0,0003	0,0025	0,0016	0,0036	44,55	12,52	4,80	8,57
0,0000	0,0003	0,0011	0,0008	0,0029	52,04	18,30	2,98	5,32
0,0001	0,0002	0,0009	0,0009	0,0029	52,07	18,29	2,66	4,75
0,0000	0,0005	0,0012	0,0005	0,0033	51,07	17,37	4,83	8,63
0,0000	0,0009	0,0010	0,0006	0,0052	45,71	13,50	11,11	19,86
0,0001	0,0010	0,0035		0,0087	36,94	9,77	17,45	31,18
	0,0002	0,0009	0,0003	0,0026	43,14	14,42	19,03	34,01
0,0000	0,0002	0,0009	0,0004	0,0030	48,69	16,64	9,52	17,02
	0,0005	0,0008	0,0007	0,0027	51,53	17,60	5,16	9,22
0,0001	0,0001	0,0021		0,0028	40,43	14,39	20,59	36,79
	0,0004	0,0012	0,0003	0,0026	49,45	16,97	8,03	14,34
0,0001	0,0009	0,0009	0,0003	0,0029	47,29	16,02	12,06	21,56

0,0001	0,0002	0,0011		0,0028	40,94	13,99	19,96	35,67
	0,0007	0,0010	0,0006	0,0028	49,99	17,62	6,61	11,82
0,0000	0,0003	0,0009	0,0005	0,0023	49,67	17,26	8,49	15,17
0,0000	0,0003	0,0009	0,0004	0,0026	49,67	17,49	7,76	13,87
	0,0003	0,0012	0,0007	0,0028	50,08	16,90	8,22	14,68
0,0001	0,0003	0,0011	0,0006	0,0028	49,52	16,39	8,25	14,75
0,0001	0,0004	0,0015	0,0006	0,0024	45,83	15,73	11,26	20,13
0,0001	0,0003	0,0008	0,0005	0,0024	45,47	15,84	11,30	20,19
0,0001	0,0002	0,0015	0,0011	0,0025	48,00	14,59	10,91	19,50
0,0001	0,0011	0,0010	0,0008	0,0040	52,03	16,90	1,56	2,78
0,0001	0,0002	0,0015	0,0009	0,0036	47,75	12,95	10,31	18,42
0,0000	0,0002	0,0023	0,0008	0,0029	48,73	15,71	10,89	19,46
0,0001	0,0003	0,0010	0,0005	0,0023	50,11	16,29	11,21	20,04
	0,0002	0,0010	0,0006		45,74	15,90	12,23	21,85
0,0001	0,0006	0,0010	0,0005	0,0026	50,13	16,43	10,34	18,47
0,0001	0,0002	0,0012	0,0006	0,0029	48,22	15,30	11,18	19,97
0,0001	0,0006	0,0012	0,0008	0,0037	52,09	17,44	1,55	2,76
0,0001	0,0002	0,0011	0,0014	0,0032	44,14	12,48	7,70	13,76
0,0002	0,0003	0,0017	0,0012	0,0032	46,79	13,45	6,88	12,28
0,0002	0,0002	0,0013	0,0015	0,0027	47,64	15,08	8,38	14,97
0,0001	0,0004	0,0018	0,0019	0,0033	38,62	9,68	8,81	15,73
0,0002	0,0006	0,0024	0,0017	0,0030	42,97	11,43	8,30	14,84
0,0001	0,0006	0,0014	0,0013	0,0026	47,51	13,71	9,44	16,87
0,0001	0,0003	0,0012	0,0010	0,0034	49,70	15,51	7,85	14,02
0,0001	0,0003	0,0009	0,0007	0,0029	50,48	16,79	9,00	16,09
0,0001	0,0011	0,0011	0,0009	0,0036	44,17	12,44	5,42	9,69
0,0000	0,0003	0,0010	0,0006	0,0031	49,50	15,24	6,95	12,42
0,0000	0,0003	0,0009	0,0009	0,0024	49,06	15,20	8,65	15,46
0,0001	0,0002	0,0008	0,0003	0,0025	48,95	15,75	11,32	20,22
	0,0002	0,0008	0,0005	0,0023	49,96	16,72	10,41	18,59
	0,0003	0,0011	0,0007		40,33	11,29	16,07	28,70
	0,0002	0,0010	0,0009		42,92	12,97	11,02	19,70
	0,0007	0,0011	0,0011	0,0039	38,76	9,30	11,15	19,92
	0,0003	0,0008	0,0007	0,0025	49,32	16,13	12,84	22,95
0,0001	0,0010	0,0008	0,0007	0,0028	48,73	15,34	8,85	15,81
	0,0003	0,0017	0,0013		35,39	8,44	14,61	26,10
0,0001	0,0004	0,0020	0,0009	0,0031	42,55	12,33	10,45	18,67
0,0002	0,0003	0,0012	0,0011	0,0035	47,58	13,60	6,90	12,33
0,0003	0,0003	0,0018	0,0016	0,0037	45,22	11,72	7,93	14,17
0,0002	0,0003	0,0017	0,0012	0,0035	45,19	12,17	9,14	16,33
0,0002	0,0003	0,0014	0,0011	0,0038	47,58	12,36	10,24	18,29
0,0001	0,0009	0,0015	0,0009	0,0031	50,36	15,02	6,87	12,28
0,0001	0,0003	0,0011	0,0008	0,0030	47,68	15,01	9,65	17,24
0,0001	0,0003	0,0013	0,0008	0,0031	50,85	14,65	7,46	13,33
0,0001	0,0005	0,0010	0,0008	0,0026	53,76	15,28	7,14	12,75
0,0002	0,0002	0,0012	0,0005	0,0024	52,19	20,30	1,38	2,46
0,0002	0,0002	0,0010	0,0006	0,0025	56,29	18,80	0,84	1,51

0,0002	0,0002	0,0011	0,0008	0,0020	55,38	19,30	0,96	1,72
0,0001	0,0002	0,0013	0,0006	0,0021	54,49	18,32	4,09	7,31
0,0002	0,0002	0,0014	0,0006	0,0024	49,77	16,39	8,89	15,88
0,0001	0,0001	0,0012	0,0006	0,0019	51,02	17,52	10,25	18,32
0,0003	0,0003	0,0014	0,0007	0,0027	48,47	14,65	9,71	17,35
0,0002	0,0002	0,0009	0,0007		42,08	10,53	22,41	40,05
0,0003	0,0003	0,0014	0,0008		34,79	9,51	28,37	50,70
0,0002	0,0002	0,0015	0,0008	0,0025	38,84	13,06	19,20	34,30
0,0002	0,0002	0,0018	0,0007	0,0034	42,71	12,49	14,82	26,48
0,0002	0,0003	0,0011	0,0007	0,0024	46,49	14,39	12,59	22,49
0,0003	0,0003	0,0011	0,0006	0,0032	48,30	12,41	11,56	20,65
0,0004	0,0003	0,0021	0,0012	0,0026	51,20	15,59	9,86	17,61
0,0004	0,0002	0,0023	0,0014	0,0023	51,17	14,82	9,94	17,76
0,0003	0,0002	0,0024	0,0014	0,0022	49,14	13,46	12,68	22,65
0,0001	0,0002	0,0011	0,0014	0,0023	51,53	15,64	11,66	20,84
0,0002	0,0003	0,0016	0,0016	0,0026	48,69	13,84	14,18	25,33
0,0001	0,0001	0,0017	0,0017	0,0020	50,72	14,36	10,27	18,36
0,0002	0,0003	0,0025	0,0019	0,0030	46,33	10,91	6,12	10,94
0,0002	0,0003	0,0020	0,0014	0,0030	45,86	12,42	9,92	17,73
0,0003	0,0003	0,0036	0,0014	0,0025	43,44	11,10	12,63	22,56
0,0002	0,0002	0,0025	0,0011	0,0027	45,09	12,45	9,85	17,61
0,0001	0,0002	0,0012	0,0022	0,0024	50,44	14,08	7,97	14,25
0,0001	0,0001	0,0014	0,0019	0,0024	49,20	13,08	10,63	19,00
0,0002	0,0002	0,0015	0,0014	0,0027	52,01	12,87	10,08	18,01
0,0001	0,0001	0,0014	0,0018	0,0022	54,87	15,51	6,48	11,57
0,0001	0,0002	0,0011	0,0008	0,0021	51,97	16,56	8,79	15,70
0,0001	0,0002	0,0014	0,0004	0,0020	44,94	13,82	17,63	31,51
0,0002	0,0002	0,0009			39,56	8,93	28,98	51,77
0,0002	0,0003	0,0013	0,0005		45,35	11,76	18,25	32,61
0,0003	0,0003	0,0016	0,0010	0,0035	47,54	12,14	13,56	24,22
0,0001	0,0002	0,0011	0,0005	0,0025	48,40	15,36	13,03	23,28
0,0001	0,0002	0,0013	0,0006	0,0022	49,99	16,53	13,48	24,08
0,0001	0,0003	0,0013	0,0005	0,0021	48,64	15,41	13,49	24,11
0,0001	0,0002	0,0011	0,0005	0,0022	51,44	16,58	11,84	21,15
0,0002	0,0003	0,0015	0,0007	0,0021	48,18	15,34	13,45	24,02
0,0002	0,0002	0,0012	0,0006	0,0025	49,64	16,16	14,06	25,12
0,0002	0,0006	0,0010	0,0005	0,0025	48,12	15,38	14,00	25,01
0,0002	0,0002	0,0014	0,0007	0,0023	50,56	16,74	12,26	21,90
0,0002	0,0003	0,0016	0,0006	0,0025	49,13	15,25	13,01	23,24
0,0003	0,0003	0,0026	0,0014	0,0026	48,99	14,30	10,73	19,18
0,0002	0,0003	0,0017	0,0013	0,0034	45,60	12,61	8,53	15,25
0,0005	0,0003	0,0030	0,0020	0,0029	43,51	12,19	8,97	16,02
0,0004	0,0004	0,0032	0,0028		35,46	9,27	18,58	33,20

0,0003	0,0003	0,0017	0,0014	0,0026	47,19	14,04	10,00	17,87
0,0003	0,0004	0,0013	0,0013	0,0028	46,96	14,32	11,10	19,84
0,0003	0,0010	0,0013	0,0016		40,66	10,64	12,24	21,87
0,0004	0,0004	0,0024	0,0020	0,0033	42,28	10,82	15,23	27,22
0,0003	0,0003	0,0014	0,0011		42,06	10,55	20,43	36,50
0,0003	0,0003	0,0020	0,0014	0,0035	40,83	9,78	16,02	28,62
0,0003	0,0002	0,0039	0,0021		40,37	9,83	13,94	24,90
0,0003	0,0002	0,0013	0,0011	0,0025	46,80	13,52	15,85	28,33
0,0003	0,0002	0,0017	0,0011	0,0026	43,55	11,64	15,59	27,86
0,0003	0,0003	0,0024	0,0014	0,0029	44,18	11,20	14,63	26,14
0,0002	0,0002	0,0018	0,0014	0,0028	48,63	13,69	10,33	18,47
0,0002	0,0002	0,0018	0,0012	0,0028	49,02	13,97	9,99	17,84
0,0002	0,0007	0,0017	0,0013	0,0031	47,84	12,92	11,55	20,64
0,0001	0,0002	0,0011	0,0007	0,0025	49,37	14,79	11,07	19,78
0,0003	0,0008	0,0025	0,0010	0,0034	45,58	12,23	14,45	25,82
0,0002	0,0006	0,0018	0,0013	0,0027	49,86	13,34	10,21	18,25
0,0001	0,0003	0,0013	0,0008	0,0026	53,05	17,14	8,10	14,47
0,0003	0,0008	0,0023	0,0012	0,0032	50,67	13,50	6,17	11,03
0,0002	0,0003	0,0018	0,0013	0,0033	49,53	13,69	9,18	16,41
0,0002	0,0003	0,0021	0,0011	0,0027	48,98	13,07	10,78	19,27
0,0001	0,0002	0,0017	0,0015	0,0031	52,60	12,84	6,09	10,89
0,0002	0,0003	0,0033	0,0014	0,0032	43,44	10,58	14,20	25,37
0,0001	0,0003	0,0010	0,0007	0,0027	49,86	15,02	9,09	16,23
0,0001	0,0003	0,0011	0,0009	0,0030	44,84	12,22	14,39	25,71
0,0001	0,0003	0,0016	0,0009	0,0027	48,66	13,75	14,24	25,45
0,0001	0,0004	0,0011	0,0006	0,0030	54,14	16,29	6,53	11,66
0,0001	0,0004	0,0018	0,0010	0,0033	42,80	11,18	13,64	24,38
0,0001	0,0013	0,0009			41,37	9,45	18,12	32,38
	0,0003	0,0012	0,0008	0,0029	43,18	11,26	19,60	35,01
	0,0012	0,0016	0,0007		38,89	9,98	20,35	36,36
	0,0004	0,0013	0,0010		39,28	10,76	21,97	39,26
	0,0006	0,0011			30,33	7,55	28,23	50,43
	0,0012	0,0012	0,0010		34,21	7,70	15,63	27,92
0,0001	0,0003	0,0011	0,0006	0,0027	47,92	13,17	16,18	28,92
	0,0004	0,0017	0,0011	0,0039	36,68	8,94	16,79	30,00
	0,0007	0,0011	0,0006	0,0027	47,56	12,53	17,26	30,84
0,0000	0,0003	0,0013	0,0006	0,0030	49,07	14,10	14,77	26,39
0,0000	0,0002	0,0011	0,0006	0,0022	51,06	16,38	13,51	24,14
	0,0003	0,0008	0,0007		43,21	13,26	15,63	27,93
	0,0003	0,0009	0,0004		44,78	13,85	19,73	35,25
	0,0002	0,0012	0,0004		44,49	13,20	20,43	36,50
	0,0003	0,0010	0,0004		46,15	14,65	18,86	33,71
0,0000	0,0002	0,0010	0,0004		47,62	14,55	19,76	35,30
0,0001	0,0003	0,0011			46,04	13,25	19,40	34,66
	0,0003	0,0009	0,0006		45,12	11,72	19,89	35,55
0,0001	0,0009	0,0011	0,0006		43,39	10,97	22,52	40,24
0,0000	0,0002	0,0021	0,0010	0,0020				

K2O	K2O/Rb	EFSi	EFTi	EFFe	EFMn	EFCa	EFMg
2,04	355,17	0,4652	0,5168	1,4022	14,9827	1,5176	
1,92	359,93	0,4387	0,5046	1,5620	27,5616	1,5239	0,3898
1,39	374,91	0,4580	0,3367	2,8111	24,0135	5,6953	0,6207
2,20	361,11	0,4161	0,4915	1,0283	9,6592	1,5134	0,2245
2,27	347,74	0,4153	0,4880	0,8334	7,2404	1,6708	0,2502
1,60	370,91	0,4362	0,3484	1,6814	16,7285	3,5848	0,3203
1,92	356,42	0,4199	0,4414	1,5337	22,8839	2,6856	0,3386
1,27	414,81	0,4533	0,2784	4,1943	36,2964	5,0249	
2,42	340,77	0,3844	0,4350	0,9265	2,4047	1,4512	0,3196
2,07	331,81	0,4678	0,5161	1,1841	2,0026	1,8931	
1,45	345,84	0,4580	0,4125	3,0073	32,0272	3,5184	0,5022
2,45	352,56	0,4073	0,4697	0,9397	2,1244	1,5940	0,1973
2,34	333,01	0,4187	0,4937	0,8736	2,0015	1,7486	0,3438
0,82	359,98	0,4539	0,2341	8,8032	27,5157	8,8184	
2,21	356,64	0,3928	0,4181	0,7433	2,8639	2,1625	0,5009
2,20	386,97	0,4146	0,4271	0,8777	1,4388	2,7250	
1,61	414,12	0,4276	0,3056	2,4092	3,8976	5,0513	
2,16	396,16	0,4025	0,4072	0,9130	1,7868	3,1407	0,3222
1,96	419,23	0,3634	0,2967	1,4316	2,1941	2,6418	0,3471
2,15	305,40	0,4139	0,5697	1,0026	2,3341	1,2232	0,2250
2,26	320,61	0,4475	0,6486	0,9955	1,4891	1,0573	0,3542
2,03	347,17	0,4543	0,5215	1,9493	2,5994	0,5326	0,4529
1,76	369,31	0,4431	0,4186	2,0437	12,2585	1,3792	0,5478
1,94	192,48	0,4198	0,4863	1,7429	4,9839	1,1325	0,4451
1,96	373,70	0,4255	0,3483	2,1222	5,3084	0,8118	0,4582
1,96	177,76	0,4088	0,4883	1,5317	2,9772	1,0171	0,4027
1,82	331,42	0,4468	0,4838	1,5276	8,7693	1,9506	0,4324
2,08	330,88	0,4136	0,4880	1,5988	8,5493	1,0265	0,3651
0,99	402,94	0,5409	0,2582	6,0204	15,7688	5,9471	0,6647
2,07	171,84	0,4204	0,5676	1,3503	9,7950	0,2882	0,4669
2,09	187,69	0,4117	0,4658	0,9542	6,8568	1,6232	0,4179
1,95	341,76	0,4265	0,3882	2,0722	7,5055	0,1934	0,3845
2,18	180,63	0,4189	0,5417	1,2651	0,5724	0,2921	0,3734
2,02	317,31	0,4173	0,5315	1,4180	1,1000	0,2298	0,3948
1,99	337,41	0,4079	0,5282	1,5375	1,0208	0,2545	0,4329
1,98	354,22	0,4015	0,5375	1,5758	1,4779	0,2012	0,4274
1,84	316,20	0,5045	0,6686	1,5326	0,9765	1,4541	0,4810
2,25	349,60	0,4032	0,5162	1,3137	1,0281	0,6177	0,3849
2,09	174,77	0,4035	0,5229	1,3638	0,7539	0,5508	0,4201
1,99	358,16	0,4169	0,4792	1,3906	7,0817	1,0553	0,4717
1,57	396,55	0,4800	0,3530	2,8354	14,4301	3,1230	0,4621
0,90	462,24	0,5359	0,1939	6,6102	17,4423	6,7726	0,6285
1,60	396,19	0,4242	0,3040	1,3857	4,4843	5,0084	0,4661
1,90	412,76	0,4149	0,4400	1,4418	6,8950	2,1716	0,4656
2,04	184,41	0,4150	0,4645	1,4200	2,8323	1,1117	0,4071
1,55	390,43	0,3983	0,3128	1,2926	2,6133	5,4275	0,5930
1,94	183,23	0,4131	0,4865	1,5057	2,3112	1,7943	0,4701
1,85	382,86	0,4185	0,4241	1,4131	18,4015	2,8567	0,4017

1,42	[redacted]	366,86	[redacted]	0,4148	0,5273	1,1642	2,8474	5,4116	0,5420
2,05	[redacted]	190,78	[redacted]	0,4022	0,4693	1,2673	2,6270	1,4241	0,4467
1,91	[redacted]	178,11	[redacted]	0,4079	0,4914	1,1721	3,3688	1,8654	0,4731
1,99	[redacted]	373,96	[redacted]	0,4025	0,4820	1,1143	3,8762	1,6833	0,4216
1,97	[redacted]	358,39	[redacted]	0,4200	0,4697	1,2424	6,5790	1,8442	0,4646
1,88	[redacted]	346,91	[redacted]	0,4284	0,4541	1,3102	1,8994	1,9109	0,4376
1,76	[redacted]	201,24	[redacted]	0,4131	0,4066	1,2376	3,2502	2,7173	0,5032
1,60	[redacted]	411,40	[redacted]	0,4068	0,3857	1,3704	1,9263	2,7059	0,4977
1,73	[redacted]	354,12	[redacted]	0,4665	0,4645	1,1402	0,8563	2,8384	0,4490
2,03	[redacted]	363,87	[redacted]	0,4366	0,3870	2,1680	1,9766	0,3495	0,4515
1,73	[redacted]	362,85	[redacted]	0,5225	0,5059	1,4568	1,6091	3,0193	0,4447
1,91	[redacted]	349,54	[redacted]	0,4397	0,4747	1,1354	2,4844	2,6296	0,4363
1,92	[redacted]	348,50	[redacted]	0,4360	0,4360	1,0958	2,5053	2,6111	0,3625
1,75	[redacted]	351,69	[redacted]	0,4079	0,3555	0,8814	1,0284	2,9183	0,5621
1,99	[redacted]	355,48	[redacted]	0,4326	0,4460	1,1042	1,6305	2,3870	0,3792
1,92	[redacted]	351,82	[redacted]	0,4469	0,4430	1,0938	1,5282	2,7721	0,4248
2,10	[redacted]	179,78	[redacted]	0,4234	0,5302	1,9194	1,9311	0,3361	0,4290
1,84	[redacted]	332,69	[redacted]	0,5013	0,5458	1,3160	1,2163	2,3402	0,3439
1,81	[redacted]	361,56	[redacted]	0,4932	0,5384	1,5234	0,6844	1,9391	0,3663
1,82	[redacted]	329,25	[redacted]	0,4477	0,4982	0,9784	0,9324	2,1076	0,4501
1,57	[redacted]	353,37	[redacted]	0,5657	0,5950	1,4095	1,1441	3,4513	0,4011
1,75	[redacted]	342,54	[redacted]	0,5328	0,6311	1,2130	1,0563	2,7552	0,3563
1,77	[redacted]	347,34	[redacted]	0,4911	0,4895	1,1875	1,0356	2,6117	0,3873
1,95	[redacted]	364,26	[redacted]	0,4543	0,4813	1,1724	0,7092	1,9196	0,4234
2,01	[redacted]	219,63	[redacted]	0,4262	0,4077	1,3388	1,9394	2,0342	0,4254
1,79	[redacted]	328,85	[redacted]	0,5031	0,4718	2,1877	6,6672	1,6524	0,4790
2,01	[redacted]	374,27	[redacted]	0,4604	0,4409	1,6173	4,1074	1,7295	0,4360
1,87	[redacted]	347,02	[redacted]	0,4576	0,4082	1,2879	1,3264	2,1595	0,4681
1,96	[redacted]	371,92	[redacted]	0,4407	0,3917	1,2052	5,0330	2,7266	0,4670
2,00	[redacted]	362,36	[redacted]	0,4236	0,4023	1,0738	1,5599	2,3610	0,4634
1,69	[redacted]	376,21	[redacted]	0,5062	0,4444	1,3854	6,4718	5,3966	0,3385
1,73	[redacted]	358,38	[redacted]	0,4690	0,3551	1,3769	5,4298	3,2239	0,4952
1,57	[redacted]	359,41	[redacted]	0,5910	0,3827	1,5308	4,1412	4,5481	0,4296
1,87	[redacted]	217,47	[redacted]	0,4336	0,3414	1,1765	1,6999	3,0212	0,4819
1,87	[redacted]	361,42	[redacted]	0,4503	0,3941	1,5186	1,3080	2,1886	0,4496
1,50	[redacted]	345,64	[redacted]	0,5944	0,4740	1,3245	1,8673	6,5649	0,5138
1,72	[redacted]	343,47	[redacted]	0,4892	0,4834	1,3428	0,7744	3,2155	0,3856
1,92	[redacted]	321,90	[redacted]	0,4958	0,5412	1,3568	0,6141	1,9247	0,3997
1,85	[redacted]	332,59	[redacted]	0,5469	0,6266	1,4666	0,8667	2,5662	0,4047
1,81	[redacted]	334,98	[redacted]	0,5264	0,5803	1,4202	1,2618	2,8488	0,3550
1,70	[redacted]	365,67	[redacted]	0,5458	0,5126	1,4543	3,7455	3,1421	0,4234
1,94	[redacted]	334,94	[redacted]	0,4754	0,4950	1,4837	1,1706	1,7361	0,3852
1,85	[redacted]	327,09	[redacted]	0,4504	0,4871	1,0987	2,3580	2,4394	0,2945
1,91	[redacted]	340,15	[redacted]	0,4921	0,4796	1,4045	3,6713	1,9316	0,3911
1,83	[redacted]	351,79	[redacted]	0,4987	0,4722	1,1112	0,6423	1,7711	0,4179
2,07	[redacted]	307,41	[redacted]	0,3645	0,5801	0,9602	0,3223	0,2571	0,3140
2,26	[redacted]	175,40	[redacted]	0,4244	0,5775	0,8850	0,4606	0,1701	0,3621

2,18	[redacted]	315,65	[redacted]	0,4067	0,5835	0,8680	0,4542	0,1893	0,3366
2,07	[redacted]	184,39	[redacted]	0,4216	0,5403	0,8429	0,6970	0,8468	0,3712
2,02	[redacted]	325,09	[redacted]	0,4304	0,4685	0,9023	0,7538	2,0573	0,3597
1,98	[redacted]	196,51	[redacted]	0,4127	0,4036	0,7489	0,9231	2,2199	0,3956
1,73	[redacted]	356,62	[redacted]	0,4689	0,4544	1,1721	1,3559	2,5135	0,3978
1,23	[redacted]	406,55	[redacted]	0,5664	0,4024	0,9234	2,7923	8,0728	0,4690
1,08	[redacted]	413,84	[redacted]	0,5186	0,3494	0,9903	2,3708	11,3184	0,6940
1,39	[redacted]	352,59	[redacted]	0,4215	0,4695	0,9854	1,4145	5,5756	0,4663
1,58	[redacted]	384,22	[redacted]	0,4848	0,4781	1,2102	0,9038	4,5012	0,4704
1,66	[redacted]	376,69	[redacted]	0,4579	0,4619	1,1676	0,9589	3,3179	0,3226
1,63	[redacted]	383,53	[redacted]	0,5515	0,4537	1,5522	0,7127	3,5321	0,4675
1,84	[redacted]	353,45	[redacted]	0,4657	0,5100	1,0939	0,6810	2,3991	0,4062
1,76	[redacted]	342,31	[redacted]	0,4893	0,5163	1,0318	0,7690	2,5439	0,4127
1,64	[redacted]	344,90	[redacted]	0,5177	0,4882	0,8956	0,5925	3,5742	0,4738
1,79	[redacted]	363,28	[redacted]	0,4671	0,4441	0,6919	0,4363	2,8289	0,4226
1,63	[redacted]	398,59	[redacted]	0,4988	0,4431	1,0892	0,9168	3,8874	0,3972
1,74	[redacted]	365,79	[redacted]	0,5007	0,5121	0,8242	0,6886	2,7141	0,3980
1,73	[redacted]	333,33	[redacted]	0,6022	0,6903	1,4238	1,7977	2,1304	0,4020
1,83	[redacted]	344,11	[redacted]	0,5234	0,6196	1,0937	1,1672	3,0300	0,3741
1,57	[redacted]	385,47	[redacted]	0,5549	0,5528	1,2696	1,1683	4,3167	0,4512
1,64	[redacted]	357,31	[redacted]	0,5134	0,5743	1,1030	0,4880	3,0027	0,3518
1,80	[redacted]	340,86	[redacted]	0,5080	0,5435	0,8495	0,3852	2,1488	0,3840
1,64	[redacted]	361,65	[redacted]	0,5334	0,5288	0,7941	0,5207	3,0847	0,4235
1,59	[redacted]	380,76	[redacted]	0,5729	0,5149	1,0004	0,5750	2,9718	0,4149
1,86	[redacted]	366,19	[redacted]	0,5014	0,5122	0,8028	0,3348	1,5837	0,3384
1,98	[redacted]	353,66	[redacted]	0,4449	0,4671	0,7260	0,4700	2,0134	0,3688
1,47	[redacted]	355,08	[redacted]	0,4611	0,4302	0,8541	0,6805	4,8417	0,4383
1,53	[redacted]	644,14	[redacted]	0,6278	0,4999	0,9753	2,7406	12,3066	0,5321
1,29	[redacted]	375,20	[redacted]	0,5466	0,4880	1,3301	0,9862	5,8870	0,4645
1,52	[redacted]	380,87	[redacted]	0,5551	0,4483	1,7232	1,3071	4,2360	0,3874
1,80	[redacted]	351,52	[redacted]	0,4466	0,4923	0,9817	0,9662	3,2181	0,4000
1,83	[redacted]	211,38	[redacted]	0,4286	0,4404	0,8206	0,4904	3,0924	0,4317
1,78	[redacted]	360,64	[redacted]	0,4476	0,4687	0,8921	0,6323	3,3221	0,3911
1,86	[redacted]	368,45	[redacted]	0,4398	0,4663	0,9033	0,5676	2,7089	0,3610
1,79	[redacted]	379,95	[redacted]	0,4453	0,4343	0,9443	0,6721	3,3254	0,3950
1,80	[redacted]	379,36	[redacted]	0,4354	0,4265	0,8727	0,6339	3,2995	0,4101
1,83	[redacted]	369,69	[redacted]	0,4436	0,4554	0,9411	0,6520	3,4523	0,4178
1,93	[redacted]	204,20	[redacted]	0,4282	0,4231	0,8859	0,5520	2,7774	0,4062
1,87	[redacted]	360,61	[redacted]	0,4566	0,4485	0,9828	0,6691	3,2350	0,4187
1,63	[redacted]	370,27	[redacted]	0,4856	0,5214	1,0169	0,7224	2,8471	0,4000
1,58	[redacted]	367,24	[redacted]	0,5127	0,5554	1,4029	1,2794	2,5676	0,4677
1,57	[redacted]	359,93	[redacted]	0,5059	0,5761	1,2503	0,9300	2,7901	0,3790
1,24	[redacted]	374,37	[redacted]	0,5424	0,4491	1,1503	0,8492	7,6042	0,4708

1,61	342,65		0,4765	0,5260	1,0940	0,5709	2,7014	0,3542
1,70	342,03		0,4648	0,4584	1,1328	0,5899	2,9409	0,3600
1,51	366,78		0,5416	0,4577	1,1616	0,6391	4,3633	0,4631
1,33	383,39		0,5539	0,4931	1,3923	1,0216	5,3407	0,3827
1,20	396,38		0,5653	0,4149	1,0152	1,6514	7,3464	0,3685
1,30	386,80		0,5920	0,4677	1,2158	1,3408	6,2155	0,4830
1,36	381,26		0,5822	0,4869	1,0417	0,9901	5,3788	0,5092
1,50	379,03		0,4907	0,4458	0,9653	0,7623	4,4481	0,3544
1,39	392,87		0,5302	0,4734	1,0104	1,2895	5,0803	0,4974
1,34	344,18		0,5591	0,4842	1,0261	0,9845	4,9536	0,4279
1,64	352,40		0,5035	0,5019	0,9788	0,7709	2,8632	0,3935
1,62	349,96		0,4975	0,4910	1,0535	0,9618	2,7117	0,3967
1,61	364,92		0,5247	0,5133	1,0695	0,7678	3,3907	0,4597
1,76	363,74		0,4731	0,4342	1,1609	1,0665	2,8395	0,3942
1,46	355,31		0,5285	0,4858	1,2504	1,2104	4,4845	0,3476
1,54	347,59		0,5300	0,5314	1,1231	0,8921	2,9047	0,3864
1,88	201,99		0,4388	0,4923	1,0010	1,1414	1,7928	0,3946
1,68	357,50		0,5320	0,5546	1,4656	0,5902	1,7345	0,3582
1,68	338,89		0,5129	0,5523	0,9838	0,6232	2,5447	0,3865
1,58	340,04		0,5312	0,5167	1,1080	0,8236	3,1294	0,4195
1,74	342,17		0,5806	0,5613	1,1847	1,7405	1,7997	0,3722
1,39	378,54		0,5822	0,4785	1,1634	1,5081	5,0930	0,4596
1,69	362,54		0,4707	0,4853	1,3122	1,1964	2,2955	0,3828
1,60	375,08		0,5201	0,4079	1,2910	1,6951	4,4662	0,3522
1,74	379,78		0,5017	0,4184	1,1233	1,5921	3,9289	0,4633
1,98	364,49		0,4712	0,4709	1,5650	1,2351	1,5202	0,3948
1,70	381,58		0,5425	0,5334	1,5443	1,9233	4,6276	0,3643
1,47	392,63		0,6206	0,4276	2,3318	6,8044	7,2749	0,4924
1,56	408,53		0,5436	0,3756	1,2552	2,7586	6,6013	0,3426
1,39	388,36		0,5526	0,4454	1,5983	4,9844	7,7383	0,5552
1,40	383,26		0,5174	0,3608	1,6471	4,0780	7,7441	0,5329
1,17	572,99		0,5697	0,2339	1,3308	8,1342	14,1885	0,6023
1,41	373,73		0,6295	0,5106	2,1583	9,1663	7,6965	0,4636
1,60	369,60		0,5159	0,3614	1,3610	3,0262	4,6631	0,3268
1,62	383,82		0,5813	0,5308	1,6158	2,2798	7,1205	0,5194
1,56	397,12		0,5380	0,3858	1,1193	1,6599	5,2250	0,4535
1,74	378,20		0,4931	0,3921	1,2779	2,0636	3,9721	0,4584
1,76	355,22		0,4420	0,4278	0,8324	1,6650	3,1301	0,3459
1,53	335,79		0,4620	0,4093	1,2640	3,9613	4,4713	0,3775
1,55	363,89		0,4584	0,3691	1,1826	3,8997	5,4041	0,4109
1,47	392,12		0,4778	0,3580	0,9906	4,1767	5,8719	0,3853
1,59	382,47		0,4466	0,3309	1,0876	5,0046	4,8854	0,3693
1,56	385,00		0,4639	0,3358	1,0380	3,9552	5,1494	0,4019
1,44	413,21		0,4927	0,3241	1,1948	7,5209	5,5553	0,4661
1,34	429,59		0,5457	0,3532	1,2592	3,2089	6,4383	0,5053
1,17	404,21		0,5606	0,3148	1,4988	20,9633	7,7859	0,3999
		Maximum	0,6295	0,6903	8,8032	36,2964	14,1885	0,6940
		Minimum	0,3634	0,1939	0,6919	0,3223	0,1701	0,1973
		Average	0,4758	0,4615	1,3832	3,7333	3,2876	0,4207

		St.dev	0,0580	0,0815	0,8755	5,8387	2,2243	0,0728
		Median	0,4643	0,4697	1,2077	1,6006	2,7838	0,4138

EFK	EFP	EFZr	EFTh	EFNb	EFSr	EFRb	EFPb	EFBa
0,6186		0,5986	0,5411	0,4356	0,5785	0,2240	1,1153	0,8875
0,5855	1,1159	0,5092	0,5345	0,4110	0,5263	0,2091	1,0118	0,9712
0,5434	4,9438	0,2930		0,6007	1,3271	0,1864	0,5882	1,5516
0,5378	1,1078	0,5248	0,3894	0,3906	0,5396	0,1915	0,9594	0,6716
0,5751	0,6496	0,5521	0,4942	0,4123	0,5143	0,2127	0,9655	0,7192
0,5049	17,9268	0,3960		0,9453	1,2361	0,1750	0,7195	1,0881
0,5742	1,0862	0,4284		0,4572	0,5026	0,2072	0,7635	0,7429
0,5504	4,6006	0,3038		0,5289	0,8664	0,1706	0,5508	0,8945
0,5570	0,6326	0,5435	0,4524	0,3547	0,6616	0,2102	0,7136	0,6070
0,7611	0,8799	0,6738	0,6283	0,4556	1,1517	0,2949	1,0019	0,8100
0,5914	0,8765	0,4358		0,3809	0,7401	0,2199	0,6477	1,6850
0,5982	1,7310	0,6247	0,5095	0,4128	0,7213	0,2182	1,0548	0,6253
0,6207	0,8388	0,6861	0,5525	0,4071	0,6785	0,2397	0,9023	0,6571
0,4871	1,6899	0,2818		0,4371	1,1701	0,1740		2,7090
0,5317	0,9507	0,5778	0,4212	0,3801	0,6849	0,1917	0,7689	0,5948
0,5693	0,6036	0,5931	0,4367	0,3581	0,6723	0,1892	0,6570	0,6237
0,5668	34,6567	0,4149		1,0927	1,2754	0,1760	0,5815	1,1171
0,5669	0,8097	0,4997	0,5166	0,3405	0,7563	0,1840	0,7634	0,6150
0,4343	2,0809	0,2697		0,3151	0,4674	0,1332	0,3352	0,5864
0,6900	1,0722	0,6920	0,4810	0,4799	0,5867	0,2905	0,7024	0,6731
0,6539	1,0196	0,9001	0,6507	0,5307	0,5688	0,2623	0,5254	0,6296
0,5865	0,4563	0,7505	0,5372	0,4508	0,3861	0,2172	2,3623	0,9170
0,5142	1,0581	0,3881		0,4180	0,2945	0,1790	1,0129	0,9272
0,5276	0,9262	0,5888	0,6012	0,4048	0,4394	0,3525	1,1762	0,6976
0,5400	1,2334	0,3669		0,3841	0,2499	0,1858	1,0386	0,4906
0,5137	0,5933	0,5771	0,4665	0,3451	0,4111	0,3716	1,2089	0,6744
0,5624	0,6449	0,6845	0,6008	0,4722	0,6170	0,2182	1,2599	0,7485
0,5601	0,8280	0,5871	0,5111	0,3738	0,4318	0,2177	1,7196	0,5930
0,4791	3,6467	0,2903		0,4504	0,9927	0,1529		0,8470
0,5370	0,6392	0,5888	0,6346	0,4077	0,3137	0,4018	0,8017	0,5864
0,5532	1,2052	0,5622	0,5818	0,4402	0,5724	0,3790	0,5521	0,5686
0,5304	0,6508	0,3857		0,3977	0,1976	0,1996	1,5457	0,4139
0,5479	0,8324	0,6262	0,4869	0,4043	0,3528	0,3901	1,2852	0,5042
0,5128	1,2549	0,6256	0,5794	0,4880	0,3623	0,2078	1,1465	0,5972
0,5048	1,1442	0,6315	0,5768	0,4577	0,3580	0,1924	1,1673	0,5416
0,4984	0,6794	0,5901	0,4643	0,4076	0,3482	0,1809	1,0995	0,5946
0,6815	1,9671	0,8648	0,7035	0,7359	0,6901	0,2771	1,3306	0,6539
0,5713	0,8555	0,6236	0,5178	0,4438	0,3933	0,2101	1,1740	0,5200
0,5303	1,0325	0,6567	0,5920	0,4402	0,3995	0,3902	1,0974	0,5649
0,5310	0,7140	0,6073	0,4893	0,3811	0,4908	0,1906	1,0999	0,7438
0,5394	1,8022	0,3387		0,4996	0,6663	0,1749		0,6015
0,4262	1,9305	0,2095		0,3607	0,9870	0,1186		0,8602
0,5157	4,2609	0,4472	0,5085	0,5399	1,6384	0,1674	0,9332	0,8272
0,5290	1,5571	0,5128	0,5906	0,4040	0,9959	0,1648	0,7562	0,6995
0,5386	1,0002	0,5883	0,5506	0,3810	0,5261	0,3756	0,8539	0,5555
0,4993	3,2559	0,5429	0,4073	0,4742	1,5120	0,1644	0,5929	0,8818
0,5299	1,5782	0,6470	0,4206	0,3499	0,7216	0,3719	0,9964	0,6697
0,5362	0,8382	0,3971		0,3639	0,6279	0,1801	0,4738	0,8222

0,4707	1,6035	1,0896	0,4295	0,3944	1,0633	0,1650	0,9052	0,9449
0,5390	1,3245	0,6112	0,5345	0,4504	0,5434	0,3633	0,9976	0,5096
0,5137	1,4589	0,6361	0,4532	0,4128	0,6594	0,3709	0,9450	0,5876
0,5286	1,4429	0,5752	0,5162	0,3442	0,6330	0,1818	1,0318	0,5918
0,5416	1,9431	0,6313	0,5329	0,4367	0,8341	0,1943	1,0269	0,5874
0,5329	1,0889	0,5701	0,5573	0,4770	0,8660	0,1975	0,9216	0,6231
0,5185	1,6147	0,4702	0,4524	0,3003	0,8799	0,3313	0,7787	0,6245
0,4696	1,6463	0,4657	0,4851	0,3458	0,8293	0,1468	0,8621	0,6733
0,5499	1,2306	0,5374	0,4901	0,4211	0,7485	0,1997	0,7226	0,5169
0,5568	1,0195	0,3428	0,5680	0,4082	0,2675	0,1968	0,8949	0,6263
0,6184	2,0609	0,6798	0,4980	0,4924	0,8092	0,2191	0,8095	0,6050
0,5637	1,1592	0,5842	0,4554	0,4157	0,7803	0,2074	0,9381	0,6714
0,5456	0,9132	0,5300	0,4805	0,4245	0,7700	0,2013	0,8982	0,6546
0,5104	0,9025	0,4552	0,4857	0,3545	0,8579	0,1866	0,8607	0,6219
0,5632	1,0346	0,5001	0,3665	0,4458	0,7181	0,2037	0,9232	0,6392
0,5828	0,8007	0,5680	0,5773	0,3666	0,8201	0,2130	0,8979	0,6866
0,5589	1,5234	0,5622	0,6224	0,4256	0,4039	0,3997	0,8487	0,6323
0,6851	0,9217	0,6567	0,6464	0,4979	0,7512	0,2648	1,3247	0,6256
0,6232	1,8484	0,6721	0,6535	0,5039	0,6984	0,2216	1,1213	0,5095
0,5607	0,8451	0,6744	0,4159	0,4622	0,7247	0,2190	1,0261	0,5550
0,7520	1,3865	0,8250	0,8101	0,4630	1,1687	0,2736	1,4391	0,8029
0,7108	1,4673	0,7306	0,6277	0,5229	1,0949	0,2668	1,1378	0,5449
0,5996	1,5420	0,6981	0,5958	0,5083	0,9804	0,2220	1,1719	0,6087
0,5832	1,1357	0,5301	0,5195	0,4414	0,6708	0,2059	0,9715	0,5339
0,5549	1,0558	0,4738	0,5041	0,3464	0,6687	0,3249	0,8254	0,6205
0,6683	1,1595	0,4344		0,4648	0,4591	0,2613	0,8935	0,9229
0,6124	1,6889	0,5314	0,6735	0,4428	0,6182	0,2104	0,9592	0,7678
0,5719	0,9207	0,5111	0,4424	0,4544	0,7151	0,2119	0,8556	0,6503
0,5784	1,2040	0,5048	0,6330	0,4112	1,0384	0,2000	0,8552	0,6522
0,5551	1,0317	0,5266	0,3608	0,4192	0,8188	0,1970	0,7776	0,5951
0,6942	1,5000	0,5775	0,5398	0,4387	1,9403	0,2373	1,0176	0,8793
0,6195	0,9596	0,5294	0,5665	0,4069	1,4284	0,2223	0,9165	0,9918
0,7853	1,3645	0,5024		0,4620	1,3957	0,2809	0,8196	1,4329
0,5384	1,2053	0,4392	0,4894	0,3722	1,2207	0,3183	0,6399	0,7461
0,5663	1,0650	0,5247	0,4130	0,4079	0,6498	0,2015	0,7288	0,8566
0,8222	1,4311	0,9749	0,7548	0,5814	2,5403	0,3059	1,0813	1,3133
0,6476	0,7499	0,7342	0,5339	0,5392	1,1887	0,2425	1,0426	0,7584
0,6556	0,8401	0,6892	0,6868	0,5731	0,9094	0,2619	1,2321	0,5629
0,7337	0,9512	0,8523	0,7064	0,6177	1,0228	0,2836	1,3501	0,7184
0,6907	1,3545	0,7643	0,6602	0,5454	1,0276	0,2651	1,3920	0,8059
0,6370	1,6710	0,6301	0,6487	0,5097	1,1393	0,2240	1,1595	0,7088
0,5981	0,9911	0,5857	0,4371	0,4818	0,6860	0,2296	1,2263	0,6464
0,5705	0,9988	0,5319	0,5419	0,4958	0,9946	0,2243	1,0501	0,6531
0,6048	0,8445	0,5935	0,5110	0,4743	0,9163	0,2286	1,0166	0,7198
0,5538	1,1808	0,5164	0,5283	0,4276	0,8013	0,2024	1,0650	0,6231
0,4740	0,4976	0,6944	0,5600	0,4113	0,2911	0,1983	1,0117	0,4748
0,5567	0,6960	0,7082	0,5872	0,4075	0,3168	0,4081	1,0129	0,4397

0,5230	0,6049	0,6562	0,5256	0,4235	0,3053	0,2130	1,2180	0,5343
0,5240	0,7462	0,6452	0,4353	0,4035	0,4584	0,3654	1,0355	0,8269
0,5727	0,8231	0,6021	0,5627	0,4292	0,6814	0,2265	1,0110	0,6459
0,5233	1,0927	0,4004	0,3515	0,3918	0,7601	0,3424	0,8561	1,0805
0,5476	1,6426	0,5785	0,4554	0,4719	0,7072	0,1975	0,8807	0,5947
0,5405	1,9590	0,6072	0,4979	0,4655	1,5600	0,1709	1,0496	0,9870
0,5268	2,5491	0,5825	0,4312	0,3941	2,1360	0,1637	0,8001	1,0595
0,4931	1,9962	0,5157	0,3936	0,3785	1,1760	0,1798	1,0741	0,7027
0,5854	2,4954	0,6446	0,5004	0,4649	1,0912	0,1959	0,8738	0,6289
0,5349	2,8504	0,5506	0,5567	0,4370	0,8918	0,1826	0,8090	0,6467
0,6097	2,8750	0,6843	0,5109	0,5411	0,9756	0,2044	0,9321	0,7525
0,5480	1,6425	0,6244	0,4711	0,4423	0,7284	0,1994	0,8922	0,5757
0,5513	1,6126	0,6584	0,5300	0,4781	0,7549	0,2071	1,1863	0,5522
0,5651	1,6979	0,6573	0,4598	0,5177	0,9544	0,2107	1,1078	0,7526
0,5300	1,2801	0,5834	0,5371	0,4095	0,7335	0,1876	0,6359	0,5513
0,5465	1,7727	0,6075	0,4679	0,4787	1,9355	0,1763	0,8133	0,6329
0,5618	1,9516	0,6388	0,4739	0,4303	0,8225	0,1975	1,0284	0,5938
0,7352	1,2184	0,8207	0,7640	0,6691	0,8765	0,2836	1,4153	0,7930
0,6839	1,7436	0,7456	0,5805	0,5862	0,9722	0,2556	1,1331	0,7462
0,6564	2,7206	0,9487	0,5339	0,5601	1,2238	0,2190	1,2340	0,9718
0,6115	1,5830	0,7749	0,6628	0,5753	0,8513	0,2201	1,1489	0,7071
0,5947	1,7077	0,6523	0,4989	0,5147	0,7398	0,2243	1,0652	0,5088
0,5827	1,3753	0,6207	0,3892	0,4534	0,8476	0,2072	1,0086	0,5712
0,5747	1,9502	0,7916	0,5715	0,4138	0,9448	0,1941	0,8986	0,5539
0,5573	1,5662	0,5387	0,4059	0,4135	0,5945	0,1957	0,9536	0,4387
0,5549	0,9677	0,5894	0,4176	0,3740	0,6031	0,2017	0,7101	0,5034
0,4931	1,5433	0,7561	0,5078	0,3908	1,0931	0,1786	0,7850	0,6480
0,7931	2,2321	1,2936	0,5135	0,5468	2,6351	0,1583	0,6025	1,3651
0,5102	1,6364	0,8270	0,5932	0,5087	1,3139	0,1748	0,8218	0,9073
0,5792	2,5836	0,6432	0,5012	0,5250	1,1292	0,1955	1,2048	1,0226
0,5429	1,3763	0,6676	0,4572	0,4339	0,9186	0,1986	0,8667	0,6060
0,5146	1,2068	0,5332	0,3518	0,3922	0,8438	0,3130	0,8181	0,7855
0,5371	1,2671	0,5523	0,4090	0,4212	0,8637	0,1915	0,7631	0,5561
0,5208	1,3190	0,5247	0,4805	0,4166	0,7347	0,1818	0,8041	0,5203
0,5426	1,0059	0,5264	0,5209	0,4016	0,8919	0,1836	0,8626	0,5988
0,5172	1,1818	0,5289	0,4805	0,4110	0,8588	0,1753	0,7089	0,5597
0,5519	1,4074	0,5760	0,5128	0,4446	0,8951	0,1920	0,9210	0,5289
0,5342	1,1617	0,5211	0,4971	0,4495	0,7949	0,3364	0,8940	0,5171
0,5695	1,3436	0,5347	0,3659	0,4260	0,9062	0,2031	0,9225	0,5826
0,5294	1,4348	0,6963	0,5082	0,4956	0,9727	0,1839	0,9004	0,5217
0,5809	2,2364	0,6792	1,8663	0,6397	0,9948	0,2034	1,1931	0,7326
0,5969	1,9299	0,7205	0,4634	0,5345	0,9008	0,2132	1,2229	0,6768
0,6218	2,4285	0,7370	0,4393	0,5885	2,9693	0,2136	1,2783	0,8912

0,5312	1,2790	0,6759	0,5885	0,4952	0,9894	0,1993	0,8366	0,6512
0,5511	1,2721	0,5706	0,5174	0,4517	1,0567	0,2072	0,8404	0,5571
0,6585	2,8735	0,8069	0,5137	0,6516	1,6836	0,2309	1,1079	1,2913
0,5713	2,7149	0,8436	0,5037	0,6036	1,6789	0,1916	1,0891	0,8801
0,5288	1,7636	0,7785	0,4733	0,4894	2,3924	0,1715	0,8412	0,9380
0,6173	2,4645	0,7805	0,5405	0,6936	1,7703	0,2052	1,1661	0,8822
0,6416	3,0099	0,6744	0,6481	0,5739	1,8222	0,2164	1,1379	0,8392
0,5158	1,7530	0,5634	0,4090	0,4354	1,7218	0,1750	1,0801	0,7110
0,5541	1,8193	0,6661	0,4833	0,5083	1,2778	0,1814	0,9784	0,7473
0,5540	2,3873	0,7606	0,5830	0,5797	1,2583	0,2070	0,9638	0,7372
0,5561	1,6072	0,6663	0,5283	0,4397	0,8597	0,2029	0,9238	0,6291
0,5386	1,3834	0,6598	0,4655	0,5303	0,8047	0,1979	1,1270	0,6051
0,5770	1,6109	0,6746	0,5323	0,5118	0,9521	0,2033	1,0177	0,5827
0,5503	0,9383	0,5520	0,4060	0,4933	0,8137	0,1945	0,9268	1,4617
0,5530	2,3612	0,6334	0,3892	0,6082	1,1762	0,2001	0,9598	0,7520
0,5360	1,9248	0,6555	0,4871	0,5165	0,8504	0,1983	1,1336	0,6651
0,5093	1,0542	0,5500	0,5142	0,3814	0,6934	0,3242	0,7435	0,5534
0,5779	3,0368	0,7710	0,5061	0,6081	0,7078	0,2079	0,9464	0,5958
0,5683	2,2821	0,7579	0,5268	0,4906	0,7926	0,2156	0,8708	0,6003
0,5604	2,1291	0,6941	0,5000	0,5032	0,8698	0,2119	0,9160	0,6282
0,6269	1,9274	0,7338	0,4689	0,5884	0,7369	0,2356	0,9941	0,6054
0,6088	2,3690	0,7386	0,5390	0,5258	1,2111	0,2068	0,9415	0,8032
0,5234	1,5554	0,6029	0,4890	0,4164	0,6555	0,1856	0,9031	0,6143
0,6057	1,4648	0,6672	0,5747	0,4969	1,0034	0,2077	0,7836	1,8019
0,5872	1,8519	0,6433	0,5015	0,5313	1,0316	0,1988	0,8230	0,7408
0,5632	0,7724	0,5258	0,6169	0,4318	0,5614	0,1987	0,9144	0,6236
0,7062	0,8198	0,6677	0,5645	0,5549	1,3170	0,2380	1,2189	0,8685
0,7232	2,5418	0,4343		0,5777	1,2785	0,2369	0,7016	1,2622
0,6418	1,9130	0,5468	0,5962	0,4820	1,4738	0,2020	0,8736	1,0608
0,6478	0,9084	0,7653	0,6861	0,5179	1,8428	0,2145	0,8049	1,0657
0,6037	1,1178	0,6027	0,6297	0,4935	1,8148	0,2025	0,9063	1,1285
0,7166	1,6092	0,2859		0,2649	1,7336	0,1608	0,5652	1,8323
0,8490	1,6276	0,4827		0,6311	1,2259	0,2921	0,9533	1,5372
0,5647	1,2123	0,5234	0,5312	0,4217	1,0870	0,1964	1,0337	0,8524
0,8405	2,1941	0,6428	0,7257	0,6462	1,6607	0,2816	1,0832	0,9942
0,5779	1,0639	0,5560	0,5603	0,4926	1,1756	0,1871	0,8424	0,8408
0,5716	0,8729	0,5179	0,6069	0,4361	1,0634	0,1943	1,1392	0,7724
0,4997	0,6906	0,5432	0,5353	0,4469	0,7789	0,1809	0,8125	0,5618
0,5337	0,9188	0,6543	0,6175	0,4544	1,3839	0,2044	0,9662	1,0044
0,5191	1,4052	0,5533	0,4939	0,4840	1,6513	0,1834	0,9005	0,7567
0,5176	1,2560	0,4994	0,4857	0,4210	2,1484	0,1697	0,7554	0,9018
0,5022	1,4088	0,4303	0,4626	0,3911	1,7308	0,1688	0,7770	0,7706
0,4974	1,2359	0,4358	0,4845	0,3780	1,5138	0,1661	0,8396	0,7083
0,5056	1,6957	0,4439	0,5331	0,4222	1,4557	0,1573	1,1169	0,8378
0,5303	2,1112	0,4774	0,5571	0,4111	1,6010	0,1587	0,7913	0,8370
0,4955	2,0644	0,3355		0,4786	1,1973	0,1576	0,7129	2,6892
0,8490	34,6567	1,2936	1,8663	1,0927	2,9693	0,4081	2,3623	2,7090
0,4262	0,4563	0,2095	0,3515	0,2649	0,1976	0,1186	0,3352	0,4139
0,5743	1,7657	0,5978	0,5326	0,4669	0,9571	0,2219	0,9583	0,7706

0,0719	2,8237		0,1463	0,1347	0,0975		0,4730	0,0584	0,2313	0,3192
0,5567	1,3645		0,5891	0,5142	0,4464		0,8583	0,2040	0,9327	0,6715

EFMo	EFAs	EFZn	EFCu	EFCr
1,7593	1,2888	0,5307	0,5949	1,3456
	3,4795	0,5327	0,5863	1,4607
	2,7109	0,5185		
	1,2220	0,4369	0,4419	1,1127
	1,0092	0,3884	0,3187	1,0749
	2,1981	0,4956		1,4756
2,1543	2,8205	0,5707	0,3369	1,2241
	3,0910	0,6971	0,6150	2,9657
1,2886	0,7669	0,4324	0,3427	1,0667
	2,6529	0,5822	0,8513	1,1720
	4,8050	0,6456	0,7423	
1,5326	0,9213	0,4139	0,3801	1,1759
1,7305	1,1141	0,4752	0,4085	0,9410
	4,2076	0,7397		5,4050
1,8912	0,6310	0,3995	0,4255	0,8957
	0,7048	0,4413	0,2883	1,0021
		0,4549	0,7950	2,1445
	0,5628	0,4782	0,5877	1,1654
1,9306	1,1987	0,3911		1,3547
	1,0497	0,6165	0,7675	1,0915
2,5791	0,6188	0,6467	0,5243	1,3403
1,9231	2,3546	0,5932	0,6611	1,7429
1,7746	3,9667	0,4853	0,4708	1,7437
	1,6860	0,4860	0,5392	1,7042
1,9174	4,4031	0,4607	0,5250	1,9277
	3,7750	0,4766	0,4137	1,6009
	2,4791	0,5146	0,4725	1,5916
2,0828	1,6983	0,7072	0,6296	1,8884
	6,4000	0,6152	1,0471	3,3475
1,7250	1,7843	0,5210	0,4946	1,2416
	1,5782	0,4590	0,5855	1,1323
	4,7780	0,4869	0,7944	1,6138
3,6429	1,0385	0,5571	0,8415	1,4161
1,6992	1,3384	0,6689	0,7512	1,4121
3,6778	1,4130	0,6094	0,9204	1,5655
2,5117	1,5695	0,4725	0,5678	1,6033
5,6361	1,3873	1,1672	1,6156	1,7907
1,9938	1,3386	0,5280	0,7724	1,4342
2,2408	1,0013	0,4367	0,8715	1,4449
1,6248	2,0704	0,5499	0,5096	1,6029
2,1090	4,0857	0,4827	0,6118	2,5585
3,2462	4,2619	1,6235		4,2814
	1,0013	0,3974	0,3111	1,2551
2,1380	1,0103	0,4085	0,3686	1,4677
	1,9976	0,3696	0,7148	1,3452
2,2628	0,6603	0,9818		1,3936
	1,9672	0,5499	0,3392	1,2995
2,3139	4,1493	0,4164	0,3032	1,4074

2,4104	0,8394	0,5338		1,3928
	2,9401	0,4743	0,5706	1,3559
1,6833	1,4990	0,4089	0,5318	1,1167
1,6513	1,1154	0,3998	0,3803	1,2861
	1,4826	0,5424	0,6418	1,3592
6,0991	1,4114	0,5183	0,5566	1,3757
2,5059	1,6193	0,6801	0,6267	1,1865
2,6665	1,5066	0,3541	0,4984	1,1970
4,2132	0,8942	0,6829	1,0856	1,2495
3,7162	5,0080	0,4509	0,7844	1,9535
3,5321	1,1041	0,6848	0,8699	1,7866
1,8442	0,8700	1,0783	0,7403	1,4410
2,8237	1,2151	0,4762	0,4872	1,1530
	0,8461	0,4767	0,5527	
3,1557	2,8183	0,4449	0,4884	1,2948
3,8646	0,8777	0,5487	0,5781	1,4258
2,8150	2,4646	0,5436	0,7622	1,8280
4,3611	1,0167	0,5102	1,3370	1,5537
10,5407	1,2397	0,7733	1,1555	1,5630
6,7370	1,0424	0,6272	1,5135	1,3136
6,3233	1,5623	0,8238	1,8681	1,6377
6,9514	2,6090	1,0951	1,7080	1,4879
5,8320	2,7851	0,6376	1,2734	1,2648
4,8181	1,1526	0,5768	0,9898	1,6646
2,3370	1,4509	0,4179	0,6986	1,4011
3,4619	4,8836	0,5253	0,9323	1,7544
2,0379	1,4315	0,4774	0,6021	1,5418
1,8236	1,1310	0,4208	0,8842	1,1761
2,6566	1,0520	0,3822	0,3123	1,2333
	1,0821	0,3536	0,4797	1,1512
	1,4986	0,5093	0,6955	
	1,0105	0,4776	0,8867	
	3,1259	0,5270	1,0349	1,8929
	1,1080	0,3550	0,6671	1,2033
2,4546	4,2208	0,3918	0,6405	1,3754
	1,3433	0,7834	1,2914	
6,0613	1,6498	0,9481	0,9019	1,5291
7,1556	1,5103	0,5395	1,0335	1,7014
11,1404	1,3562	0,8194	1,5227	1,8052
10,2422	1,5415	0,7893	1,2129	1,7303
8,5795	1,4085	0,6295	1,0621	1,8515
4,5472	3,8668	0,7194	0,8740	1,5177
5,5809	1,1790	0,5154	0,8115	1,4688
3,5393	1,2715	0,5950	0,7551	1,5162
5,0037	2,0867	0,4688	0,8295	1,2862
7,8594	1,0928	0,5459	0,5241	1,1652
7,3304	0,9213	0,4760	0,5880	1,2268

7,3457	0,7281	0,4975	0,8275	0,9578
5,8730	0,7231	0,5858	0,5996	1,0382
7,7723	0,9341	0,6392	0,5547	1,1705
5,9987	0,5780	0,5789	0,6060	0,9330
14,9211	1,3867	0,6637	0,7223	1,3300
8,4663	0,9235	0,4252	0,6914	
11,8960	1,1440	0,6356	0,7808	
7,8618	0,8546	0,7073	0,7649	1,2110
10,2672	1,1036	0,8306	0,6658	1,6581
9,3976	1,2611	0,5032	0,7228	1,1892
13,6332	1,4380	0,5268	0,5929	1,5542
18,6534	1,1486	0,9937	1,1663	1,2745
17,7242	0,8589	1,0780	1,4109	1,1330
13,6248	0,7973	1,1031	1,4156	1,0572
5,9038	0,7980	0,5063	1,4148	1,1073
9,6130	1,3379	0,7219	1,5900	1,2583
5,4427	0,5007	0,7939	1,6924	0,9949
11,0170	1,2816	1,1852	1,8368	1,4796
7,5480	1,1204	0,9198	1,3489	1,4913
14,5895	1,1640	1,6949	1,3860	1,2094
9,6102	1,0321	1,1802	1,0811	1,3331
4,5966	0,9152	0,5523	2,1629	1,1899
5,6829	0,5536	0,6344	1,8915	1,1924
6,6375	0,8422	0,7035	1,3721	1,3338
3,7245	0,6356	0,6727	1,7813	1,0911
4,1046	0,8799	0,5268	0,7628	1,0333
5,9582	0,9185	0,6686	0,3955	0,9764
7,2259	1,0470	0,4344		
8,4902	1,2835	0,6118	0,5352	
13,4872	1,3329	0,7237	0,9464	1,7171
6,4626	0,9811	0,4937	0,5077	1,2121
5,7769	0,8761	0,5970	0,6016	1,0983
6,1019	1,1234	0,6116	0,5287	1,0540
6,3097	0,8002	0,4893	0,5236	1,1000
8,3560	1,2074	0,7042	0,6696	1,0477
6,8757	0,9076	0,5611	0,5504	1,2230
7,1608	2,6233	0,4827	0,5158	1,2428
6,9980	0,7417	0,6568	0,6716	1,1400
6,8360	1,1089	0,7272	0,5463	1,2328
13,8365	1,4146	1,2054	1,3940	1,2853
10,8527	1,4548	0,8041	1,2896	1,6918
22,4459	1,1730	1,3901	1,9669	1,4241
16,3765	1,5782	1,4994	2,7090	

14,2834	1,1596	0,8083	1,3656	1,2613
12,0893	1,8093	0,6075	1,3001	1,3841
13,8227	4,5422	0,6169	1,5564	
17,8408	1,6413	1,1237	1,9324	1,6064
13,1634	1,2483	0,6573	1,0422	
14,0826	1,1068	0,9345	1,3528	1,7305
12,3087	1,1043	1,8009	2,0791	
12,4496	0,7997	0,5856	1,0733	1,2105
11,5728	0,7335	0,8090	1,1045	1,2608
13,7505	1,2349	1,1004	1,3748	1,4343
10,0124	0,7025	0,8276	1,4095	1,3724
10,2268	1,0221	0,8287	1,1732	1,3787
8,9468	3,1259	0,7890	1,2296	1,5235
4,6683	0,8925	0,5206	0,7108	1,2316
13,4464	3,5818	1,1673	0,9766	1,6680
8,7516	2,6236	0,8175	1,2739	1,3406
4,7114	1,1377	0,6259	0,7435	1,2978
13,2083	3,4548	1,0771	1,1475	1,5890
7,7395	1,1582	0,8366	1,2913	1,6063
9,6128	1,3279	0,9542	1,0855	1,3246
3,8682	1,0454	0,7817	1,4479	1,5375
10,3089	1,4208	1,5221	1,3959	1,5595
5,0433	1,2678	0,4718	0,7148	1,3496
3,1019	1,4942	0,5087	0,8612	1,4702
2,3801	1,5458	0,7375	0,9017	1,3118
3,8602	1,5795	0,5004	0,5480	1,4628
2,7920	1,6543	0,8253	0,9385	1,6279
3,8699	5,5752	0,4064		
	1,2968	0,5750	0,7983	1,4392
	5,4613	0,7340	0,6388	
	1,8603	0,6014	0,9594	
	2,5557	0,5244		
	5,3719	0,5753	0,9917	
2,5746	1,2436	0,5118	0,5627	1,3495
	1,8109	0,7946	1,1038	1,9219
	3,1685	0,5111	0,5615	1,3208
1,8883	1,1720	0,6067	0,6063	1,4926
1,6518	0,8958	0,5056	0,5702	1,0780
	1,3203	0,3546	0,6537	
	1,2269	0,4225	0,4251	
	0,9495	0,5735	0,3475	
	1,1058	0,4547	0,3545	
1,7898	0,9517	0,4764	0,4255	
2,3822	1,1659	0,4928		
	1,3868	0,4047	0,5427	
2,9678	3,9769	0,5030	0,5843	
22,4459	6,4000	1,8009	2,7090	5,4050
1,2886	0,5007	0,3536	0,2883	0,8957
6,4991	1,7258	0,6484	0,8713	1,4551

	4,4934	1,1840	0,2607	0,4381	0,5100
	5,6829	1,2715	0,5721	0,7435	1,3559

Correlation of XR

	Ti	Mo	Zr	Sr	Rb	Th	Pb	As	Zn	Cu	Fe
Ti	1,00	-0,03	**0,84**	-0,55	0,70	0,54	0,68	-0,07	0,29	0,15	-0,13
Mo		1,00	0,10	0,22	-0,18	-0,18	-0,10	-0,24	0,49	0,43	-0,39
Zr			1,00	-0,25	0,52	0,37	0,55	-0,29	0,31	0,18	-0,33
Sr				1,00	-0,42	-0,44	-0,49	-0,41	-0,15	-0,09	-0,42
Rb					1,00	0,42	0,46	0,08	0,05	-0,06	0,05
Th						1,00	0,40	0,15	-0,05	-0,10	0,47
Pb							1,00	0,14	0,23	0,11	0,32
As								1,00	-0,19	-0,21	0,57
Zn									1,00	0,54	-0,11
Cu										1,00	-0,26
Fe											1,00
Mn											
Cr											
Ca											
K											
S											
Ba											
Nb											
Al											
P											
Si											
Mg											

RF values

Mn	Cr	Ca	K	S	Ba	Nb	Al	P	Si	Mg
-0,20	-0,04	**-0,80**	**0,84**	-0,05	-0,23	0,51	**0,79**	-0,17	**0,81**	0,35
-0,43	-0,38	0,10	-0,32	0,21	-0,30	0,08	-0,29	0,26	-0,15	-0,38
-0,40	-0,24	-0,54	0,64	-0,03	-0,25	0,42	0,56	-0,17	0,63	0,22
-0,18	-0,48	**0,75**	-0,47	0,09	0,04	-0,21	-0,42	0,14	-0,42	-0,29
-0,07	0,11	-0,63	0,70	-0,08	-0,02	0,33	0,67	-0,11	0,58	0,46
0,17	0,45	-0,55	0,52	-0,11	0,01	0,49	0,48	-0,16	0,43	0,31
-0,09	0,43	-0,69	0,58	-0,09	-0,13	0,33	0,56	-0,18	0,59	0,32
0,45	0,56	-0,25	0,03	-0,12	0,17	0,00	0,06	0,00	-0,02	0,20
-0,24	-0,14	-0,26	0,03	0,14	-0,35	0,20	0,04	-0,05	0,16	-0,05
-0,38	-0,24	-0,24	-0,11	0,17	-0,42	0,15	-0,20	0,00	0,05	-0,24
0,54	**0,90**	-0,22	-0,07	-0,18	0,23	0,01	0,08	0,14	-0,13	0,39
1,00	0,44	0,02	-0,09	-0,22	0,45	-0,05	-0,01	0,11	-0,22	0,12
	1,00	-0,30	0,00	-0,24	0,19	0,04	0,17	0,10	-0,06	0,42
		1,00	**-0,74**	0,03	0,21	-0,46	-0,62	0,14	-0,66	-0,32
			1,00	-0,12	-0,10	0,49	**0,84**	-0,11	**0,79**	0,39
				1,00	-0,13	-0,11	-0,04	0,21	-0,07	0,10
					1,00	-0,03	-0,02	0,15	-0,19	0,06
						1,00	0,48	0,60	0,49	0,18
							1,00	-0,05	**0,86**	0,64
								1,00	-0,13	-0,05
									1,00	0,43
										1,00